

Adaptation of a High-Accuracy Spectrophotometer for Ultraviolet Work

K. D. Mielenz, R. Mavrodineanu, and E. D. Cehelnik*

Institute for Materials Research, National Bureau of Standards, Washington, D.C. 20234

(May 31, 1974)

A high-accuracy spectrophotometer, originally designed for work at visible wavelengths, was modified to permit measurements in the ultraviolet without degradation of its original performance. This was accomplished by equipping the spectrophotometer with a stable deuterium arc source, a highly efficient averaging sphere with fluorescent wavelength converter, a new grating, and achromatic sample-compartment optics. The modified spectrophotometer will be used for the development of new Standard Reference Materials, as well as for materials research, in the region between 200 and 300 nm.

Key words: Averaging sphere; deuterium arc lamp; fluorescent wavelength converter; grating; spectrophotometry; standard reference materials; ultraviolet; UV achromats; visible.

1. Introduction

A primary goal of the current NBS program in spectrophotometry has been the design of high-accuracy instrumentation for the certification of calibration standards and the development of improved measurement techniques. For transmittance measurements at visible wavelengths, this goal was accomplished by specially constructing two highly accurate single-beam spectrophotometers [1, 2],¹ which are presently used in the Institutes for Materials Research (IMR) and Basic Standards (IBS) for standards work at visible wavelengths (400 to 800 nm, approximately). The instrumental accuracy achieved with these spectrophotometers is 10^{-4} transmittance units (0.01 percent). Although similar in some design aspects, these two spectrophotometers differ significantly in others, and therefore can be employed for in-house comparisons to ensure the accuracy and consistency of all spectrophotometric measurements at NBS. The purpose of this work was to extend these capabilities into the ultraviolet spectral region by developing the means for modifying either spectrophotometer for applications down to about 200 nm.

The particular instrument that was modified was the IMR spectrophotometer described in reference [1]. As originally designed, this spectrophotometer employed a current-stabilized, 100-W tungsten ribbon lamp as the radiation source; a 1-meter, $f/8.7$ Czerny-

Turner grating monochromator (1200 lines/mm, 500-nm blaze) with a fused-silica prism predisperser as the dispersing element; and an 11-stage, S-20 photomultiplier tube attached to a 125-mm, BaSO₄-coated averaging sphere as the signal detector. The tungsten lamp is imaged on the predisperser entrance slit by a fused-silica lens. Two additional fused-silica lenses are used in the sample compartment to focus the monochromator exit slit at the sample, and to refocus it into the averaging sphere [3]. The photomultiplier signal is measured by means of a current-to-voltage converter and a digital voltmeter, interfaced with a computer.

It may be estimated that, for a spectrophotometer of this type, a clear-space signal of at least 10^{-7} A is required if measurements are to be made with a standard deviation of at least 10^{-4} transmittance units [4]. The actual clear-space signal current obtained with this spectrophotometer at different wavelengths and for typical values of tungsten-lamp power, monochromator slit width, photomultiplier anode voltage, etc. is shown as curve (a) in figure 1, and thus indicates an inadequate performance of the instrument in the spectral region below approximately 370 nm. In order to effect the desired improvement of ultraviolet performance, the spectrophotometer was equipped with a deuterium arc source, a re-designed averaging sphere, and a differently blazed grating. These components were chosen to achieve a wide spectral range (200 to 800 nm) of the modified spectrophotometer, requiring only a change back to the tungsten lamp for work above 400 nm. In order to facilitate the usage of the instrument throughout this extended range, it was necessary to replace the two sample-compartment lenses by fused-silica, lithium-fluoride achromats.

* This paper describes a cooperative project on the part of the three authors. The basic design concepts and the accomplishment of a functioning instrument are due to K. D. Mielenz and R. Mavrodineanu. The optimization of the fluorescent wavelength converter for the averaging sphere was achieved by E.D. Cehelnik.

¹ Figures in brackets indicate the literature references at the end of this paper.

2. Modification of Spectrophotometer

2.1. Deuterium Arc Lamp

To a significant extent, the sharp drop of ultraviolet signal level shown by curve (a) in figure 1 is attributed

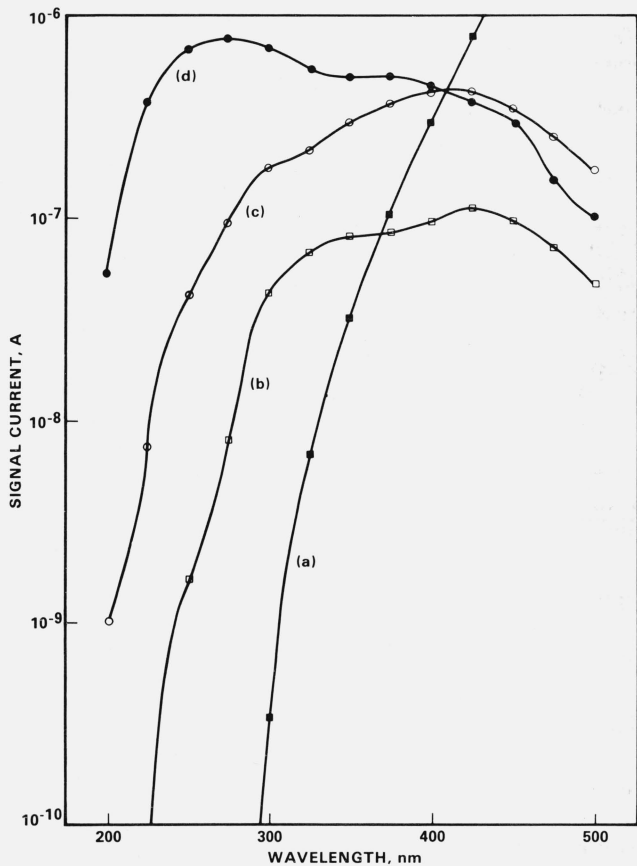


FIGURE 1. Successive improvement of clear-space signal level of original spectrophotometer (curve a) obtained by: (b) deuterium arc lamp, (c) improved averaging sphere, and (d) new grating.

utable to the tungsten lamp of the original spectrophotometer. A rapid decrease of radiant intensity with decreasing wavelength is typical for incandescent filament lamps, and therefore makes any source of this kind a poor choice for work at short wavelengths [5]. In contrast, a deuterium arc lamp exhibits an increase of radiant intensity with decreasing wavelength, and thus provides much better power levels in the ultraviolet.

A 60-W deuterium lamp with high-purity fused-silica window was chosen for the modified spectrophotometer. This lamp has a line-free continuous emission in the ultraviolet extending to below 180 nm, and is rated to have the same output at 200 nm as a 150-W xenon arc lamp. In comparison to a 250-W tungsten-bromide filament lamp, its output is about 1000 times greater at 250 nm, and 4 times greater at 300 nm. For work above 400 nm, tungsten lamps are preferable because of the decreasing intensity of the deuterium-arc spectrum and its line structure in the visible. The clear-space signal obtained after the deuterium lamp was installed in the spectrophotometer is shown as curve (b) in figure 1.

The stability of the radiant-intensity output of the deuterium lamp was tested by performing regularly repeated measurements of the spectrophotometer signal over extended periods of time. The long-term stability of lamp power so observed may be seen from figure 2, showing a gradually decreasing signal drift at the rates of 1.5, 0.6, and 0.08 percent per hour after the lamp had been operated for 1, 3, and 5 h, respectively. The average short-term instability (random noise plus drift) of the deuterium lamp was found to be 0.02 percent for a total of 15 sets of 20 individual readings, taken at 5-s intervals and at arbitrary times during an 8-h period of lamp operation. Since all data obtained with this spectrophotometer are derived by averaging a large number of individual measurements of transmittance, performed in a time-symmetrical sequence which eliminates the effects of drifting, this stability of the deuterium lamp is adequate for routine

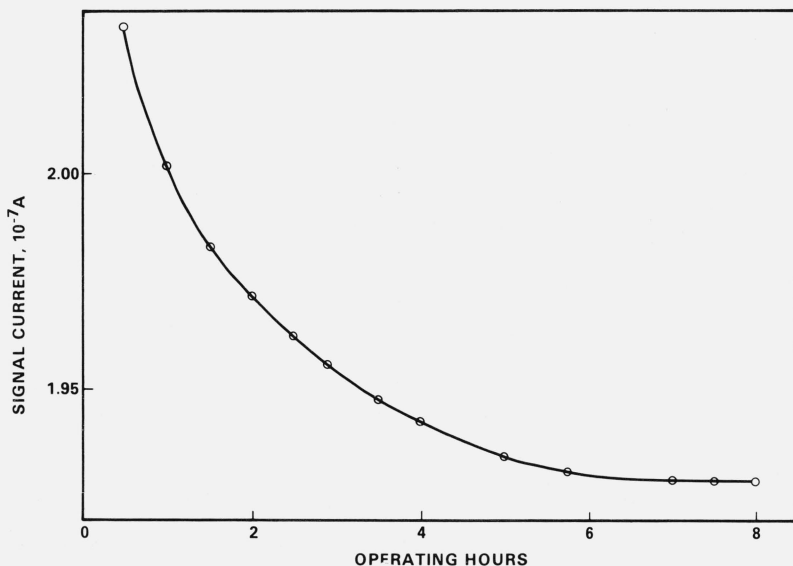


FIGURE 2. Long-term signal drift observed with deuterium lamp.

measurements with a precision better than 10^{-4} transmittance units. The above results for the deuterium lamp compare favorably with the stability data found for a current-stabilized tungsten lamp [2].

2.2. Averaging Sphere

The original averaging sphere of the spectrophotometer was designed as shown in figure 3a. It has an internal diameter of 125 mm, and circular entrance and exit ports 20 and 50 mm in diameter, respectively. The circular target, 35 mm in diameter, is located at the center of the sphere. The inside of the sphere, both sides of the target, and the thin target support rod are coated with several layers of specially prepared barium sulfate and polyvinyl alcohol coatings as developed by Grum and Luckey [6]. The photomultiplier tube is attached to the sphere, so that its 50-mm cathode is located 16 mm behind the exit port. The efficiency of this sphere was determined by successively measuring photomultiplier signals obtained at different wavelengths with and without sphere, using the deuterium arc lamp. These measurements showed a steep decrease of sphere efficiency from about 15 percent for visible wavelengths near 500 nm to

less than 0.1 percent at 200 nm, and thus indicated the necessity to equip the spectrophotometer with an improved, more efficient sphere [7].

According to theory [8], the efficiency of an averaging sphere of the type considered is, approximately,

$$\phi_D/\phi = [r^2/(1-r)](1-e/d)d^2/16s^2 \quad (1)$$

where

ϕ = radiant flux into sphere,

ϕ_D = flux reaching detector,

r = wall reflectance (assumed close to, but not equal to unity),

s = sphere radius,

d = radius of sensitive area of detector (assumed equal to radius of exit-port)

e = distance between exit port and detector.

It may be seen from this equation that, to a large extent, the poor efficiency of the original spectrophotometer sphere is due to inadequate coupling of exit port and detector. The collection efficiency of the detector (i.e.; the fraction of the diffuse flux from the exit port which actually reaches the photocathode) appears in Eq (1) as the factor $(1-e/d)$, which in this case has the numerical value 0.64 and thus shows that more than one third of the available flux is lost through the gap between exit port and detector. Therefore, a large increase in efficiency could be gained by modifying the sphere as shown in figure 3b. The sphere wall was tapered in a pear-like fashion and was extended into the detector housing, so that the exit port is butted directly against the photocathode. This simple modification of the sphere resulted in a large increase of efficiency (from 15 to 70 percent at 500 nm). However, the efficiency in the ultraviolet (now 2.5 percent at 200 nm) was still inadequate.

The averaging effectiveness of this sphere was tested by Mr. K. L. Eckerle of the Optical Radiation Section of NBS. The sphere was found to be insensitive to beam displacements from the target center of ± 1.5 mm within a $\pm 10^{-4}$ limit of signal variation. This is to be compared with a ± 5 percent variation for a ± 1 mm beam displacement on the same photomultiplier used without the sphere.

The high efficiency of the modified sphere in the visible suggested that a near-optimal sphere geometry had been achieved, and that the limiting factor in the ultraviolet was now the reduced reflectance of the barium-sulfate sphere coating. In order to overcome this remaining difficulty, a fluorescent dye was used to shift the incident short-wave radiation into the longer wavelength region for which the reflectance of barium sulfate is high. This dye, which is contained in a cell placed in front of the sphere target as shown in figure 3b, had to be chosen such that virtually all of the incident flux at short wavelengths is absorbed and is converted into fluorescence with a quantum efficiency as nearly equal to unity as possible. In order to avoid impairing the high sphere efficiency at longer wavelengths, it was also required that visible light be not absorbed, so that it passes through the dye unaffected and is reflected from the target as before. The fluores-

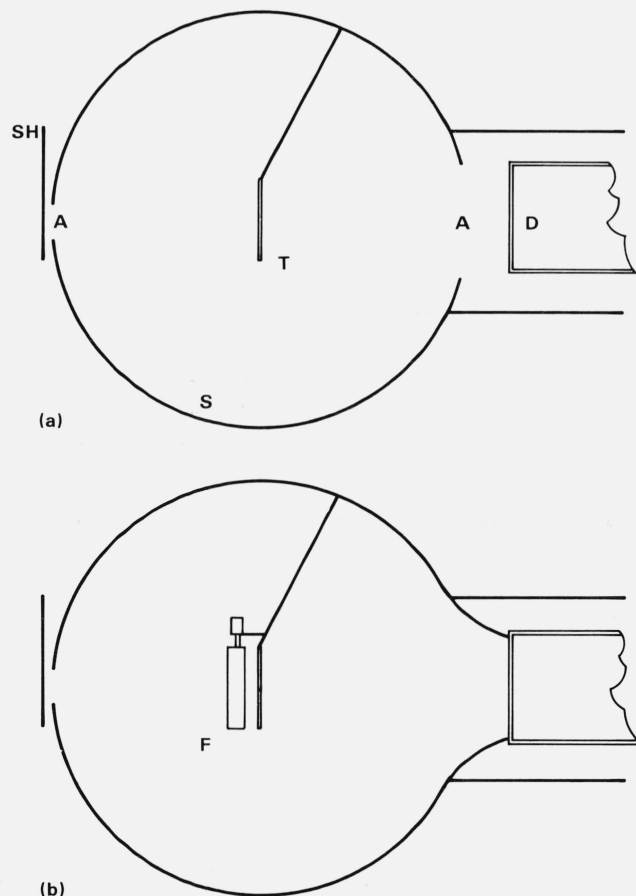


FIGURE 3. Geometry of (a) original averaging sphere and (b) improved sphere.

A: entrance port, A': exit port, D: detector, F: fluorescent dye cell, S: sphere wall, SH: shutter, T: target.

cent material selected was a 0.923 g/l solution of 2,5-diphenyloxazole (PPO) in *n*-hexane in a 10 × 10 × 2 mm high-purity fused-silica cell. It is effectively transparent for wavelengths above 360 nm, and below 340 nm absorbs more than 99 percent of the incident radiation. Its estimated quantum efficiency is 0.9, with the peak emission occurring near 370 nm. The use of this dye proved highly successful, and resulted in a sphere efficiency of 20 percent at 200 nm.

The marked enhancement of signal level obtained with this improved sphere is shown by comparing curve (c) in figure 1 with curve (b). The measured efficiency of the sphere is roughly constant and equal to 20 percent between 200 and 300 nm, followed by a gradual increase to a constant level between 60 and 65 percent for wavelengths from 400 to beyond 650 nm. A further increase of sphere efficiency was obtained in a final design by reducing the sphere diameter and further optimization of the dye [8].

It was also ascertained that the fluorescence wavelength converter did not affect the linearity of the detection system. Theoretically, the radiant intensity of fluorescence from the dye can be expressed as

$$I_e = QI_a, \quad (2a)$$

where Q is the quantum efficiency of the dye and I_a is the intensity absorbed. The latter is given by Beer's law as

$$I_a = I_o(1 - 10^{-\epsilon cb}) \quad (2b)$$

where I_o is the initial intensity, and where ϵ , c , and b denote molar absorptivity, concentration, and path length, respectively. Thus, I_e is proportional to I_o under the applicable assumptions that Beer's law is valid and that the quantum efficiency of the dye is independent of intensity. This conclusion was verified by measuring the linearity of the detection system at one wavelength (250 nm) for which the dye is effective, and at another (400 nm) for which it is not. These two measurements, which were made using the double-aperture method [9], yielded indistinguishable results within the limits of experimental uncertainty, and also agreed with previously performed linearity measurements of the same photomultiplier tube at 575 nm [1].

2.3. Grating

The previously obtained clear-space signal level, curve (c) in figure 1, was still judged inadequate for accurate work at short wavelengths. Since the original grating of the spectrophotometer (blazed for 500 nm in the first order) had been chosen for work in the visible, it was obvious that a further improvement could be effected by substitution of another grating. This new grating has 600 lines/mm, is blazed for 200 nm in the first order, and resulted in the final clear-space signal current plotted as curve (d) in figure 1. Since the signal level near 200 nm can easily be raised by adjusting the photomultiplier gain, the original goal of achieving a

clear-space signal of at least 10^{-7} A throughout the ultraviolet had thus been accomplished.

The loss of signal level in the visible due to the change of gratings [curves (d) and (c) in figure 1] is relatively small, and is more than offset by the higher efficiency of the new sphere [curves (c) and (b)]. Thus the modified spectrophotometer can be used above 400 nm by merely interchanging deuterium and tungsten lamps, without need to substitute gratings.

2.4. Achromatic Sample-Compartment Optics

In view of the wide spectral range of the modified spectrophotometer, the chromatic aberration of the original sample-compartment lenses proved to be a limiting factor of instrumental performance. Significant losses of signal level were caused by the fact that these lenses, when initially focused by eye, were out of focus in the ultraviolet and thus caused less-than-optimal illumination of sample and detector.

If the monochromator exit slit is focused at the sample with unit magnification at a wavelength λ_0 , the diameter of the blur circle in the sample plane for a wavelength $\lambda < \lambda_0$ can easily be shown to be equal to

$$\delta = D[2f(\lambda_0)/f(\lambda) - 1], \quad (3)$$

where f is the focal length and D is the effective diameter of the focusing lens. For the particular lenses of the original spectrophotometer [$f(200 \text{ nm}) = 168 \text{ mm}$, $f(500 \text{ nm}) = 200 \text{ mm}$, $D = 38 \text{ mm}$], and assuming that the focusing was done at 500 nm, the computed blur-circle diameter at 200 nm is 14 mm. This numerical example illustrates the large defocusing caused by chromatic lenses in the sample compartment, although it should be pointed out that due to the opposing effect of the second lens a smaller blur circle is incurred at the detector. Nevertheless, it was found empirically that the ultraviolet signal level of the spectrophotometer could be improved as much as 30 percent by repositioning the sample-compartment lenses.

The most effective way to overcome this deficiency of the spectrophotometer would have been to use mirror optics, but since this would have required a redesign of the sample compartment and its enclosure it was more expedient to employ achromatic lenses. The lenses selected are $f/3$ lithium-fluoride, fused-silica (non fluorescent) achromats, with 200 mm focal length, best correction for longitudinal chromatic aberration between 200 and 400 nm, and with anti-reflection coating for 400 nm.

On account of the limited spectral regions for which the deuterium and tungsten lamps of the modified spectrophotometer are employed, it was not found necessary to use an achromat in the source compartment as well.

3. Conclusion

As a result of the work reported here, the modified high-accuracy spectrophotometer is now used, throughout the spectral region between 200 and 800 nm, for

the certification of solid and liquid Standard Reference Materials for routine applications in spectrophotometry, as well as for materials research aimed at establishing inorganic and organic molar absorptivity standards.

The modified spectrophotometer may also serve as a model for improved commercial instrumentation. In particular, it is anticipated that the development of a highly efficient averaging sphere for visible and ultraviolet wavelengths will lead to a more widespread use of spheres in routine spectrophotometry.

4. References and Notes

- [1] Mavrodineanu, R., *J. Res. Nat. Bur. Stand. (U.S.)*, **76A** (Phys. and Chem.), No. 5, 405-425 (Sept.-Oct. 1972).
- [2] Mielenz, K. D., Eckerle, K. L., Madden, R. P., and Reader, J., *Appl. Optics* **12**, 1630-1641 (1973); Mielenz, K. D., and Eckerle, K. L., *Nat. Bur. Stand. (U.S.)*, Tech. Note 729, 60 pages (June 1972).
- [3] The systematic error due to interreflection between the sample-compartment lenses is accounted for in all measurements made with this spectrophotometer. See Mielenz, K. D., and Mavrodineanu, R., *J. Res. Nat. Bur. Stand. (U.S.)*, **77A** (Phys. and Chem.), No. 6, 699-703 (Nov.-Dec. 1973).
- [4] K. D. Mielenz, *J. Res. Nat. Bur. Stand. (U.S.)*, **76A** (Phys. and Chem.), No. 5, 455-467 (Sept.-Oct. 1972).
- [5] Although tungsten-halogen lamps are frequently used in ultraviolet spectrophotometry, such a source was unsuitable for this application. A 250-W, single-coil tungsten-bromide lamp was tried, but merely resulted in an over-all increase of signal level which could also have been achieved by choosing a more intense tungsten lamp or increasing the photomultiplier gain. The tungsten-bromide lamp exhibited essentially the same steep drop of signal toward shorter wavelengths as the tungsten lamp, and was found to be inadequate for accurate work below 320 nm. A further difficulty is that tungsten-halogen lamps are generally too unstable for high-accuracy spectrophotometry in a single-beam geometry. See Clarke, F. J. J., *J. Res. Nat. Bur. Stand. (U.S.)*, **76A** (Phys. and Chem.), No. 5, 375-403 (Sept.-Oct. 1972).
- [6] Grum, F., and Luckey, G. W., *Appl. Optics* **7**, 2289-2294 (1968).
- [7] A significant improvement of the visible and ultraviolet signal levels was found with a flux averager consisting of two double-ground fused-silica plates, 1 mm in thickness and spaced by a diffusely reflecting, cylindrical Al_2O_3 tube with 50 mm length and internal diameter. Although this type of averager has been used successfully for other applications (See Budde, W., *Proc. Fourth Imeko Symposium, Prague 1969*, p. 167), the averaging effectiveness of the particular unit used in this work was inadequate for this application since a beam displacement of ± 1 mm at the entrance window of the averager still caused a 0.4 percent change in the photomultiplier signal. These measurements were performed by Mr. K. L. Eckerle of the Optical Radiation Section of NBS.
- [8] Mielenz, K. D., Mavrodineanu, R., and Cehelnik, E. D., *Appl. Optics* (to be published).
- [9] Mielenz, K. D. and Eckerle, K. L., *Appl. Optics* **11**, 2294-2303 (1972).

(Paper 78A5-838)

Publications of the National Bureau of Standards*

Citations with Selected Abstracts

J. Res. Nat. Bur. Stand. (U.S.), 78A (Phys. and Chem.), No. 4, (July-Aug. 1974), SD Catalog No. C13.22/sec.A:78/4.

The glass transition temperature of monodispersed polystyrenes and their binary mixtures, L. A. Wall, Roestamsjah, and M. H. Aldridge.

A method of measuring the solubilities of hydrocarbons in aqueous solutions, R. L. Brown and S. P. Wasik.

Theoretical and experimental Compton scattering cross sections at 1.12 MeV in the case of strongly bound K-shell electrons, P. N. Baba Prasad and P. P. Kane.

Standardization of ^{60}Co and ^{137}Cs gamma-ray beams in terms of exposure, T. P. Loftus and J. T. Weaver.

Investigation of freezing temperatures of National Bureau of Standards aluminum standards, G. T. Furukawa.

Prediction of the viscosities of "soda-lime"-silica glass, K. C. Lyon.

The system NaCl-AlCl_3 , E. M. Levin, J. F. Kinney, R. D. Wells, and J. T. Benedict.

Simultaneous measurements of heat capacity, electrical resistivity and hemispherical total emittance by a pulse heating technique: zirconium, 1500 to 2100 K, A. Cezairliyan and F. Righini.

Measured enthalpy and derived thermodynamic properties of crystalline and liquid potassium chloride, KCl, from 273 to 1174 K, T. B. Douglas and A. W. Harman.

Monogr. 140. **Time and frequency: Theory and fundamentals**, B. E. Blair, Ed., Nat. Bur. Stand. (U.S.), Monogr. 140, 470 pages (May 1974) SD Catalog No. C13.44:140, \$8.65.

Key words: accuracy; Allan variance; atomic frequency standards; atomic time scales; AT(NBS); BIH; buffer gases; CCIR; clock ensembles; clocks; crystal aging; Cs frequency standard; dissemination techniques; figure of merit; flicker noise; frequency stability; frequency standards; frequency/time metrology; hydrogen maser; leap seconds; Loran-C; magnetic resonance; masers; NBS-III; NBS-5; NBS/USNO time coordination; Omega; optical pumping; precision; quartz crystal oscillators; radio T/F dissemination; Rb frequency standards; satellite T/F dissemination; short-term stability; SI Units; TAI; television T/F dissemination; thallium beam standards; time; time dispersion; time domain; time/frequency statistics; time scale algorithm; time scales; "unified standard"; URSI; USA standard time zones; UTC (NBS); UTC (USNO).

*Publications with prices and SD Catalog numbers may be purchased directly from the Superintendent of Documents, U.S. Government Printing Office, Washington, D.C. 20402 (foreign: one-fourth additional). Microfiche copies are available from the National Technical Information Service (NTIS), Springfield, Va. 22151. Reprints from outside journals and the NBS Journal of Research may often be obtained directly from the authors.

This is a tutorial Monograph describing various aspects of time and frequency (T/F). Included are chapters relating to elemental concepts of precise time and frequency; basic principles of quartz oscillators and atomic frequency standards; historical review, recent progress, and current status of atomic frequency standards; promising areas of developing future primary frequency standards; relevance of frequency standards to other areas of metrology including a unified standard concept; statistics of T/F data analysis coupled with the theory and construction of the NBS atomic time scale; an overview of T/F dissemination techniques; and the standards of T/F in the USA. This Monograph addresses both the specialist in the field as well as those desiring basic information about time and frequency. The authors trace the development and scope of T/F technology, its improvement over periods of decades, its status today, and its possible use, applications, and development in days to come.

SP236, 1974 Edition. **NBS frequency and time broadcast services. Radio stations WWV, WWVH, WWVB, and WWVL**, P. P. Viezicke, Ed., (Supersedes NBS Special Publication 236, 1973 and previous editions) Nat. Bur. Stand. (U.S.), Spec. Publ. 236, 1974 Edition, 19 pages (Mar. 1974) SD Catalog No. C13.10:236, 1974 Ed., 60 cents.

Key words: broadcast of standard frequencies; high frequency; low frequency; standard frequencies; time signals; very low frequency.

Detailed descriptions are given of the technical services provided by the National Bureau of Standards radio stations WWV, WWVH, WWVB and WWVL. These services are: 1. Standard radio frequencies; 2. Standard audio frequencies; 3. Standard musical pitch; 4. Standard time intervals; 5. Time signals; 6. UTI corrections; and 7. Official announcements. In order to provide users with the best possible services, occasional changes in broadcasting schedules are required. This publication shows the schedules in effect on January 1, 1974. Annual revisions will be made. Current data relating to standard frequencies and time signals are available monthly in the Time and Frequency Services Bulletin. Advance notices of changes occurring between revisions will be sent to users of NBS broadcast services who request such notice on the basis of need. Supersedes NBS Special Publication 236, 1973 and previous editions.

SP260-48. **Standard Reference Materials: Description and use of precision thermometers for the clinical laboratory, SRM 933 and SRM 934**, B. W. Mangum and J. A. Wise, Nat. Bur. Stand. (U.S.), Spec. Publ. 260-48, 23 pages (May 1974) SD Catalog No. C13.10:260-48, 60 cents.

Key words: clinical laboratory; enzymology; health care; liquid-in-glass thermometers; standard reference material; SRM 933; SRM 934; thermometers.

Because of the high sensitivity to temperature of many facets of the clinical laboratory, e.g., in enzyme reactions and in pH and blood gas analysis, there is a need for accurate temperature measurements and its control. In order to help satisfy these needs and to aid in getting a usable and accurate temperature scale into the clinical laboratory, the National Bureau of Standards has developed SRM 933 and SRM

934. These are precision thermometers, which are calibrated at 0, 25, 30, and 37 °C and their description, their calibration, and the procedures for their proper usage are discussed.

SP388. The public need and the role of the inventor. Proceedings of a Conference held in Monterey, Calif., June 11-14, 1973, F. Essers and J. Rabinow, Eds., Nat. Bur. Stand. (U.S.), Spec. Publ. 388, 215 pages (May 1974) SD Catalog No. C13.10:388, \$5.55.

Key words: antitrust doctrine; employed inventors; entrepreneurship; innovation; invention; needs of society; new enterprises; Patent Office; patent system; technological policy making; technology.

This book presents the proceedings of the Conference on the Public Need and the Role of the Inventor, held at Monterey, Calif., on June 11-14, 1973. The conference, based on a recommendation of the National Inventors Council, was sponsored by the Office of Invention and Innovation, Institute for Applied Technology, under a grant from the Experimental Technology Incentives Program, NBS. The purpose of the conference was to study the climate for invention and how to make it one in which America's inventors can flourish for the common good. Eighteen invited papers were presented. In addition, the proceedings includes statements from the chairmen of the three sessions: Charles S. Draper, Jacob Rabinow, and Myron Coler. The proceedings are divided into three sessions with an edited version of the floor discussions following the papers. Following the presentation of papers, the participants of the conference separated into six workshop panels. Their recommendations are presented at the end of this volume.

SP391. Report of the 58th National Conference on Weights and Measures 1973, S. J. Wilson and R. N. Smith, Eds., Nat. Bur. Stand. (U.S.), Spec. Publ. 391, 208 pages (May 1974) SD Catalog No. C13.10:391, \$2.50.

Key words: administration; automated checkstand systems; Conference; consumers; laws and regulations; metrication; open dating; procedures; technical requirements; technology; universal product coding; weights and measures.

This is a report of the proceedings (edited) of the Fifty-Eighth National Conference of Weights and Measures, sponsored by the National Bureau of Standards, held in Minneapolis, Minn., July 22-27, 1973, and attended by state, county, and city weights and measures officials, the Federal Government, business, industry, and consumer organizations.

SP394. MFPG. The role of cavitation in mechanical failures. Proceedings of the 19th Meeting of the Mechanical Failures Prevention Group, held at the National Bureau of Standards, Oct. 31, Nov. 1 and 2, 1973, Boulder, Colo. 80302, T. R. Shives and W. A. Willard, Eds., Nat. Bur. Stand. (U.S.), Spec. Publ. 394, 183 pages (Apr. 1974) SD Catalog No. C13.10:394, \$2.25.

Key words: bubble collapse; cavitation; cavitation damage; cavitation erosion prevention; erosion; surface roughness.

These proceedings consist of a group of 16 submitted papers and discussions from the 19th meeting of the Mechanical Failures Prevention Group which was held at the National Bureau of Standards on October 31 and November 1 and 2, 1973. The central theme of the proceedings is the role of cavitation in mechanical failures.

BSS52. The effect of impact loadings on the performance of wood joist subflooring systems, H. S. Lew, Nat. Bur. Stand. (U.S.), Bldg. Sci. Ser. 52, 35 pages (May 1974) SD Catalog No. C13.29:2/52, 70 cents.

Key words: concentrated load; deflection; floor; hardboard; housing; impact energy; Operation BREAKTHROUGH; plywood; subfloors; underlayment; wood; wood joists.

This report presents the results of an experimental study of wood-joist subflooring systems subjected to impact load. Six different types of subflooring systems were tested following the test method described in the ASTM Standard Methods (ASTM Designation E-72). The magnitude of impact load was varied by dropping a 60-lb bag from different heights.

A concentrated static load of 400 lb was applied to the subfloor after it was exposed to impact load. It is suggested that the deflection under this concentrated load be used as a measure of the impact resistance of the subfloor. Supersedes NBSIR 73-187 (PB 221-188).

BSS53. Study of the local resistance of conventional plywood subflooring to concentrated load, F. Y. Yokel, Nat. Bur. Stand. (U.S.), Bldg. Sci. Ser. 53, 43 pages (May 1974) SD Catalog No. C13.29:2/53, 85 cents.

Key words: evaluation criteria; floors; hardboard; load capacity, performance criteria; plywood subflooring; subflooring; underlayment; wood-frame construction.

Representative specimens, simulating the performance of five conventional plywood floor systems, were tested under concentrated load in order to compare their performance with that stipulated by performance criteria developed on the basis of anticipated occupancy loads.

In 24 out of 26 tests the performance of the specimens exceeded that required by the criteria. Data on failure loads, load-deflection characteristics and failure modes are presented and discussed. Supersedes NBSIR 73-116 (PB 220-432/9).

FIPS PUB10-1. Countries, dependencies, and areas of special sovereignty, H. E. McEwen, Standards Coordinator, Nat. Bur. Stand. (U.S.), Fed. Info. Process. Stand. Publ. (FIPS PUB) 10-1, 27 pages (1974) SD Catalog No. C13.52:10-1, 70 cents.

Key words: ADP standards; computers; data elements and codes; data processing; Federal Information Processing Standards; geography; information processing standards; information systems; representations and codes; standards; statistical data.

This publication provides a list of geographical-political entities of the world and associated standard codes. These entities include independent states, dependent areas, areas of quasi-independence, non-contiguous territories, possessions without population, areas with special sovereignty associations, areas without sovereignty, political regimes not recognized by the United States, and outlying areas of the United States.

FIPS PUB29. Interpretation procedures for Federal Standard COBOL, R. E. Rountree, Jr., Standards Coordinator, Nat. Bur. Stand. (U.S.), Fed. Info. Process. Stand. Publ. (FIPS PUB) 29, 4 pages (1974) SD Catalog No. C13.52:29, 25 cents.

Key words: COBOL; compilers; data processing; Federal Information Processing Standard; information interchange; information processing; programming language; software.

This FIPS PUB defines the procedures that will be followed in requesting interpretations of the Federal Standard COBOL and in providing responses to those requests. The provisions of this document apply to all Federal departments and agencies and to vendors of COBOL compilers in their dealings with the Federal Government.

TN594-8. Tables of diffraction losses, W. B. Fussell, Nat. Bur. Stand. (U.S.), Tech. Note 594-8, 39 pages (June 1974) SD Catalog No. C13.46:594-8, 75 cents.

Key words: diffraction; diffraction losses; Fresnel diffraction; Kirchhoff diffraction theory; photometry; radiometry; scalar diffraction theory.

Tables of diffraction losses are given for a range of typical experimental geometries for wavelengths from 0.2 to 100 micrometers. The scaling relationships for the diffraction losses for varying wavelengths and geometries are also given, and sample calculations are presented. General formulas are given for the diffraction losses; the formulas are derived from the Kirchhoff scalar paraxial diffraction theory. The accuracy of the tabulated values is estimated.

TN650. An evaluation of selected angular momentum, vortex shedding and orifice cryogenic flowmeters, J. A. Brennan, R. W. Stokes, C. H. Kneebone, and D. B. Mann, Nat. Bur. Stand. (U.S.), Tech. Note 650, 69 pages (Mar. 1974) SD Catalog No. C13.46:650, 65 cents.

Key words: angular momentum; cryogenic; flow; liquid nitrogen; mass; mass flowmeters; measurement; orifice; volume flowmeters; vortex shedding.

The National Bureau of Standards (NBS) and the Compressed Gas Association (CGA) have jointly sponsored a research program on cryogenic flow measurement. Cryogenic flowmeters operating on the principles of angular momentum (mass flow), vortex shedding (volume flow), and pressure drop are reported.

The operation and the accuracy of the flow facility is briefly described. The performance of the flowmeters in liquid nitrogen is described by reporting the precision and bias of the meters before and after an 80-hour stability test and by defining the existence of temperature, pressure, flow rate, subcooling, and time order (wear) dependencies.

Meters were evaluated with flow rates ranging from 20 to 210 gpm (0.00126 to 0.0132 m³/s), pressures ranging from 32 to 112 psia (0.22 to 0.77 MPa), and with temperatures ranging from 72 to 90 K.

TN652. Development and construction of an electromagnetic near-field synthesizer, F. M. Greene, Nat. Bur. Stand. (U.S.), Tech. Note 652, 44 pages (May 1974) SD Catalog No. C13.46:652, 50 cents.

Key words: electromagnetic-field hazards; electromagnetic-field synthesizer; electromagnetic radiation-exposure testing (non-ionizing); near fields; RF biological hazards.

This publication describes work done by the National Bureau of Standards for the USAF School of Aerospace Medicine at Brooks AF Base involving the development, design, construction and testing of a prototype EM near-field synthesizer. The purpose of the contract was to provide a means of independently generating high-level electric and magnetic near fields in the frequency range 10 to 30 MHz. These fields are to be used in various ratios by the USAFSAM in their EM radiation exposure program for determining the biological effects of hazard-level, non-ionizing EM fields on human beings.

The synthesizer consists of a balanced, parallel-plate strip line to generate the "desired" electric field, and a single-turn quadruple-fed inductor placed parallel to and midway between the plates to generate the "desired" magnetic field. Methods used to reduce the "unwanted" E- and H-field components associated with the above, as well as the methods used to reduce the coupling between the two field systems are discussed. The result is a synthesizer in which the electric- and magnetic-field components can be adjusted essentially independently over wide ranges of magnitude, relative time-phase, and spatial orientation to simulate various near-field configurations.

Previous research has been largely limited to the use of plane-wave fields for evaluating RF biological hazards. This new device will allow researchers to investigate any near-field effects that may occur at high field levels.

TN656. Standard time and frequency: Its generation, control and dissemination by the National Bureau of Standards, J. B. Milton, Nat. Bur. Stand. (U.S.), Tech. Note 656, 21 pages (June 1974) SD Catalog No. C13.46:656, 35 cents.

Key words: clock synchronization; frequency and time dissemination; primary frequency standard; standard frequency broadcasts; time interval; time scales.

The Time and Frequency Division of the National Bureau of Standards maintains primary frequency standards, which provide a realization of the internationally-defined second, and two atomic time scales, AT(NBS) and UTC(NBS). AT(NBS) is dependent upon the primary frequency standards, an ensemble of commercial cesium clocks, and a computer algorithm to process the data. The UTC(NBS) scale is derived from AT(NBS) by the addition of small annual frequency adjustments and leap second adjustments to keep its time nominally synchronous with the international time scale UTC. The UTC(NBS) time scale is used to calibrate the clocks and secondary standards necessary for the operation of the NBS radio stations, WWV, WWVH, WWVB, and WWVL. These stations transmit various standard frequency and time signals throughout the world, and, in addition, provide certain official announcements such as geolocal warnings, marine weather advisories, and radio propagation forecasts.

TN782. Application of systems analysis to the operation of a fire department, E. K. Nilsson, J. A. Swartz, and M. Westfall, Nat. Bur. Stand. (U.S.), Tech. Note 782, 52 pages (June 1974) SD Catalog No. C13.46:782, 90 cents.

Key words: Alexandria; fire department; location; operations research; resource allocation; simulation; systems analysis.

Rising labor costs and increasing competition for tax dollars to provide urban services demand that a more precise methodology be used in the management of fire departments. A pilot program was conducted with the cooperation of the Alexandria, Va. Fire Department to evaluate the applicability and usefulness of selected Operations Research tools. These tools, in the form of computer models, were modified and adapted to assure that they could be implemented to provide information which would facilitate fire department management. In this effort queueing, facility location, and simulation models were applied to sample data extracted from the historical records of the Alexandria Fire Department. It was established that such models do provide valuable information which may assist managerial decisions. This paper describes the city of Alexandria and its fire department, the O.R. models, output from their application, and evaluations of the output.

TN801. Research considerations in computer networking to expand resource sharing, D. W. Fife, Nat. Bur. Stand. (U.S.), Tech. Note 801, 24 pages (June 1974) SD Catalog No. C13.46:801, 60 cents.

Key words: computer networking research; computer network management; management evaluation; resource sharing.

Computer networking technology is adequately developed now to support research and experimentation to expand computing resource sharing. Whether progress will be made depends upon organizational initiative among multiple institutions, to pool personnel and capital so as to effectively address the major issues in management approach, support and software design that limit the feasible interdependence of computing operations. The organizational requirements are partially revealed by examining progressive stages of resource sharing in organizational and operational terms rather than such technical aspects as load sharing or program sharing that have been introduced in the past. Five stages are identified, ranging from simply establishing multiple service access to the advanced stage where multiple institutions organize for joint development of new resources. A preliminary evaluation framework for new management arrangements

results when these stages are mapped against the four functional levels inherent in computer network management. Future needs for networking experimentation and research are briefly described, and other NBS technical results are identified in context.

TN825. Properties of selected superconductive materials—1974 supplement, B. W. Roberts, Nat. Bur. Stand. (U.S.), Tech. Note 825, 1974 Supplement, 88 pages (Apr. 1974) SD Catalog No. C13.46:825, \$1.25.

Key words: bibliography; composition; critical fields; critical temperature; crystallographic data; data compilation; low temperature; superconductive materials; superconductivity.

This report includes data on additional superconductive materials extracted from a portion of the world literature up to mid-1973. The data presented are new values and have not been selected or compared to values (except for selected values of the elements) previously assembled by the Superconductive Materials Data Center. The properties included are composition, critical temperature, critical magnetic field, crystal structure and the results of negative experiments. Special tabulations of high magnetic field materials with Type II behavior and materials with organic components are included. All entries are keyed to the literature and a list of reviews centered on superconductive materials is included. Extends NBS Technical Note 724.

TN827. Controlled accessibility workshop report. A report of the NBS/ACM Workshop on Controlled Accessibility, Rancho Santa Fe, Calif., Dec. 10-13, 1972, S. K. Reed and D. K. Branstad, Eds., Nat. Bur. Stand. (U.S.), Tech. Note 827, 86 pages (May 1974) SD Catalog No. C13.46:827, \$1.25.

Key words: access control; computer security; controlled accessibility; EDP management control; identification; measurement; security audit.

A report has been prepared of the NBS/ACM Workshop on Controlled Accessibility, December 1972, Rancho Santa Fe, Calif. The Workshop was divided into five separate working groups: access controls audit, EDP management controls, identification, and measurements. The report contains the introductory remarks outlining the purpose and goals of the Workshop, summaries of the discussions that took place in the working groups and the conclusions that were reached. A list of participants is included.

TN828. Measures for air quality (1972-1973). Annual report—FY 1973, J. R. McNesby, Nat. Bur. Stand. (U.S.), Tech. Note 828, 143 pages (May 1974) SD Catalog No. C13.46:828, \$1.70.

Key words: air pollution; measurement; standard reference material; water pollution.

This report is a project-by-project description of the Measures for Air Quality program covering the fiscal years 1972 and 1973. Participation in the program is bureau-wide but the program office operates out of the Institute for Materials Research. Although air pollution measurement science has formed the major thrust of the program, it has been extended in FY 73 to include the beginnings of a water pollution effort to respond to new needs, particularly those arising out of the requirements of the Federal Water Pollution Control Act of 1972. A report on the MAQ program for FY 72 was not issued. However, the project reports in the current document include progress made during FY 72 for those FY 73 projects which were active in FY 72. Where a project was terminated at the end of FY 72 its description is included in the present document with appropriate notation.

In water pollution the situation is much more complex since there are many more pollutants in more types of water that will be subject to control under the Federal Water Pollution Control of 1972. When a pollutant is of concern in the discharge permit program, water quality standards, the toxic pollutant list and in the specimen bank

program, the state of the measurement art is scrutinized at NBS and the need for development assessed.

TN830. NBS cryogenic thermometry and the proposed cryogenic extension of the IPTS, G. Cataland, R. P. Hudson, B. W. Mangum, H. Marshak, H. H. Plumb, J. F. Schooley, R. J. Soulen, Jr., and D. B. Utton, Nat. Bur. Stand. (U.S.), Tech. Note 830, 32 pages (May 1974) SD Catalog No. C13.46:830, 65 cents.

Key words: acoustical thermometry; γ -ray anisotropy thermometry; noise thermometry; nuclear magnetic resonance; nuclear quadrupole resonance; paramagnetism; superconductivity; temperature.

This article outlines a comprehensive and long-term program being carried out by NBS scientists of the Cryogenic Physics and Temperature Sections. The goals of the program are the extension of IPTS 68 below 13.81 K and the development of devices which make practical realizations of that scale convenient and reliable. We propose to contribute to international adoption of a thermodynamically accurate scale below 13.81 K by analyzing the results of three thermometers: the NBS Acoustical Thermometer (already in operation for several years), noise thermometry using the Josephson effect (recently developed), and γ -ray anisotropy thermometry (recently studied in detail at NBS). Such a temperature scale will most likely be disseminated by the use of certain superconductors as thermometric reference points. Practical interpolation devices will be based on the principles of nuclear and electronic paramagnetism, nuclear quadrupole resonance, and nuclear magnetic resonance. Details of operation, measurement schemes and experimental progress made to date are included in nine appendices.

TN831. Introduction to liquid flow metering and calibration of liquid flowmeters, L. O. Olsen, Nat. Bur. Stand. (U.S.), Tech. Note 831, 60 pages (June 1974) SD Catalog No. C13.46:831, 95 cents.

Key words: calibration; liquid flow; liquid flowmeters; metering.

These notes are intended to serve as an instruction manual for technicians and engineers engaged in metering liquids and calibrating liquid flowmeters. It is a condensed review of the properties of liquids and the mathematical relations required in this work. References to more complete sources of properties of liquids, theoretical relations and instructions for metering liquids are included. Separate chapters discuss liquids and their properties as they affect flow, the theory of incompressible flow of liquids and the measurements required in the metering of liquids. One chapter describes several different apparatus and their use in the calibration of liquid flowmeters. The last chapter contains brief descriptions of the many types of flowmeters such as differential pressure, positive displacement, electromagnetic and ultrasonic. It also includes a discussion of the physical principles involved in their design and use.

TN834. Information handling needs within the U.S. Patent Office, S. Jeffery, Nat. Bur. Stand. (U.S.), Tech. Note 834, 17 pages (June 1974) SD Catalog No. C13.46:834, 55 cents.

Key words: administrative operations; data handling; data storage and retrieval; information handling technology; information processing; intellectual process; patent examination; Patent Office; patent storage; production statistics.

This paper examines aspects of the Patent Office's needs that make it different from other existing information retrieval systems. The paper then reviews current technology and assesses its ability to provide effective and economical tools to aid the Patent Office.

TN836. Detector actuated automatic sprinkler systems—a preliminary evaluation, R. L. P. Custer, Nat. Bur. Stand. (U.S.), Tech. Note 836, 27 pages (July 1974) SD Catalog No. C13.46:836, 65 cents.

Key words: bedding fires; design criteria; detector actuated automatic sprinklers; detectors; levels of protection; life safety; sprinklers.

An investigation was conducted to evaluate the capabilities of a detector actuated automatic sprinkler system to protect individuals who are intimately associated with the first materials ignited such as bedding materials. Tests were conducted in a simulated nursing home bedroom. System response was evaluated for both smoldering and open flaming ignition sources. It was determined that barring electrical or mechanical failure the system could be nearly 100 percent effective with smoldering fires. The effectiveness with open flaming fires was difficult to evaluate. Although these fires were extinguished with minimum damage in times as short as 36 seconds the possible effects of flammable blankets and sleepwear were not tested. It was estimated that perhaps one third of the potential victims of open flaming fires might be saved. Although these tests were limited in scope, some tentative design criteria for detector actuated sprinkler systems are presented and possible alternatives offered.

NBSIR 73-211. LEAA police equipment survey of 1972.

Volume II: Communications equipment and supplies, S. Mumford, P. Klaus, E. Bunten, and R. Cunitz, 175 pages (Final July 1971-July 1973). Order from NTIS as COM 74-10950.

Key words: communications; mobile radio; police; police equipment; portable radio; standards.

The report outlines the methodology of and summarizes a portion of the data from the LEAA Police Equipment Survey of 1972. One of a series of seven reports resulting from this nationwide mail survey of a stratified random sample of police departments, the present report summarizes the answers of 428 police departments concerning their communications equipment and supplies: use of mobile radios and portable radios; power supplies for portable radios; scramblers; portable/mobile radios; helmets with built-in communications; needs for standards and problems associated with communications equipment and supplies. The data are presented by all responding departments and by seven department types.

NBSIR 73-212. LEAA police equipment survey of 1972.

Volume III: Sirens and emergency warning lights, P. Klaus and E. Bunten, 141 pages (July 1971-Sept. 1973). Order from NTIS as COM 74-11009.

Key words: emergency warning lights; police equipment; sirens; standards.

The report outlines the methodology of and summarizes a portion of the data from the LEAA Police Equipment Survey of 1972. One of a series of seven reports resulting from this nationwide mail survey of a stratified random sample of police departments, the present report summarizes the answers of 437 police departments concerning their sirens and emergency warning lights: use of sirens and lights; experience with most commonly used electronic sirens, electromechanical sirens, and emergency warning lights; purchasing, repair and replacement of this equipment; and training of officers in use of this equipment. The data are presented by all responding departments and by seven department types.

NBSIR 73-215. LEAA police equipment survey of 1972.

Volume VI: Body armor and confiscated weapons, G. B. Hare, P. A. Klaus, and E. D. Bunten, 104 pages (Oct. 1973). Order from NTIS as COM 74-11010.

Key words: ballistic protective equipment; body armor; confiscated weapons; police; standards.

The report outlines the methodology of and summarizes a portion of the data from the LEAA Police Equipment Survey of 1972. One of a series of seven reports resulting from this nationwide mail survey of a stratified random sample of police departments, the present report summarizes the answers of 440 police departments concerning body

armor and confiscated weapons: preference for hidden or visible body armor; use of other ballistic protective equipment; routine operations where body armor would be most useful; current problems and failures with present equipment; needs for standards for the testing and assessment of penetration capabilities of body armor; disposition of confiscated weapons. The data are presented by all responding departments and by seven department types.

NBSIR 73-216. LEAA police equipment survey of 1972.

Volume VII: Patrolcars, E. D. Bunten and P. A. Klaus, 115 pages (July 1973). Order from NTIS as COM 74-11011.

Key words: patrolcar; police; police vehicles; standards.

The report outlines the methodology of and summarizes a portion of the data from the LEAA Police Equipment Survey of 1972. One of a series of seven reports resulting from this nationwide mail survey of a stratified random sample of police departments, the present report summarizes the answers of 449 police departments concerning their patrolcars: purchasing practices; types of options and accessories usually selected; types of equipment stored in the patrolcar; typical patterns of use; and needs for standards for systems or aspects of patrolcars. The data are presented by all responding departments and by seven department types.

NBSIR 73-246. Fire research publications, 1969-1972, N. H.

Jason, R. G. Katz, and P. A. Powell, 14 pages (July 1973). Order from NTIS as COM 74-10989.

Key words: bibliographies; construction materials; fire departments; Fire Research and Safety Act; fire tests; flammability tests; flammable fabrics; Flammable Fabrics Act; protective clothing.

A list of publications is provided representing the papers and journal articles prepared by Fire Technology Division and by Building Fires and Safety Section of the Center for Building Technology personnel and by external laboratories under contract to the Fire Technology Division from 1969 through 1972.

NBSIR 73-254. A mercury vapor generation and dilution

system, E. P. Scheide, R. Alvarez, B. Greifer, E. E. Hughes, and J. K. Taylor, 12 pages (Oct. 1973). Order from NTIS as COM 74-10987.

Key words: atomic absorption; gas generation system; mercury; occupational safety.

This report describes a system capable of producing well-defined test atmospheres of mercury in air or other diluent gas at concentrations between 0.005 and 0.5 $\mu\text{g}/\text{l}$ and an analytical system for the analysis of these gas mixtures. Various parameters that affect the generator and analytical system and their interactions are discussed. This system provides a means of calibration of the various analytical systems for mercury now in use. The analytical unit of the system can also be used for the determination of mercury in industrial atmospheres by collecting the mercury on a silver wool collector, and then desorbing it by heat into a flameless atomic absorption spectrometer.

NBSIR 73-290. Development of a dynamic pressure calibration

technique. A progress report, P. S. Lederer, 4 pages (Oct. 15, 1973). Order from NTIS as COM 74-10974.

Key words: dynamic calibration; pressure; transducer.

Plans are described for experimental investigation of a hydraulic sinusoidal pressure calibrator as a basis for development of dynamic pressure calibration techniques for frequencies up to 2000 Hz.

NBSIR 73-329. Theory of adjoint reciprocity for electroacoustic transducers, A. D. Yaghjian, 78 pages (Feb. 1974).

Order from NTIS as COM 74-10608.

Key words: adjoint operators; electroacoustic transducers; reciprocity; scattering matrices.

Analytical techniques for the measurement of the external characteristics of electroacoustic transducers have been developed by D. M. Kerns using a plane-wave scattering-matrix (PWSM) formulation. Foldy and Primakoff, in their classic papers on linear electroacoustic transducers, utilize a spatial impedance-matrix (SIM) formulation. Both formulations involve a continuous, linear "matrix" transformation in which reciprocity is defined as a relationship between elements of the matrix.

The first portion of the present report demonstrates that a transducer satisfying the "SIM relations" also satisfies the "PWSM equations" (but that the converse theorem does not hold), and that the alternate expressions of reciprocity are equivalent for transducers that obey both formulations.

The second portion of the report examines the equations which characterize the internal behavior of a large class of electroacoustic transducers. A linear operator approach is employed to develop a generalized reciprocity lemma which is used to establish adjoint reciprocity relations between the fields of a given transducer and its adjoint transducers. The linear operator approach facilitates the identification of self-adjoint (reciprocal or antireciprocal) transducers, and the adjoint reciprocity relations have utility in the extrapolation techniques of the PWSM formulation. An adjoint "reciprocity theorem" and "principle of reciprocity" are derived from the generalized reciprocity relations. Finally it is shown that the total power inputs for the adjoint transducers belong to the same "value class" as the original transducer.

NBSIR 73-330. Frequency domain measurement of baseband instrumentation, N. S. Nahman and R. M. Jickling, 68 pages (July 1973). Order from NTIS as COM 74-10609.

Key words: bandwidth; diode; impedance; sampling; slotted line.

Microwave measurement techniques were developed for characterizing the wideband feed-through sampling heads associated with time domain sampling oscilloscopes and frequency domain network analyzers. Such characterization or modeling is necessary for the removal of the oscilloscope distortion from the observed waveform to yield the input waveform; also, it is useful for extrapolation in estimating oscilloscope performance at higher frequencies.

The techniques were developed through measurements on a sampling oscilloscope having a 28 picosecond transition time (10 to 90%) and a 12.4 GHz baseband bandwidth. The major results of the work are the development of voltage and impedance measurement techniques which provide the means for determining the sampling-head equivalent circuit parameters. The techniques are based upon slotted-line measurements and are not inherently limited to any particular frequency range. Experimental results were obtained for the sampling-head input impedance over the 7-12 GHz frequency range, and for the 10 GHz sampling loop impedance (vs. sampling-diode bias current).

NBSIR 73-341. Test results for the Mooring Line Data Line, D. A. Ellerbruch, 46 pages (Oct. 1973). Order from NTIS as COM 74-10885.

Key words: characteristic impedance; coupler; current; impedance, input impedance; Mooring Line Data Line; propagation characteristics; transmission line.

Results obtained from the Mooring-Line-Data-Line (MLDL) measurements program are presented. Frequency and time domain measurements are made to determine characteristic impedance, input impedance, current, and propagation parameters. Most of the measurements were made with an MLDL deployed specifically for this program; however, some were made on an MLDL deployed buoy.

NBSIR 73-344. Heat transfer and mixing of slush hydrogen, C. F. Sindt and P. R. Ludtke, 40 pages (Nov. 1973). Order from NTIS as COM 74-10749.

Key words: heat transfer; liquid hydrogen; mixing; mixing power; paddle mixers; slush hydrogen; turbine mixers.

Heat transfer to slush hydrogen and mixing were investigated in a 1 m³ cylindrical vessel. The effects of heat transfer rates on thermal stratification and on self-pressurization were measured. Temperature profiles in thermal stratification were found to be more dependent on slush level and slush settling rates than on liquid level. Solids in the slush appear to be involved in the heat transfer mechanism as slush level affected the amount of warm liquid reaching the top of the dewar and therefore affected the self-pressurization rates.

Mixing effectiveness and power requirements to mix slush hydrogen were determined for two configurations of turbine mixers and one paddle mixer. Mixing power requirements were found to be sensitive to the mixer location and configuration.

NBSIR 73-347. Active and passive mode locking of continuously operating rhodamine 6G dye lasers, A. Scavennec and N. S. Nahman, 54 pages (Feb. 1974). Order from NTIS as COM 74-10674.

Key words: DODCI; dye laser; laser; mode-lock; picosecond; rhodamine 6G.

Using confined and unconfined fluid flow dye cells with suitable mode locking methods continuously operating rhodamine 6G dye lasers have been built to produce narrow pulses (less than 40 ps) at about a 140 MHz pulse repetition rate. For active (acoustic) amplitude modulation mode locking methods optical pulses were obtained having about a 32 ps pulse width (FWHM). For passive mode locking methods optical pulses of ≤ 35 ps pulse width (FWHM) were obtained.

A three mirror cavity was used for the active mode locking studies while three and five mirror cavities were used in the passive studies. The three mirror passive mode locked laser employed a single dye cell containing both the rhodamine 6G (gain) and DODCI (loss) solutes in a single solution having glycol as the solvent. The active and passive mode locked carrier wavelengths were about 5900 Å and 5800 Å, respectively.

NBSIR 73-404. Mass transport and physical properties of large crystals of calcium apatites: Studies of Ca(OH)₂ crystals for use in electrolytic conversion of calcium fluorapatite crystals to calcium hydroxyapatite, A. D. Franklin and K. F. Young, 37 pages (Sept. 1, 1972-Aug. 31, 1973). Order from NTIS as PB 203952.

Key words: ac impedance; calcium apatites; calcium hydroxide; crystal growth; electrolysis; interfacial polarization; ionic conduction; mass transport.

In order to convert single crystals of calcium fluorapatite to calcium hydroxyapatite, an electrolytic cell technique will be explored. To utilize such a technique, the cathode compartment must consist of a source of hydroxyl ions and a barrier to the flow of all others. Examination of the literature on metallic hydroxides suggests that a suitable cathode might be composed of an oriented Me(OH)₂ crystal, where Me is Mg, Ca, Sr, or Ba, backed up by a Pt electrode in an atmosphere containing H₂O and O₂. Ca(OH)₂ crystals have been grown from aqueous solution, and Pt electrodes evaporated onto them. An apparatus has been built to study their ac admittance as a function of temperature and atmosphere, and measurements begun. A computer program for handling the complex admittance data has been devised and tested.

NBSIR 73-407. Report on a pre-test of a survey plan for estimating incidence of lead based paint, L. S. Joel and H. W. Berger, 86 pages (Dec. 1973). Order from NTIS as COM 74-11078.

Key words: lead; lead paint poisoning; paints; poisoning; retail inventory; statistics; survey.

Lead in paint has been indicted as a major cause of lead poisoning of children. Federal regulations have been established to limit the amount of lead which may be added to paints that are intended for residential use. The intent of such a limitation is to curtail the incidence of present and future lead based paint poisoning of children.

This report presents the results of a "pre-test" for a nationwide survey plan that would be used to determine the availability, to the public, of paints that may contain lead compounds in hazardous quantities. Statistical summaries of the chemical analysis of 250 paints purchased by random selection at five retail outlets, are presented along with comments regarding the possible implications of those results. Recommendations are made about survey action beyond the pre-test described herein.

NBSIR 73-420. Survey on metallic implant materials, J. R. Parsons and A. W. Ruff, 55 pages (Dec. 1973). Order from NTIS as COM 74-11092.

Key words: biomaterials; corrosion; implant materials; mechanical properties; metals.

The application of metallic materials as orthopedic implants in the human body is reviewed, concentrating on materials presently in clinical use and undergoing laboratory evaluation for possible future use. The criteria considered explicitly are tissue compatibility, mechanical properties, corrosion resistance, and toxicity. The three principal metallic implant materials, stainless steel, cobalt alloys, and titanium, are discussed in detail. Wherever possible, comparisons are made between the materials in terms of the intended application.

NBSIR 74-426. Survey plans and data collection and analysis methodologies: Results of a pre-survey for the magnitude and extent of the lead based paint hazard in housing, W. Hall, T. Ayers, and D. Doxey, 110 pages (Jan. 1974). Order from NTIS as COM-11074.

Key words: housing; housing survey; lead; lead hazard; lead paint; lead poisoning; survey; urban health problems.

A pilot survey of housing in Washington, D.C. was carried out in order to develop and test methodologies, data collection procedures and formats that will be used in subsequent full scale surveys of cities to determine the magnitude and extent of the lead-based paint hazard in housing.

On site measurements of lead contents of interior and exterior surfaces were made (with portable x-ray fluorescence lead detectors, hereafter referred to as XRF's) on 115 dwelling units which were randomly selected from a Washington, D.C. city directory.

This report describes the procedures for identifying the survey sample, drawing the sample, and carrying out the survey. Computer programs for data handling and analysis are included and a brief summary of the data obtained from the pilot survey is presented.

NBSIR 74-438. Pilot demonstration of lead based paint hazard elimination methods, T. H. Boone, T. R. Ray, W. G. Street, 26 pages (Dec. 1973). Order from NTIS as COM 74-10980.

Key words: cost analysis; housing; lead based paint; lead poisoning; surface preparation; surface refinishing; water wash paint removal.

This report describes the removal of lead base paint from exterior surfaces of a single family attached house using alkaline/solvent thixotropic liquid paint removers followed by a high-pressure/low-volume water spray.

The extent of the reduction of the lead based paint hazard, the cost of the process and the observed problems and merits of this water wash paint removal system are presented.

NBSIR 74-439. Preparation of reference materials for stationary source emission analysis: Beryllium, T. C. Rains, C. D. Olson, R. A. Velapoldi, S. A. Wicks, O. Menis, and J. K. Taylor, 12 pages (Mar. 1974). Order from NTIS as COM 74-10985.

Key words: air pollution; atomic absorption spectrometry; beryllium; chemical analysis; fluorimetric analysis.

Techniques are described for the preparation of reference materials useful for evaluating the accuracy and precision of analytical methods for measurement of beryllium emissions from stationary sources. These reference materials consist of membrane filters upon which are deposited microgram quantities of high-fired beryllium oxide and ampoules containing soluble beryllium and suspended beryllium oxide. Methods for measurement of the beryllium content of such materials by atomic absorption spectrometry and by spectrofluorimetry are described.

NBSIR 74-443. Weight cleaning procedures, H. E. Almer, 9 pages (Nov. 1973). Order from NTIS as COM 74-11003.

Key words: cleaning; standards; steam generator; storage; temperature equilibrium; weights.

Accurate and meaningful results in the calibration of weights depend on clean weights. This paper describes a method of cleaning weights.

NBSIR 74-454. The equivalence of gravimetric and volumetric test measure calibration, R. M. Schoonover, 16 pages (Feb. 1974). Order from NTIS as COM 47-10988.

Key words: check standard; closure; gravimetric calibration; standard deviation; test measure; volumetric transfer calibration.

This report discusses the statistical importance of observed differences between gravimetric and volume transfer calibrations of volumetric test measures. The data presented are results from the present NBS calibration program and conclusively show there are negligible differences between the two methods of calibration.

NBSIR 74-458. Laser damage in materials, A. Feldman, D. Horowitz, and R. M. Waxler, 16 pages (Mar. 1974). Order from NTIS as AD 776-337.

Key words: absorption coefficient; damage threshold; electrostriction; inclusion damage; intrinsic damage; Kerr effect; laser damage; laser glasses; laser rod materials; modulator crystals; nonlinear index of refraction; optical glasses; polarizer materials; self-focusing.

This report summarizes the study of damage and self-focusing in materials used in Q-switch solid-state laser systems. In borosilicate crown glass, fused silica, dense flint glass, and yttrium aluminum garnet, self-focusing appears to be the main cause of damage. An analysis of damage threshold measurements with linearly polarized radiation suggests that the Kerr effect is the dominant self-focusing mechanism with a significant contribution to self-focusing from the thermal effect. The electrostrictive effect is negligible. The damage threshold in Nd:doped laser glasses appears to be intrinsic. In all the above materials, the damage threshold for circular polarization is greater than the damage threshold for linear polarization. In lithium niobate, calcite, potassium dihydrogen phosphate, and deuterated dihydrogen phosphate, damage at the lowest levels is caused by inclusions. Bulk and surface damage thresholds in Nd:doped thoria:yttrium oxide ceramic are obtained relative to bulk damage thresholds in several optical materials. Relationships under different geometric boundary conditions are also derived for solid materials between the stress-optic coefficients and the electrostrictive coefficients.

NBSIR 74-466. Management of data elements in information processing, H. E. McEwen, Ed., (Proceedings of a Symposium Sponsored by the American National Standards Institute and by

The National Bureau of Standards, held at NBS, Gaithersburg, Maryland, Jan. 24-25, 1974), 490 pages (Apr. 1974). Order from NTIS as COM 74-10700.

Key words: American National Standards; American National Standards Institute; data; data base systems; data elements; data management; data processing; Federal Information Processing Standards; information interchange; information processing; information systems.

Recent technological advances in computers and communications make possible the integration of data systems and the exchange of data among them on an expanding scale. However, the full effect of these advances cannot be realized unless the need for uniform understanding of the common information (data elements) and their expression in data systems is recognized and a means provided to effectively manage this information. The increasing interrelationships among the data systems of Federal, State, and local governments, and with industry and the public add emphasis and dimension to the need for the improved management of data elements in information processing.

These Proceedings are for the first Symposium on the Management of Data Elements in Information Processing held at the National Bureau of Standards on 1974 January 24 and 25. Over 400 representatives of Federal and State governments, industry and universities from 30 states, from Canada, and Sweden were in attendance. Thirty-four speakers discussed data element management in the fields of health care, water resources, state government information systems, transportation, libraries, market research, manufacturing, banking, information retrieval systems, military systems, computer programming and software systems, and motor vehicle registration.

NBSIR 74-470. Interaction of plasma proteins with surfaces, C. A. Fenstermaker, W. H. Grant, B. W. Morrissey, L. E. Smith, and R. R. Stromberg, 83 pages (Mar. 22, 1974). Order from NTIS as COM 74-10984.

Key words: adsorption; blood protein; bound fraction; ellipsometry; polymer adsorption; protein adsorption.

The interaction of blood proteins with surfaces has been investigated with principal attention focused on those proteins that are either major constituents of blood plasma or are implicated as being important in the clotting process. Emphasis has been placed on molecular conformational changes occurring upon the interaction of such proteins with surfaces. The extension of adsorbed molecules of fibrinogen, albumin, and prothrombin on a number of selected materials was studied by ellipsometry. The results indicate a dependence of conformation on surface energy. Measurements of the bound fraction (number of carbonyl surface attachments) of these adsorbed blood proteins on a silica surface showed that approximately ten percent of the carbonyl groups were attached to the surface for prothrombin and serum albumin at all values of surface population for the solution concentrations studied. Competitive interactions of prothrombin and fibrinogen during the process of adsorption, displacement, and desorption have been measured and rates of adsorption of albumin were measured on chrome and silica surfaces.

NBSIR 74-471. Life cycle costing of police patrol cars: Summary report, R. T. Ruegg, 23 pages (Mar. 1974). Order from NTIS as COM 74-10981.

Key words: fleet management; life cycle costing; patrol cars; police fleets; vehicle leasing; vehicle management.

There are many different choices to be made with respect to police vehicle acquisition, utilization, maintenance, and disposition. Cost comparisons among the different alternatives are an important element in the choices to be made. To make valid cost comparisons, it is necessary to employ the techniques of life-cycle costing. This means the inclusion of all relevant costs and the conversion of costs to an

equivalent basis to take into account differences in the timing of expenditures.

This report briefly summarizes the results of a larger study which compares the life cycle costs of some of the alternatives associated with police fleet management. The full report from which this report is derived is entitled *Life Cycle Costing: Efficiency in Vehicle Acquisition, Operation, and Disposition*.

The focus of the study is on police patrol cars, but the methods are applicable to other types of vehicles. Specific topics addressed by the larger study and summarized here are the cost effects of purchasing different sizes of patrol cars and different optional equipment, the advantages and disadvantages of direct ownership of vehicles as compared with leasing, the costs of contracting out maintenance as compared with self-maintenance of vehicles, the cost effects of alternative utilization practices, the optimal timing of vehicle replacement, and the comparative efficiency of different methods of vehicle disposition.

NBSIR 74-474. Metallurgical analysis of wear particles and wearing surfaces, A. W. Ruff, 59 pages (Apr. 1974). Order from NTIS as AD 778340.

Key words: bearings; electron diffraction; electron microscopy; gears; lubrication; particles; wear.

Results are presented from a program involved in characterizing the wear particles and surface degradation produced by wear in bearing and gear tests in which the effects of several variables on failure of the wearing surfaces has been examined. The information obtained has been correlated with the results of allied studies conducted by others in an attempt to develop an understanding of the processes producing wear and degradation of metal surfaces in sliding, rubbing, rolling, and/or rotating contact and the effects of lubricants, lubricant additives, bearing materials, etc. on these processes. The characterization of the wear particles and wearing surfaces should aid in the establishment of the interrelationships between wear particle shape, size, size distribution, chemical compositions, metallurgical structure, and surface damage prior to failure.

NBSIR 74-487. Proposed revision of American National Standard COBOL, R. E. Rountree, Jr., Ed., 544 pages (Jan. 1974). Order from NTIS as COM 74-10886.

Key words: COBOL; data processing; Federal Information Processing Standard; information interchange; information processing; programming language; software.

This document is for review purpose only in anticipation of its becoming an American National Standard and subsequent adoption as a Federal Information Processing Standard. The American National Standard COBOL defines the elements of the COBOL programming language and the rules for their use. The standard is used by implementors as the reference authority in developing compilers and by users for writing programs in COBOL. The primary purpose of the standard is to promote a high degree of interchangeability of programs for use on a variety of automatic data processing systems.

This column lists all outside publications by the NBS staff, as soon after issuance as practical. For completeness, earlier references not previously reported may be included from time to time.

Abrams, M. D., Lindamood, G. E., Pyke, T. N., Jr., Measuring and modelling man-computer interaction, Proc. 1st Annual SIGME Symp. on Measurement and Evaluation, Palo Alto, Calif., Feb. 26-28, 1973, pp. 136-142 (Feb. 1973).

Key words: dialogue; interaction; man-computer; measure; model; monitor.

The Dialogue Monitor has been developed as a tool for the measurement of computer service. The objectives of such measurement are defined. A set of models and measures is developed. Operation of

the Dialogue Monitor and analysis of the data obtained are briefly discussed.

Abrams, M. D., Rosenthal, R., **On the passing of MOBIDIC-B**, *Computer* **6**, No. 3, 10-18 (Mar. 1973).

Key words: computer; MOBIDIC-B; teleprocessing system.

The history, design, hardware configuration, instruction set and operating system of the MOBIDIC-B used in the National Bureau of Standards (NBS) computer research facility is described using conventional methods and Bell and Newell's PMS and ISP notations. As modified at NBS, MOBIDIC-B is the nucleus of an experimental remote access computer system, with variable partition multiprogramming capability, that supports conversational terminal usage.

Allan, D. W., Gray, J. E., Machlan, H. E., **The National Bureau of Standards atomic time scale: Generation, dissemination, precision, and accuracy**, (Proc. Conf. Electromagnetic Measurement, Boulder, Colo., June 26-29, 1972), *1972 CPEM Digest*, p. 165 (1972).

Key words: atomic clock; cesium clock; coordinate time; Flicker noise; frequency standard; time dissemination; time scale.

The atomic time scale at the National Bureau of Standards, AT(NBS), depends upon an ensemble of continuously operating cesium clocks calibrated occasionally by the NBS primary frequency standard. The data of interclock comparisons and frequency calibrations are statistically processed to provide near optimum time stability and frequency accuracy. Each clock is represented by a simple mathematical model of its noise spectrum, with parameters determined by the behavior of that clock. These noise parameters are used in a nearly optimum procedure for periodically recalibrating the frequency of each clock and for combining the clock readings to produce AT(NBS). The long-term fractional frequency stability of AT(NBS) is shown to be a few parts in 10^{14} , and the accuracy is inferred to be 1 part in 10^{12} .

A small coordinate rate is added to the rate of AT(NBS) to generate UTC(NBS); this small addition is for the purpose of maintaining synchronization within a few microseconds of other international timing centers. UTC(NBS) is readily and operationally available over a large part of the world via WWV, WWVH, WWVB, and telephone; also via some time transfer systems, e.g., Loran-C and the TV line-10 system; and also experimentally via satellite and WWVL. The precision and accuracy of these dissemination systems will be discussed.

Bagchi, A., Gomer, R., Penn, D. R., **The field emission total energy distribution in the presence of adsorbates**, *Surface Sci.* **41**, 555-558 (1974).

Key words: adsorbed molecules on metal surfaces; Anderson Model; energy distribution of field emitted electrons; field emission theory; metal surface; overcomplete states.

The total energy distribution (TED) of field-emitted electrons from an adsorbate-covered metal surface is studied within the framework of the Anderson Hamiltonian, but taking overcompleteness of states into account. The correct asymptotic behavior of the adsorbate wavefunction, postulated in the previous work, is now established, and a numerical correction factor (~ 15) to the adsorbate induced current density is obtained.

Bass, A. M., Laufer, A. H., **Extinction coefficients of azomethane and dimethyl mercury in the near ultra-violet**, *J. Photochem. Short Communication* **2**, 465-470 (1973/74).

Key words: absorption spectrum; azomethane; dimethyl mercury; extinction coefficient; ultraviolet.

The absorption spectra and extinction coefficients of azomethane and dimethyl mercury have been measured between 170-360 nm. In each case the absorption consists of an intense broad band upon

which is superimposed a vibrational sequence of a single frequency. For azomethane the vibrational spacing is about 470 cm^{-1} ; for dimethyl mercury it is about 347 cm^{-1} . The vibrational frequencies of the upper states have been tentatively assigned.

Beatty, R. W., **Methods for automatically measuring network parameters**, *Microwave J.* **17**, No. 4, 45-49, 63 (Apr. 1974).

Key words: automatic measurements; automatic network analyzer; complex reflection coefficients; complex transmission coefficients; computer controlled measurement systems; computer-operated transmission measurements; envelope delay; group delay; network parameters.

A survey is presented of techniques, from 1934 to the present time, used in the automatic measurement of network parameters. Some of the computer-controlled measurement systems developed in the U.S.A. since 1968 are described. The direction that future developments may take is forecast. Numerous references are given.

Beatty, R. W., **2-Port $\lambda_c/4$ waveguide standard of voltage standing-wave ratio**, *Electronics Letters* **9**, No. 2, 24-26 (Jan. 25, 1973).

Key words: coaxial line; impedance standard; reflection coefficient standard; VSWR standard; waveguide.

A new calculable standard of voltage-reflection coefficient and voltage standing-wave ratio consists of a quarter-guide-wavelength section of waveguide having cross-sectional dimensions different from those of the waveguide system into which it is inserted. Design equations are given for waveguide of rectangular and coaxial cross-sections.

Becker, D. A., LaFleur, P. D., **Characterization of a nuclear reactor for neutron activation analysis**, (Proc. Int. Conf. on Modern Trends in Activation Analysis, Saclay, France, Oct. 1972), *J. Radioanal. Chem.* **19**, 149-157 (1974).

Key words: cadmium ratio; fast neutron flux; neutron activation analysis; sample pressure; thermal neutron flux; threshold foil.

Evaluation of some of the neutron activation analysis irradiation characteristics for the NBS Nuclear Reactor (NBSR) are reported, along with a description of a measurement technique developed. The characteristics discussed here are the thermal (sub-cadmium) neutron flux determination, neutron energy distribution measurements using cadmium ratios and threshold foil detectors, and the determination of excess sample pressures generated during irradiation.

Bennett, L. H., Swartzendruber, L. J., Watson, R. E., **Critical temperatures in Fe-doped copper-rich Cu-Ni alloys**, (Proc. 17th AIP Conf. on Magnetism and Magnetic Materials, Chicago, Ill., Nov. 15-18, 1971), Chapter in *Magnetism and Magnetic Materials*, C. D. Graham, Jr., and J. J. Rhyne, Eds., No. 5, pp. 1190-1194 (June 1972).

Key words: alloys; copper; critical temperatures; iron; magnetism; Mössbauer effect; nickel.

Systematics of magnetic ordering as a function of Fe and Ni content have been investigated by use of the Mössbauer effect in Cu-based alloys with up to a few percent Fe and up to 40 percent Ni. The halfwidth of the magnetic transition is $\sim 1 \text{ K}$ in all the "weak" ferromagnets (i.e., when the critical temperature, $T_c \leq 10 \text{ K}$), and is a similar, or smaller, fraction of T_c for the strong ferromagnets. T_c is sharply defined for all compositions, despite the distribution of hyperfine fields and magnetic moments existing in these alloys. For any Ni concentration, T_c increases with increasing Fe. As a function of Ni, a minimum in T_c occurs near 30 percent Ni. These results indicate that the long-range conduction electron interaction between Fe atoms in Cu is reduced by Ni addition, with strong short-range in-

teractions becoming more important for ferromagnetism at higher Ni concentrations.

Berger, M. J., Seltzer, S. M., Maeda, K., **Some new results on electron transport in the atmosphere**, *J. Atmos. Terrest. Phys.* **36**, 591-617 (1974).

Key words: atmosphere; backscattering; bremsstrahlung; electron; energy deposition; flux spectrum; Monte Carlo calculations.

The penetration, diffusion and slowing down of electrons in a semi-infinite air medium has been studied by the Monte Carlo method. The results are applicable in the atmosphere at altitudes up to ~ 300 km. Most of the results pertain to monoenergetic electron beams, with energies between 2 keV and 2 MeV, injected into the atmosphere at a height of 300 km, either vertically downwards or with a pitch-angle distribution isotropic over the downward hemisphere. Some results were also obtained for various initial pitch angles between 0 and 90°. Information has been generated concerning the following topics: (a) the backscattering of electrons from the atmosphere, expressed in terms of backscattering coefficients, angular distributions and energy spectra; (b) the altitude dependence of energy deposition by electrons and by secondary bremsstrahlung, for incident electron beams that are monoenergetic or have exponential spectra with e-folding energies between 5 and 200 keV; (c) the evolution of electron flux spectra as function of the atmospheric depth, for incident beam energies between 2 and 20 keV.

Blanc, R., **Minicomputer trends and applications—1973**, *Computer* **6**, No. 6, 28-29 (June 1973).

Key words: minicomputer applications; minicomputer maintenance; minicomputer peripherals; minicomputer software.

The present trends in the growth and utilization of minicomputers as presented and discussed at a recent Symposium cosponsored by NBS are reviewed. In addition, problems are identified in the areas of minicomputer software, peripherals, and maintenance.

Bonnelle, C., Karnatak, R. C., Sugar, J., **Photoabsorption in the vicinity of 3d absorption edges of La, La₂O₃, Ce, and CeO₂**, *Phys. Rev. A* **9**, No. 5, 1920-1923 (May 1974).

Key words: absorption; Ce; La; x-rays.

Observations of photoabsorption in La, La₂O₃, Ce, and CeO₂, in the vicinity of the 3d edges are given. Calculations of relative absorption intensities for Ce are shown to correspond well with the experimental data.

Brauer, G. M., **Adhesives and composites in dentistry—present and future**, *Proc. Symp. Dental Biomaterials-Research Priorities, Des Plaines, Ill., Aug. 1973*, DHEW Publ. No. (NIH) 74-548, pp. 63-99 (Department of Health, Education, and Welfare, Bethesda, Md., 1974).

Key words: adhesion to tooth structure; adhesives; dental composites; dental restorative materials.

Probably no subject matter affects as many facets of dental biomaterials as that of the modification of and adhesion to tissues. The many techniques that are available to gain valuable information of the structure of tooth surfaces and methods to vary their characteristics are reviewed. Materials and procedures have become available that exhibit clinically significant adhesion to enamel. Bonding to collagenous surfaces such as dentin under conditions encountered in the oral cavity appears to be a realizable goal. Composite restoratives possess unusually good esthetics and their overall properties are considerably better than those of unfilled resins. Investigations of reactions at the interfaces and optimization of the ingredients, as well as the rapidly expanding wealth of experience with these materials, should lead to further improvements. For many composite restorations a nonadhesive protective liner is needed. This requirement

negates the use of a tooth-composite coupling agent unless this agent protects the pulp from the noxious effects of the composite. Nonetheless, the evidence today suggests that continuing progress will lead to clinically acceptable adhesive restoratives that will substantially improve the quality of dental services.

Brennan, J. A., **LNG measurement projects at NBS**, *Proc. 49th Int. School of Hydrocarbon Measurement, Norman, Okla., Apr. 16-18, 1974*, pp. 464-465 (1974).

Key words: description; LNG; projects.

This paper presents, in summary form, the projects at the Cryogenics Division of NBS involved with LNG or LNG related measurements. A brief description of each project is given along with identification of the sponsoring agency.

Broadhurst, M. G., Malmberg, C. G., Mopsik, F. I., Harris, W. P., **Piezo- and pyroelectricity in polymer electrets**, (Proc. Conf. on Electrets, Charge Storage and Transport in Dielectrics, Miami Beach, Fla., Oct. 8-13, 1972), Chapter in *Electrets, Charge Storage and Transport in Dielectrics*, M. M. Perlman, Ed., pp. 492-504 (Electrochemical Society, New York, N.Y., 1973).

Key words: dipoles; electret; glass transition; polymer; pyroelectric.

A model for a polymer electret, based on an elastically isotropic solid with orientationally frozen molecular dipoles, was developed and tested experimentally. This electret is shown to be both piezoelectric and pyroelectric. The polarization is shown to change with mechanically and thermally induced strains in the polarization direction. The currents generated by the electret will be proportional to the strain rate and, for thin contact electrodes and uniform strains, unaffected by the presence of real charges. Poly (vinyl chloride) films were poled at 80 °C, just above their glass transition temperature. The pressure- and temperature-induced short-circuit currents in the polarization direction equalled 0.15(pA/cm²)/(bar/min) and 2.2 (pA/cm²)/(K/min) respectively for a specimen poled at 320 kV/cm. These currents were 1) reversible and proportional to the rate of temperature or pressure change, 2) proportional to poling voltage up to 320 kV/cm, 3) in the direction corresponding to increasing polarization with increasing pressure and decreasing temperature, 4) stable with time without special storage conditions, 5) about 1.6 times as great for temperature induced strains as for equivalent pressure induced strains and 6) about 2-4 times as great in magnitude as expected from dielectric constant measurements. The apparent polarization from temperature measurements for the 320 kV/cm specimen was about 1.7 μC/cm², or about 1/3 the value expected for maximum alignment of dipoles. In the same specimen the pyroelectric coefficient was found to be $p_3 = -0.39$ nC/cm² K and, assuming elastic isotropy, the piezoelectric strain coefficients were found to be $d_{31} = d_{32} = d_{33} = -0.89$ pC/N.

Brower, W. S., Parker, H. S., Roth, R. S., **Reexamination of synthetic parkerite and shandite**, *Amer. Mineral.* **59**, 296-301 (1974).

Key words: chalcogenides; parkerite; shandite; subsulfides.

A reinvestigation of synthetic parkerite, Ni₃Bi₂S₂, has demonstrated that the unit cell is 4 times the volume of that previously reported (Michener and Peacock, 1943). It has monoclinic symmetry, most probable space group C2/m with $a = 11.066$, $b = 8.085$, $c = 7.965$ Å, $\beta = 134.0^\circ$. The larger cell was confirmed by single crystal x-ray diffraction data, but can be deduced from the presence of extra lines in the powder pattern of a specimen which has been annealed after grinding. This same technique revealed the rhombohedral distortion of shandite, Ni₃Pb₂S₂, space group R $\bar{3}m$, previously thought to be dimensionally cubic. The unit cell of shandite was found to be $a = 5.591$, $c = 13.579$ Å. The Sn analogue of shandite, Ni₃Sn₂S₂, reported for the first time, is hexagonal with $a = 5.465$, $c = 13.196$ Å. We were

unable to synthesize any Mn, Fe, Co, or Cu analogs of the parkerite-shandite series.

Brown, W. E., **Physicochemical mechanisms of dental caries**, *J. Dent. Res.* **53**, No. 2, 204-216 (Mar./Apr. 1974).

Key words: caries models; dental caries; phase diagrams; physicochemical mechanism; solubility of enamel.

A review of models for physicochemical mechanisms of dental caries is presented. The existing models belong to three general categories: Equilibrium, steady-state and cyclic. A new interpretation is provided for these models by the application of phase diagram consideration in a generalized four component system, $\text{Ca}(\text{OH})_2\text{-H}_3\text{PO}_4\text{-HX-H}_2\text{O}$, in which HX is a bioorganic acid; the role of important factors in caries process is evaluated and advantages and shortcomings of the existing models are discussed. New directions for future research are recommended.

Burke, J. M., Ritter, J. J., Lafferty, W. J., **Infrared and Raman spectra of ethynyl difluoroborane (HC_2BF_2) and ethynyl dichloroborane (HC_2BCl_2)**, *Spectrochim. Acta* **30A**, 993-999 (1974).

Key words: ethynyl dichloroborane; ethynyl difluoroborane; gas phase; infrared; Raman; spectra.

The vapor phase infrared and Raman spectra of several isotopic species of ethynyl difluoroborane (HC_2BF_2) and ethynyl dichloroborane (HC_2BCl_2) have been obtained. Vapor phase band contours, Raman polarization data, characteristic group frequencies, and isotopic frequency shifts have been used to make the vibrational assignments for these molecules.

Burns, G. W., Hurst, W. S., **Some studies on the behavior of W-RE thermocouple materials at high temperatures**, *NASA CR-72884*, 42 pages (National Aeronautics and Space Administration, Washington, D.C., Feb. 1972). (Available as N 7220401 from the National Technical Information Service, Springfield, Va. 22151).

Key words: beryllium oxide; drift; microstructure; thermal emf-temperature; thermocouples; tungsten-rhenium alloys.

Bare 0.25 mm diameter W-Re alloy thermoelements (W, W-3% Re, W-5% Re and W-25% Re) and BeO-insulated W-3% Re and W-25% Re thermoelements have been examined for metallurgical, chemical and thermal emf changes after testing for periods up to 1000 hours at temperatures principally in the range 2000 to 2400 K. Environments for the tests consisted of high purity argon, hydrogen, helium or nitrogen gases. Commercially obtained bare-wire thermoelements typically exhibited a shift in their emf-temperature relationship upon initial exposure. The shift was completed by thermally aging the W-3% Re thermoelement for 1 hour and the W-25% Re thermoelement for 2 minutes at 2400 K in argon or hydrogen. Aged thermoelements experienced no appreciable drift with subsequent exposure at 2400 K in the gaseous environments. The chemically "doped" W-3% Re thermoelement retained a small-grained structure for exposure in excess of 50 hours at 2400 K. BeO-insulated thermoelement assemblies showed varied behavior that depended upon the method of exposure. However, when the assemblies were heated in a furnace, no serious material incompatibility problems were found if the materials were given prior thermal treatments. Thermocouples, assembled from aged W-3% Re and W-25% Re thermoelements and degassed sintered BeO insulators, exhibited a drift of only 2 to 3 K during exposure in argon at 2070 K for 1029 hours.

Butrymowicz, D. B., Manning, J. R., Read, M. E., **Diffusion in copper and copper alloys. Part 1. Volume and surface self-diffusion in copper**, *J. Phys. Chem. Ref. Data* **2**, No. 3, 643-656 (1974).

Key words: copper; diffusion; electromigration; liquid copper diffusion; nuclear magnetic resonance and diffusion; pressure effects on diffusion; self-diffusion; sintering; surface diffusion; thermomigration.

A survey, comparison, and critical analysis is presented of data compiled from the scientific literature concerning copper self-diffusion. Topics include volume diffusion, dislocation pipe diffusion, surface diffusion, sintering, electromigration, thermomigration, pressure effect on diffusion, strain-enhanced diffusion, nuclear magnetic resonance measurements of solid state diffusion and diffusion in molten copper. An extensive bibliography is presented along with figures, tabular presentation of data, and discussion of results.

Candela, G. A., Forman, R. A., Kahn, A. H., Meadowcroft, D. B., Wimmer, J., **Magnetic susceptibility of lanthanum chromite doped with strontium**, *Proc. 14th Symp. on Engineering Aspects of Magnetohydrodynamics, Tullahoma, Tenn., Apr. 8-10, 1974*, pp. IV.5.1-IV.5.3 (1974).

Key words: lanthanum chromite; lanthanum strontium chromite; magnetic susceptibility.

The magnetic susceptibility of sintered samples of Sr doped LaCrO_3 has been measured over the temperature range of 2 K to 365 K. All the samples were antiferromagnetic at low temperatures. Above 300 K all the doped samples exhibited a lower susceptibility than the pure material. Analysis of these results showed that in the doped samples not all of the chromium is in the 3^+ oxidation state. These results support the view that Sr doping modifies the valence of the Cr and thereby enhances the electronic conduction.

Carrington, C. G., Gallagher, A., **Teratomic recombination of excited RbXe** , *J. Chem. Phys.* **60**, No. 9, 3436-3444 (May 1, 1974).

Key words: molecules; recombination.

Free $\text{Rb}(5^2\text{S})$ is optically excited to $\text{Rb}^*(5^2P_{1/2})$ in the presence of Xe gas, and the $\text{RbXe}^*(A^2\Pi_{1/2}) \rightarrow \text{RbXe}(X^2\Sigma_{1/2})$ fluorescence is measured as a function of xenon pressure. The teratomic recombination process, $\text{Rb}^* + 2\text{Xe} \rightarrow \text{RbXe}^* + \text{Xe}$, and other collision processes compete with radiative decay. The radiative rate is known, so collisional rates can be inferred from the data. The molecular spectrum is observed as a continuum, whose intensity profile yields the bound-state vibrational distribution at each xenon pressure. The low-pressure limit of this distribution yields the teratomic recombination rate as a function of vibrational state, and the total recombination rate constant k_f . The recombination rate into a bound state increases with increasing binding energy, but less rapidly than the increase in equilibrium population. The transition from this initially formed distribution to the high-pressure equilibrium distribution is reported. The ratio $k_f/K_{eq} = 2.4 \times 10^{-11} \text{ cm}^3/\text{sec}$ and the equilibrium constant $K_{eq} \approx 3.4 \times 10^{-21} \text{ cm}^3$, corresponding to the experimental temperature of 300 K, are deduced from the data. The $A^2\Pi_{1/2}$ and $X^2\Sigma_{1/2}$ potentials are also obtained from analysis of the spectrum in the low-pressure and high-pressure limits.

Carroll, J. J., Melmed, A. J., **Optical constants of titanium**, *J. Opt. Soc. Amer. Letters to Editor* **64**, No. 4, 514-515 (Apr. 1974).

Key words: ellipsometry; optical constants; titanium.

Optical constants of (0001) titanium at $\lambda = 5461 \text{ \AA}$ were measured ellipsometrically under a variety of conditions. The results are compared to the appropriate literature values.

Celotta, R. J., Bennett, R. A., Hall, J. L., **Laser photodetachment determination of the electron affinities of OH^- , NH_2^- , NH_3^- , SO_2^- , and S_2^-** , *J. Chem. Phys.* **60**, No. 5, 1740-1745 (Mar. 1, 1974).

Key words: electron affinity of NH_2^- ; electron affinity of NH_3^- ; electron affinity of OH^- ; electron affinity of S_2^- ; electron affinity of SO_2^- ; photodetachment.

Using a fixed frequency argon ion laser we have studied the energy spectra of electrons photodetached from OH^- , NH_2^- , NH^- , SO_2^- , and S_2^- . We determined the following electron affinities: $E_A(\text{OH}) = 1.829 \pm 0.014$ eV, $E_A(\text{NH}_2) = 0.779 \pm 0.037$ eV, $E_A(\text{NH}) = 0.38 \pm 0.03$ eV, $E_A(\text{SO}_2) = 1.097 \pm 0.036$ eV, and $E_A(\text{S}_2) = 1.663 \pm 0.040$ eV. Additionally, the angular distribution anisotropy parameter β was measured for OH^- and NH_2^- at 4880 Å, as -0.993 ± 0.040 , and 0.027 ± 0.012 , respectively, and information about negative ion vibrational constants is presented.

Celotta, R. J., Mielczarek, S. R., Kuyatt, C. E., **Electron energy loss spectrum of ozone**, *Chem. Phys. Lett.* **24**, No. 3, 428-430 (Feb. 1, 1974).

Key words: electron energy-loss; electron excitation; gas scattering; ozone.

Electron energy loss spectra for ozone are presented over the energy loss range 1-30 eV with an incident electron energy of 300 eV. The data are obtained using an electron monochromator-analyzer combination and a static gas cell, and have a resolution of 0.035 eV fwhm.

Chandler, H. H., Bowen, R. L., Paffenbarger, G. C., Mullineaux, A. L., **Clinical evaluation of a tooth-restoration coupling agent**, *J. Am. Dental Assoc.* **88**, 114-118 (Jan. 1974).

Key words: clinical evaluation; clinical research; composite restorations; dental restorations; dentistry; monomers; operative dentistry; reinforcements.

The clinical effectiveness of a tooth-restoration coupling agent (NPG-GMA) was tested by treatment of 54 Class III and V cavity preparations with an acetone solution of this surface-active comonomer. Fifty-four additional preparations were treated with acetone alone for comparison. The teeth were restored with an experimental composite material.

The restorations were observed by three dentists for 3 1/2 years. The evaluations indicated that the restorations placed over the NPG-GMA coupling agent had significantly better margins, and a significantly higher number of the NPG-GMA associated restorations were rated better compared to those placed over the acetone control.

Chang, S. S., Bestul, A. B., **Heat capacities of selenium crystal (trigonal), glass, and liquid from 5 to 360 K**, *J. Chem. Thermodyn.* **6**, 325-344 (1974).

Key words: annealed and quenched glasses; calorimetry; glass transformation; heat capacity; selenium; supercooled liquid; thermodynamic properties; trigonal selenium.

Heat capacities of high purity selenium (better than 99.999 moles percent) have been measured for the trigonal crystal from 5 to 360 K, for the quenched and annealed glasses from 5 K to T_g (around 300 K) and for the supercooled liquid from T_g to 340 K. The glass transformation temperature T_g , as determined from plots of H against T , is 304 K for the quenched glass and 295 K for the annealed glass. C_p of the glass is higher than that of the crystal over the entire temperature range of investigation. C_p , $\{H(T) - H(c, 0)\}$, and S for the trigonal form of Se at 298.15 K are 25.05 J K⁻¹ mol⁻¹, 5509 J mol⁻¹, and 42.27 J K⁻¹ mol⁻¹, respectively. The corresponding thermodynamic properties of the annealed Se glass at 298.15 K, evaluated by incorporating the present results with recently published high-temperature data, are 26.23 J K⁻¹ mol⁻¹, 9363 J mol⁻¹, and 48.60 J K⁻¹ mol⁻¹, respectively. The residual entropy of the annealed Se glass is estimated to be 3.6 J K⁻¹ mol⁻¹ at $T=0$.

Colwell, J. H., **The heat capacity of cerous magnesium nitrate and some related materials between 0.3 and 4 K**, *J. Low Temp. Phys.* **14**, Nos. 1/2, 53-71 (Jan. 1974).

Key words: cerous magnesium nitrate; heat capacity; magnetic thermometry and adiabatic cooling.

Cerous magnesium nitrate (CMN) is the preeminent electronic paramagnet in use in cryogenic physics for magnetic thermometry

and adiabatic cooling. In demagnetization experiments designed to establish the thermodynamic temperature relations for CMN, an inexplicable heat capacity anomaly was found to occur above 20 mK and is shown here to persist to temperatures near 1 K. The anomaly is small but its presence interferes with and may cause errors in the analysis of thermometric data. We have measured the heat capacity of CMN, lanthanum magnesium nitrate (LMN), cerous nitrate hexahydrate, and a saturated aqueous solution of CMN (CMN liquor) in the temperature range 0.3-4 K in an attempt to find the source of the anomaly. The LMN heat capacity shows no anomaly and is used to approximate the lattice heat capacity of CMN. At low temperatures the CMN heat capacity, exclusive of the lattice contribution, is some 2 1/2 times larger than the magnetic heat capacity predicted by other investigations. At high temperatures an exponentially increasing heat capacity due to the first excited electronic level is observed and indicates a splitting which is in accurate agreement with the spectroscopic value. There is evidence that the lattice heat capacity in CMN is about 1 percent smaller than in LMN, which is probably the result of the crystal-field interaction with the electronic states of the cerous ions. The lattice terms and the T^{-2} term of the magnetic heat capacity for cerous nitrate have been determined, the latter being 25 times larger than the predicted T^{-2} term in CMN. The CMN liquor measurements indicate that this sample had probably become a glass on cooling. The lattice heat capacity is considerably larger than could be predicted from the separate components and there is no indication of the exponential term which would be observable if appreciable crystalline CMN were present. These measurements help to define the nature of the anomalous heat capacity and remove from consideration some possible explanations, but they do not reveal the cause of the anomaly.

Coxon, B., **Studies of carbohydrates by Fourier transform NMR spectroscopy: Structural analysis of glycosyl cyanides**, *Ann. N.Y. Acad. Sci.* **222**, 952-970 (Dec. 31, 1973).

Key words: fluorinated chemical shift reagents; Fourier transform ¹³C magnetic resonance spectroscopy; glycosyl cyanides; ¹³C-H coupling constants.

Acylated glycosyl cyanides are useful intermediates in the synthesis of C-nucleoside antibiotics, but the preparation of these intermediates from glycosyl halides and heavy metal cyanides may be complicated by the simultaneous formation of, and identification of isomeric 1,2-O-(cyanoalkylidene) derivatives. Hexopyranosyl, pentopyranosyl, and pentofuranosyl cyanides in the D-glucose, D-galactose, D-ribose, and D-xylose series and some isomeric cyanoalkylidene structures have been identified and distinguished by the characteristic chemical shifts of the CN, C-1, and alkylidene ¹³C nuclei determined by pulse-Fourier methods at 22.6 MHz. The ¹³C-H coupling constants of the cyanoalkylidene derivatives are approximately proportional to the respective ¹³C shifts from tetramethylsilane as measured by computer. The acetyl methyl ¹³C signals of carbohydrate acetates are often coincident and afford little stereochemical information. For structural analysis, these resonances may be resolved by use of the Eu(fod)₃ or Pr(fod)₃ shift reagents.

Crenshaw, R., Thomas, C., Ramsey, R., Morgenroth, D., **An approach to performance specifications for public buildings**, (Proc. Int. Conf. on Planning and Design of Tall Buildings, Lehigh Univ., Bethlehem, Pa., Aug. 21-26, 1972), Paper in *Tall Building System and Concepts*, **1a**, 797-806 (1972).

Key words: office buildings; performance criteria; systems, building.

A progress report after one year on the use of *The PBS Performance Specification for Office Buildings* for the construction of three Social Security Payment Centers. The report is mainly concerned with the shift in responsibility for the architect, industry, research and management.

Cunningham, G. W., Meijer, P. H. E., **Exact calculation of the energy and heat capacity for the triangular lattice with three different coupling constants**, *J. Math. Phys.* **15**, No. 1, 55-59 (Jan. 1974).

Key words: anisotropic coupling; elliptic integrals; heat capacity; internal energy; Ising model; triangular lattice.

Calculation of the internal energy and heat capacity of the general anisotropic triangular Ising lattice is derived from the double integral form of the partition function. The principal result is the reduction of the elliptic integrals to a standard form for three arbitrary coupling constants. Both the standard form and the method of reduction are due to Legendre. The method of reduction is one involving two linear transformations. A straightforward reduction of elliptic integrals to standard form could not be used in this application. This is because of the functional dependence of the two linear transformations on the many combinations and permutations of the signs and relative magnitudes of the coupling energies of the lattice. A relatively simple formulation is presented in which the many combinations and permutations previously mentioned are reduced to only two distinct cases. An independent numerical solution was calculated directly from the partition function as a means of verifying the formulation presented in this paper.

Cuthill, J. R., Dobbyn, R. C., McAlister, A. J., Williams, M. L., **Critical evaluation of soft x-ray emission spectra: Al metal**, *Proc. Int. Symp. X-Ray Spectra and Electronic Structure of Matter, Munchen, Germany, Sept. 18-22, 1972*, **II**, 208-219 (1973).

Key words: aluminum; critical evaluation; emission spectra; metals; soft x ray.

Measurements of the K and L valence band emission spectra of Al metal are critically compared in the light of current theory and experimental practice, and with the results of ultraviolet photoemission. The picture which emerges is one of essential agreement of experiment with one electron band theory. A number of discrepancies are noted within the existing body of data, and ascribed to inconsistencies in experimental practice.

Dalglish, W. A., Marshall, R. D., **Research review—North and South America**, (Proc. Int. Conf. on Planning and Design of Tall Buildings, Lehigh Univ., Bethlehem, Pa., Aug. 21-26, 1972), Paper in *Tall Building System and Concepts*, **Ib**, 383-398 (1972).

Key words: climatological data; meteorology; tall buildings; wind effects; wind loads; wind tunnel.

The current status of research in North and South America relevant to the prediction of tall building behavior in response to wind is reviewed under four main headings: Meteorological research—wind structure and climate; Full-scale investigations of wind action on tall buildings; Development of wind tunnel techniques for building aerodynamics; Simplified theoretical models of wind effects on tall buildings.

Day, G. W., Hamilton, C. A., Peterson, R. L., Phelan, R. J., Jr., Mullen, L. O., **Effects of poling conditions on responsivity and uniformity of polarization of PVF₂ pyroelectric detectors**, *Appl. Phys. Lett.* **24**, No. 10, 456-458 (May 15, 1974).

Key words: infrared detectors; PVF₂; pyroelectric detectors; uniform polarization.

A large number of pyroelectric detectors, fabricated from commercially available PVF₂ and poled under a variety of conditions of voltage, temperature, and time have been evaluated for responsivity and uniformity of polarization in the direction of the poling field. Results show that uniformity of polarization (a requirement for flat frequency response) can be achieved and responsivities as high as 2.9 $\mu\text{A/W}$ can be obtained.

Daywitt, W. C., **A reference noise standard for millimeter waves**, *IEEE Trans. Microwave Theory Tech.* **MTT-21**, No. 12, 845-847 (Dec. 1973).

Key words: millimeter waves; noise calibration; standard; thermal noise.

The WR15 thermal noise standard that is used as the national reference standard of noise power in the frequency range from 56 to 64 GHz is described in this short paper. The source forms a basis for both the noise-power comparison service and noise-figure service offered by the National Bureau of Standards in this frequency range.

DiChio, D., Natali, S. V., Kuyatt, C. E., **Focal properties of the two-tube electrostatic lens for large and near-unity voltage ratios**, *Rev. Sci. Instrum.* **45**, No. 4, 559-565 (Apr. 1974).

Key words: focal properties; near-unity voltage ratios; object-image curves; paraxial; two-tube electrostatic lens; weak lenses.

Accurate calculations of focal properties of the two-tube electrostatic lens are extended to cover a range of voltage ratios from 1.1 to 10000. The accuracy of the calculations is discussed in detail. For voltage ratios near 6400 the lens is found to be telescopic. Results are given in tabular form and as *P-Q* (object-image) curves. A simple analytical form for the focal properties of lenses with near-unity voltage ratios is given.

DiChio, D., Natali, S. V., Kuyatt, C. E., Galejs, A., **Use of matrices to represent electron lenses. Matrices for the two-tube electrostatic lens**, *Rev. Sci. Instrum.* **45**, No. 4, 566-569 (Apr. 1974).

Key words: focal properties; matrix elements; paraxial; strong lenses; two-tube electrostatic lens; weak lenses.

The use of matrices to represent electron lenses is discussed. It is shown that it is more convenient and natural to represent a lens by a matrix and that the matrix elements show a more regular behavior than do the focal properties. Thus matrices are more convenient to use in computer programs. Matrix elements for the two-tube electrostatic lens are presented and their properties discussed. A simple analytical form for the matrix elements of lenses with near-unity voltage ratios is given.

Dickers, R. D., **Summary report—Technical Committee No. 27, Masonry structures**, (Proc. Int. Conf. on Planning and Design of Tall Buildings, Lehigh Univ., Bethlehem, Pa., Aug. 21-26, 1972), Paper in *Tall Building System and Concepts*, **III**, 1103-1114 (1972).

Key words: bricks; building codes; buildings; concrete blocks; masonry; research; reinforced masonry; structural engineering; walls.

The re-emergence of masonry as a modern and viable structural material during the past decade is described. Buildings have been constructed up to a height of 206 ft (63 m) utilizing 10-in (254 mm) thick loadbearing masonry walls. Extensive research programs have been recently conducted but high priority should be given to additional investigations of reinforced masonry. Various needs in masonry standards and codes of practice are also identified. The use of prefabricated and prestressed masonry should continue to increase in the future.

Diller, D. E., **The Clausius-Mossotti functions (molar polarizabilities) of pure compressed gaseous and liquid methane, ethane, propane, butanes, and nitrogen**, *Cryogenics* **14**, No. 4, 215-216 (Apr. 1974).

Key words: butanes; Clausius-Mossotti function; density; dielectric constant; ethane; interpolation function; LNG components; methane; mixtures; nitrogen; propane.

This report gives accurate interpolation functions for the Clausius-Mossotti functions (molar polarizabilities) of pure compressed gase-

ous and liquid methane, ethane, propane, butanes and nitrogen; and suggests a method for calculating the dielectric constants or the densities of their mixtures. The accuracy of calculated Clausius-Mossotti functions for mixtures containing a high concentration of methane is expected to be better than 1 percent using only data for the pure components. Additional data for the dependence of the excess Clausius-Mossotti function on composition could reduce the uncertainty in Clausius-Mossotti functions for multicomponent mixtures to less than 0.2 percent.

DiMarzio, E. A., **Statistical mechanics of polymers with application to a polymer between plates**, (XXIII Int. Congress of Pure and Applied Chemistry, Special Lectures, Boston, Mass., July 26-30, 1971), *J. Pure Appl. Chem.* **8**, 239-263 (1971).

Key words: polymer statistics; statistical mechanics of polymers.

It is shown that the customary separation of the classical partition function into a translational part and a configurational part is invalid for polymers. However, the integration over momentum coordinates can always be performed resulting in a configuration integral with effective potential energies. The problem of a polymer molecule near a surface of arbitrary shape is formally solved. The polymer is allowed to experience a spatially varying potential ($V(r)$ per segment). Kakutani's theorem of probabilistic potential theory is easily derived. Using both continuum and lattice methods explicit formulae are obtained which describe the behavior of a polymer molecule constrained to be (1) on one side of an infinite plate, or (2) between two parallel plates, or (3) in a wedge of arbitrary angle. These results are applied to the problems of adsorption and adhesion and to the problem of crystallization. It is shown how an understanding of these subjects requires prerequisite knowledge of the appropriate polymer-interface problem. The notion of polymer size is not invariant but rather depends on the process in which the polymer participates. If one thrusts a plate towards another plate on which a polymer molecule resides until a first contact is made then the resulting plate separation defines a polymer size which is relevant to the problems of adhesion and crystallization. It is larger than the root-mean-square end-to-end length.

Dobbyn, R. C., McAlister, A. J., Cuthill, J. R., Erickson, N. E., **Valence band x-ray photoemission and soft x-ray emission studies of Pt**, *Phys. Lett.* **47A**, No. 3, 251-252 (Mar. 25, 1974).

Key words: electronic density of states; Pt; surface cleanliness; valence-band; x-ray photoemission.

The soft x-ray $N_{6,7}$ (5d to 4f transition) emission spectrum and the x-ray photoemission spectrum of Pt (the latter under two conditions of surface cleanliness) have been obtained, and are compared with the results of photoemission and band theoretical studies.

Drummond, D. L., Gallagher, A., **Potentials and continuum spectra of Rb-noble gas molecules**, *J. Chem. Phys.* **60**, No. 9, 3426-3435 (May 1, 1974).

Key words: molecules; rubidium.

Rubidium vapor is optically excited by either of the atomic resonance lines in the presence of typically 400 torr of He, Ne, Ar, Kr, or Xe. Normalized emission spectra of the far wings of these resonance lines are then measured as a function of temperature. These far wings, extending as much as 1000 Å from the resonance lines, are interpreted as molecular continuum radiation of Rb-noble gas molecules. Using the quasistatic theory of line broadening, or the classical Franck-Condon principle, these spectra are analyzed to yield the ground and excited state molecular potentials.

Ehrlich, M., **Dosimetry performance tests**, (Proc. Panel on National and International Radiation Dose Intercomparisons, Vienna, Austria, Dec. 13-17, 1971), Paper IAEA-PL-479/8 in *National and International Radiation Dose Comparisons*, pp. 41-57 (International Atomic Energy Agency, Vienna, Austria, 1973).

Key words: choice of dosimeters; electrons; ferrous sulfate dosimeters; medical applications; performance criteria; personnel monitoring; photographic film; photons; radiation measurements; test patterns.

This report presents a discussion of the need for critical studies of radiation measurement techniques and routine measurement performance. The aim of such studies is to improve practical measurement performance by periodic testing and by the distribution of the knowledge gained by the participants in such tests. Besides general consideration, such items as test pattern, choice of dosimeters and examples from tests are discussed.

Farabaugh, E. N., **X-ray microscopy of single-crystal potassium diduterium phosphate**, *J. Appl. Phys. Commun.* **45**, No. 4, 1905-1907 (Apr. 1974).

Key words: dislocations; KD^*P ; Lang technique; solution grown; x-ray diffraction microscopy.

Examination of solution-grown KD^*P single crystals by the Lang technique has shown that the crystals are free from growth veils, impurity segregation, and subgrain boundaries. The density of dislocations varies throughout the volume of the crystals, some areas being nearly dislocation free. One Burgers vector identified as being parallel to $\langle 100 \rangle$ is common to the similar KDP and ADP single crystals.

Fathers, D. J., Jakubovics, J. P., Joy, D. C., Newbury, D. E., Yakowitz, H., **A new method of observing magnetic domains by scanning electron microscopy. I. Theory of the image contrast**, *Phys. Status Solidi* **20**, 535-544 (1973).

Key words: contrast measurement; image contrast; iron-silicon alloy; magnetic domains; nickel; scanning electron microscopy.

A theory is developed to explain the magnetic domain contrast observed by scanning electron microscopy using the method reported recently [4,5]. The theory is based on a model which assumes that the contrast is due to the Lorentz deflection of the incident electrons inside the specimen. Using this model, the dependence of the image contrast on various experimental parameters was calculated analytically. The model was confirmed by means of calculations carried out by computer simulation of electron trajectories (Monte Carlo techniques). The theory accounts satisfactorily for previous experimental results. A more detailed comparison of the theory with experimental results will be published in a subsequent paper.

Fatiadi, A. J., **Electron spin resonance studies of chemical changes of phenylhydrazones and osazones in alkaline solution**, *Adv. Chem. Ser., No. 117, Carbohydrates in Solution*, pp. 88-105 (1973).

Key words: alkaline solution; chemical changes; electron spin resonance; free radical mechanism; nitroxide radical; osazones; phenylhydrazones.

Treatment of a solution of a sugar phenylhydrazone or osazone in methyl sulfoxide with potassium *tert*-butoxide and a trace of oxygen at room temperature gives products that have a three-line electron spin resonance (ESR) spectrum characteristic of a nitroxide radical. The apparent fragmentation of the phenylhydrazine moiety under reaction conditions used does not show evidence of any paramagnetic species derived from glyoxal bis(phenylhydrazone). The latter had been reported to be the product of degradation of the sugar phenylhydrazones under more vigorous alkaline treatment. Some inosose phenylhydrazones in alkaline methyl sulfoxide solution produce stable radical-anions in which the phenylhydrazine moiety remains intact. A free radical mechanism is advanced to account for the β -elimination reactions of the sugar phenylhydrazones under mildly basic conditions.

Fatiadi, A. J., **New applications of periodic acid and periodates in organic and bio-organic chemistry**, *Synthesis Reviews*, No. 4, 229-272 (Apr. 1974).

Key words: application; bio-organic; methods; organic; oxidation; periodates; review.

Recent applications of periodic acid and periodates to organic and bio-organic chemistry are reviewed. Unique periodate oxidations and synthetic methods employing periodates are discussed.

Filliben, J. J., **Comments on the paper "Treatment of null responses,"** by G. L. Meyer and R. L. Johnson, *Proc. 17th Conf. on the Design of Experiments in Army Research Development and Testing, Washington, D.C., Oct. 27-29, 1971, ARO-D Report 72-2*, pp. 397-402 (Sept. 1972).

Key words: camouflage; design of experiment; null responses; paired comparisons; sign test; statistics.

Comments are given on the paper "Treatment of Null Responses" by G. L. Meyer and R. L. Johnson at the 17th Conference on the Design of Experiments in Army Research Development and Testing. The statistical limitations imposed by small sample sizes are discussed. A change in the design of the experiment is suggested which would reduce or eliminate altogether the number of ties (due to null responses). A modification of the Sign Test is proposed which allows the processing of the data even in the presence of ties.

Fowlkes, C. W., **Fracture toughness tests of a rigid polyurethane foam,** *Int. J. Fract.* **10**, No. 1, 99-108 (Mar. 1974).

Key words: fracture; fracture toughness; polyurethane foam.

The results of some exploratory tests for determining the fracture toughness of a rigid polyurethane foam are presented. The specimen geometries used included center- and double-edge-cracked plates, the single-edge-cracked tensile specimen and the double cantilever beam specimen. The validity of applying the concepts of linear elastic fracture mechanics to the fracture of this foam is discussed. Some unique features of the fracture of foam are discussed.

Frederikse, H. P. R., Hosler, W. R., **Electrical conductivity of MHD-channel materials,** *Proc. 14th Symp. on Engineering Aspects of Magnetohydrodynamics, Tullahoma, Tenn., Apr. 8-10, 1974*, pp. IV.2.1-IV.2.3 (1974).

Key words: coal slag; electrical conductivity; high temperature; magnetohydrodynamics; zirconates.

This paper deals with two aspects of MHD-channel materials. The first part reports on the electrical conductivity of mixtures of coal slag and K_2SO_4 seed. The second part discusses the problem of finding electronically conducting electrode materials and describes the results of conductivity measurements performed on Ce and Ti doped $SrZrO_3$.

Frommer, M. A., Messalem, R. M., **Mechanism of membrane formation. VI. Convective flows and large void formation during membrane precipitation,** *I&EC Prod. Res. Develop.* **12**, 328-333 (Dec. 1973).

Key words: convection flows; desalination; interfacial turbulence; membranes; membrane structures; polymer precipitation; scanning electron micrographs.

The factors governing the formation of voids and large cavities in a wide variety of membranes made from different polymers cast from different solvents and precipitated in various nonsolvents have been studied. It has been shown that the formation of large voids in membranes can be eliminated by (1) lowering the tendency of the nonsolvent to penetrate into the casting solution or (2) increasing the viscosity of the cast solution or creating a thick gel layer on top of this cast solution. It is suggested that the formation of large finger-like cavities in membranes originates from convective flows formed within the cast (fluid) polymer solution upon its immersion in the bath of nonsolvent for final precipitation. It is also shown that the driving forces leading to the formation of these convective flows are not density gradients.

Gadzuk, J. W., **Surface molecules and chemisorption. I. Adatom density of states,** *Surface Sci.* **43**, 44-60 (1974).

Key words: chemisorption; molecules; surfaces.

A useful picture of chemisorption on metal surfaces is one in which a localized molecule is formed between the adatom and its nearest neighbor substrate atoms. The interaction responsible for the molecule formation is treated as the coupling between the adsorbate state and a group orbital formed from a linear combination of atomic orbitals on the substrate atoms. Within the surface molecule picture, level width and level shift functions, given by Newns modification of the Anderson theory, have been calculated and the resulting adatom density of states function has been obtained. This has been done for model systems in which the substrate is either a free electron metal or a tightbinding p-band metal and the adsorbate is s or p like. The results show how it is possible to simultaneously have narrow virtual levels due to chemisorption (~ 1 eV) which previously implied weak interactions and also high binding energies (≥ 3 eV) as are observed experimentally.

Gadzuk, J. W., **Valence-band Auger-electron spectra for aluminum,** *Phys. Rev. B* **9**, No. 4, 1978-1980 (Feb. 15, 1974).

Key words: attenuation lengths; Auger effect; electron spectroscopy of solids; surfaces.

Recent measurements of the L_{23} VV Auger spectrum of Al by Powell, have shown that the observed energy distributions do not correspond to the self-convolution of the Al bulk density of states. Attempts to account for this discrepancy in terms of energy-dependent matrix elements and inelastic scattering of the ejected electron are described here.

Giarratano, P. J., **Supercritical helium heat transfer,** (Proc. CRYO-72 Conf., Chicago, Ill., Oct. 3-5, 1972), Chapter 4 in *Applications of Cryogenic Technology* **5**, 52-89 (Scholium Int. Inc., Whitestone, N.Y., 1973).

Key words: forced convection; heat transfer; helium; supercritical.

This paper reports part of the National Bureau of Standards Cryogenics Division's program to provide helium heat transfer information to designers of helium cooling systems. An experiment on supercritical helium heat transfer is described, and its results are compared with various standard and modified correlation expressions.

Extensive appendices give tables of helium viscosity, thermal conductivity, and Prandtl numbers from 3 to 300 K.

Gilman, F. J., Kugler, M., Meshkov, S., **Transformation between current and constituent quarks and transitions between hadrons,** *Phys. Rev. D* **9**, No. 3, 715-735 (Feb. 1, 1974).

Key words: cross sections; reactions; regge pole; SU(3); symmetry breaking; trajectory.

The transformation from current- to constituent-quark basis states is discussed. Certain algebraic properties of the transformed vector and axial-vector currents are abstracted from the free-quark model and assumed to hold in nature. Supplemented by the partially conserved axial-vector current hypothesis and assumptions about the identification of the observed hadrons with simple constituent-quark states, the algebraic properties of the transformed currents are used to compute the pion and photon transitions between any two hadron states. General selection rules are stated. Many specific matrix elements for both meson and baryon decays are tabulated, and both their magnitudes and signs are compared with experiment.

Goldberg, S., Ogburn, F., **Plating standards and specifications,** Chapter 7 in *Electroplating Engineering Handbook (3d Edition)*, pp. 258-271 (Van Nostrand Reinhold Co., New York, N.Y., 1972).

Key words: coating thickness; coatings; electrodeposited coatings; electrodeposits; metal coatings; plated coatings; plating specifications; plating standards; specifications.

The electroplated coating specifications of the ISO, the ASTM, and the U.S. Government are discussed in some detail. The requirements of the specifications and the test methods are reviewed and coating thickness requirements are tabulated. A number of the applications for which various types of plated coatings suitable are discussed.

Grabner, L. H., Hosler, W. R., Frederikse, H. P. R., **Some optical and electrical properties of undoped and SR-doped LaCrO₃**, *Proc. 14th Symp. on Engineering Aspects of Magnetohydrodynamics, Tullahoma, Tenn., Apr. 8-10, 1974*, pp. IV.4.1-IV.4.3 (1974).

Key words: diffuse reflectivity; LaCrO₃; photoconductivity; photoexcitation; photoluminescence; transport data.

Transport data and optical data (photoluminescence, photoexcitation, diffuse reflectivity and photoconductivity) are presented for undoped, and Sr and Ca doped LaCrO₃. We conclude that LaCrO₃ is a wide band-gap semiconductor (~7 eV) in which an oxygen deficiency of the complex Cr³⁺ octahedrally coordinated with 6O⁻ gives rise to a donor with an activation energy of about 0.5 eV. This oxygen deficiency can be induced as a charge compensation mechanism when LaCrO₃ is doped with either Sr or Ca.

Gravatt, C. C., Jr., **Real time measurement of the size distribution of particulate matter by a light scattering method**, *APCAJ*, **23**, No. 12, 1035-1038 (Dec. 1973).

Key words: air pollution; light scattering; particulate matter.

The body of information presented in this paper is directed to those individuals concerned with the measurement of the size distribution of particulate matter in air. The light scattering instrument described herein is characterized by the fact that it can accurately size particles almost independently of their index of refraction. The basic concept involves the simultaneous measurement of the intensity of light scattered by a single particle at two small scattering angles. The ratio of the two intensities is directly related to the size of the particle, and for scattering angles of 5 and 10° the effective range of the instrument is 0.2 to 4 μm. The air flows through the optical system at such a rate that approximately 25 μs are required to determine the size of each particle, and concentrations as high as 10⁴ particles/cc can be measured without dilution and without serious coincidence effects. By employing a multichannel analyzer as the data storage and readout device it is possible to detect changes in particulate size distribution within a few seconds. Calibration of the instrument has been performed using polystyrene latex spheres and materials having a wide range of index of refraction and shape including carbon black, iron oxide and spores.

Greene, W. E., Jr., **Stochastic models and live load surveys**, (Proc. Int. Conf. on Planning and Design of Tall Buildings, Lehigh Univ., Bethlehem, Pa., Aug. 21-26, 1972), Paper in *Tall Building System and Concepts*, **1b**, 35-58 (1972).

Key words: computer simulation; live and fire loads; occupancy; stochastic predictive models; survey; techniques.

Design fire loads and live loads for office buildings are based on data collected over 30 years ago. Maximum cost efficiency in gathering this loads data requires the use of stochastic models. Explanatory models based on room characteristics such as room use, occupancy type, age of occupancy, etc. are used to determine (explain) room loads for the rooms not surveyed. Only about 10,000 rooms will be surveyed from about 100 office buildings which will serve to provide information for estimating parameters for the predictive loads models (sustained, maximum sustained, extraordinary). The explanatory models will provide the remaining room loads. The topology of these 100 buildings having been previously programed and stored in the

computer, all rooms of the building population will be loaded through mathematical simulation. A pilot study, using a limited amount of previously collected data has been initiated to verify these models as much as possible, this will be followed by a reduced survey of about 25 buildings to further refine the models before the major survey of approximately 75 buildings will be conducted.

Hagen, L., **Report of The National Bureau of Standards 1972/73, for Reports of Observatories**, *Bull. Amer. Astronom. Soc.*, **6**, No. 1, 140-144 (1974).

Key words: atomic energy levels; atomic line shapes; atomic spectra; atomic transition probabilities; bands, molecular; energy levels, atomic; line shapes, atomic; molecular bands; molecular spectra; rotational constants.

Research at the National Bureau of Standards in spectroscopy pertinent to astronomy is summarized. Publications on atomic spectra, atomic transition probabilities and line broadening, and molecular spectra are referenced and work in progress is discussed.

Haque, S. S., Lees, R. M., Saint Clair, J. M., Beers, Y., Johnson, D. R., **Microwave spectrum of ¹³C methanol**, *Astrophys. J.*, **187**, L-15-L-17 (Jan. 1, 1974).

Key words: carbon-13; methanol.

Laboratory measurements of the frequencies of some astronomically interesting transitions of the ¹³C isotopic species of methanol are reported. Most lines of the $J = 2 \leftarrow 1, 3 \leftarrow 2, 4 \leftarrow 3 \mu_a$ -type $\Delta k = 0$ transitions in the 94-, 142-, and 189-GHz regions have been measured, as well as a number of μ_b -type transitions in the 14-50 GHz region. The standard deviation of fit with the constants given is 0.098 MHz. The remaining unmeasured lines in these R-branch patterns have been predicted with an uncertainty of 0.3 MHz.

Hall, J. L., **Saturated absorption line shape**, *Proc. Esfahan Symp. on Fundamental and Applied Laser Physics, Esfahan, Iran, Sept. 1971*, pp. 463-477 (1972).

Key words: laser spectrometer; pressure broadening; resonance line shape; saturated absorption.

In this paper we demonstrate optical frequency stability of $\pm 3 \times 10^{-14}$ obtained at 3.39 μm by use of saturated molecular absorption in methane. Through Frequency Offset Locking this stability can be transferred to other lasers, thus allowing construction of a very powerful laser spectrometer. A resolution of 2×10^6 FWHM and absolute resettability of $\pm 1/2 \times 10^{-11}$ have been achieved with this spectrometer. We have studied the power- and pressure-broadening of saturation resonances in methane for several different laser spot sizes. Except near zero power and pressure, the line shape is found to be accurately Lorentzian. Based on a saturation model, a 3-parameter formula is presented which accounts for the observed broadening. The residual line width (intercept at zero power and pressure, HWHM) times laser spot radius is found to be 70 kHz mm. The saturation power turns out to be 1 mW. Pressure broadening rates of 10 to 16 kHz (HWHM)/mT are observed.

Haller, W., **A single equation relating molecular weight, pore-size, and elution coefficient in the controlled pore glass chromatography of protein-sodium dodecyl sulfate complexes**, *J. Chromatog.*, **85**, 129-131 (1973).

Key words: chromatography; controlled pore glass; denaturing solvents; glass; molecular weight; permeation; porous glass; proteins; sodium duodecyl sulfate.

Permeation chromatography elution coefficients of the sodium duodecyl sulfate complexes of thirteen different proteins on controlled pore glass columns were analyzed. A master equation, relating elution coefficient, subunit molecular weight and pore diameter of glass is described. The equation allows estimating the subunit molecular weight of the proteins from elution results on columns of any

known pore diameter, without the need for individual column calibration with a series of proteins with known subunit molecular weight.

Hanley, H. J. M., **The viscosity and thermal conductivity coefficients of dilute argon, krypton and xenon**, *J. Phys. Chem. Ref. Data* **2**, No. 3, 619-642 (1973).

Key words: dilute gas; kinetic theory; *m*-6-8 potential function; rare gases; thermal conductivity coefficient; viscosity coefficient.

The viscosity and thermal conductivity coefficients of dilute argon, krypton, and xenon are reviewed and tables of recommended values presented. The tables were generated using the appropriate kinetic theory expressions with the *m*-6-8 potential. The temperature range covers from about one-half critical temperature to 2000 K for each gas. A general estimate of the accuracy is one percent increasing to one and three-quarters percent for temperatures above 1000 K.

Hanson, D. W., Hamilton, W. F., Gatterer, L. E., **The NBS frequency and time satellite experiment using ATS-3**, *Proc. 3d Precise Time and Time Interval Strategic Planning Meeting, Washington, D.C., Nov. 16-18, 1971*, pp. 155-165 (U.S. Naval Observatory, Washington, D.C., 1971).

Key words: frequency; satellites; time.

A frequency and time dissemination experiment using NASA's ATS-3 synchronous satellite is explained. Details of frequency, bandwidth, receiving equipment requirements and recovery techniques are given to allow reader to use system. Results and data concerning accuracy and expected performance are included.

Hellner, C., Keller, R. A., **Flash photolysis of sulfur dioxide**, *J. Air Pollut. Contr. Ass.* **22**, No. 12, 959-963 (Dec. 1972).

Key words: air pollution; flash photolysis; sulfur dioxide; ultraviolet absorption.

The body of information presented in this paper is directed to photochemists and air pollution scientists interested in species which result from the interaction of SO₂ and light. When SO₂ at low pressures is subjected to an intense photolysis flash, the characteristic, very structured SO₂ absorption spectrum disappears immediately after the flash and is replaced by a continuous absorption. The continuous absorption gradually decays and the normal SO₂ absorption spectrum returns. The initial absorbance of the continuous absorption is proportional to the square of the SO₂ pressure and the square of the flash irradiance. From these facts we propose the formation of a metastable dimer of SO₂ formed by the collision of two excited molecules. Some properties of this dimer are: natural lifetime = 2 sec; energy above separated monomers = 4 kcal; lifetime at atmospheric pressure = 1 sec (quenching coefficients with several foreign gases = 10⁻²⁰ cm³/sec molecule); absorption of ultraviolet light results in photodecomposition of the dimer into monomeric SO₂. The long lifetime of this species and its low quenching cross section may make it an important intermediate in photochemical reactions of SO₂. The relatively low excitation energy of the metastable species indicates it may also be an intermediate in thermally excited reactions and perhaps an important component of smoke stack effluent.

Horton, W. S., **A relationship between the magnetic susceptibilities of pyrolytic and single crystal graphites**, *Proc. 11th Biennial Conf. on Carbon, Gatlinburg, Tenn., June 4-8, 1973*, Paper EP-2, pp. 2-3 (1973).

Key words: anisotropy; magnetic susceptibility; pyrolytic graphite; single crystal graphite.

Actual magnetic susceptibility data are compared with the relation $\chi_{\perp} + 2\chi_{\parallel} = 3\chi_r$ where the first two susceptibilities refer to those perpendicular and parallel to the deposition plane, and χ_r is that for a random mixture of perfect crystals. A parabolic rather than linear relation appears to fit better empirically. An intersection of the

straight and curved lines appears to be close to the measured values of principal magnetic susceptibilities of good single crystal graphite.

Hougen, J. T., **Comment on the paper "About the symmetries of the rotation-vibration wavefunction of molecules"**, *J. Mol. Spectrosc.* **50**, 485-486 (1974).

Key words: group theory; methane; rovibronic symmetry species; selection rules; tetrahedral point group.

Qualitative observations are presented concerning the long-standing controversy over the correct use of group-theoretical symmetry operations and symmetry species in the methane molecule. No new mathematical details are introduced; discussion focuses rather on the merits of papers in the existing literature. The observations are presented in response to a comment by Professor J. Moret-Bailly, published simultaneously, in which an opposing point of view is given.

Huebner, R. H., Celotta, R. J., Mielczarek, S. R., Kuyatt, C. E., **Electron energy loss spectroscopy of acetone vapor**, *J. Chem. Phys.* **59**, No. 10, 5434-5443 (Nov. 15, 1973).

Key words: acetone vapor; electron energy-loss spectroscopy; oscillator strength.

High resolution, inelastic electron scattering data can provide new spectroscopic information on the electronic structure of polyatomic molecules. Features in the acetone energy loss spectrum from 0 to 15 eV obtained for 100 eV incident electrons correspond to vibrational, electronic discrete, and electronic continuum excitations. These data are compared with optical measurements in a wide spectral region extending from the infrared to the vacuum ultraviolet. A comprehensive interpretation of the energy loss spectra is attempted with the use of photochemical and photoelectron data, as well as quantum-chemical calculations in the literature. Three Rydberg series with quantum defects of 1.03, 0.81, and 0.315 join onto bands previously discussed in terms of transitions to valence orbitals. These series converge to an ionization limit of 9.705 eV in good agreement with previous optical determinations. Dissociative continua underlie the Rydberg region and give rise to a variety of neutral products observed in recent photolysis work. Broad features in the ionization continuum appear to correlate generally with higher ionization potentials observed by photoelectron spectroscopy. Apparent oscillator strengths derived from the energy loss data for the bands at 4.4 and 6.35 eV and for a region (9.7-11.78 eV) of the ionization continuum agree very well with the photoabsorption measurements. Integrated oscillator strengths of 0.46 below 9.7 eV and 3.93 below 15 eV were derived from the electron impact data.

Hunt, C. M., **Simple observations of some common indoor activities as producers of airborne particulates**, (Proc. ASHRAE Symp. Cleaner Indoor Air—Progress and Problems, Cincinnati, Ohio, Oct. 19-22, 1972), Chapter in *ASHRAE*, pp. 8-14 (American Society of Heating, Refrigerating, and Air-Conditioning Engineers, New York, N.Y., 1973).

Key words: air cleaning; air pollution; dust generation; indoor pollution; particulates.

Observations were made of some common indoor particle generating and dispersing activities by performing them in a small closed room and measuring the changes in particle count as a function of time using a light scattering particle counter. Two size ranges were measured, particles larger than 0.3 μm in diameter, and particles larger than 3 μm . The activities examined were smoking, heating grease as in frying, operation of a vacuum cleaner, and use of household aerosol sprays. The particle count in a closed room without activity was also observed as well as the effect of an oscillating electric fan.

Thermal operations such as smoking and the heating of grease produced a much larger number of particles smaller than 3 μm than

the mechanical generating and dispersing activities. The mechanical activities, by comparison, tended to produce more particles larger than $3\ \mu\text{m}$. With no activity in the room the particle count in both size ranges decreased with time, and with the electric fan or vacuum sweeper operating an increase in particle count was observed, followed by a decrease qualitatively similar to that observed with no activity in the room. The increase in count by the aerosol sprays appeared to be dominated by effects due to the propellant.

Hurlock, S. C., Lafferty, W. J., Rao, K. N., **Analysis of the ν_3 band of $^{14}\text{N}^{16}\text{O}_2$** , *J. Mol. Spectrosc.* **50**, 246-256 (1974).

Key words: air pollutant; fundamental vibrational band; high-resolution; molecular constants; spin-splittings; vibration-rotation.

The rotational structure of the ν_3 fundamental of $^{14}\text{N}^{16}\text{O}_2$ has been recorded by employing a vacuum grating infrared spectrograph. The analysis has led to the assignment of over 500 *R*- and *P*-branch transitions in the spectral region 1650-1562 cm^{-1} . Molecular constants for the upper state, 001, have been presented. No *Q*-branch transitions were used in the evaluation of these constants. The presently obtained $\alpha_3^A = 0.22517\ \text{cm}^{-1}$ and the band center $\nu_0 = 1616.846\ \text{cm}^{-1}$ differ significantly from previous determinations. Spin splitting was observed but no information was extracted about upper state spin splitting parameters.

Jan, G., Mendlowitz, H., **Optical imaging with frequency-dependent spectral-density functions**, *J. Opt. Soc. Amer.* **61**, No. 7, 865-869 (July 1971).

Key words: coherence; image formation; modulation transfer; optical transfer function.

In this investigation, the quasimonochromatic condition is not assumed, and the spectral-density function of the radiation depends on frequency as well as on positions. We discuss various models for the impulse-response function of the optical system, and examine the results in temporal-frequency space. We approximate the integration by employing the method of steepest descent. An explicit relation of the mutual coherence function and the spectral-density function of the source is established with some correction factors that differ from the results of the quasimonochromatic approximation.

Johnson, C. R., **A note on matrix solutions to $A = XY - YX$** , *Proc. Amer. Math. Soc.* **42**, No. 2, 351-353 (Feb. 1974).

Key words: commutator; eigenvalues; positive definite; trace.

It is known that a square matrix A can be written as a commutator $XY - YX$ if and only if $\text{Tr}(A) = 0$. In this note it is shown further that for a fixed A the spectrum of one of the factors may be taken to be arbitrary while the spectrum of the other factor is arbitrary as long as the characteristic roots are distinct. The distinctness restriction on one of the factors may not in general be relaxed.

Jones, M. C., Giarratano, P. J., McConnell, P. M., Arp, V., **Refrigeration with forced flow of helium**, *Proc. Cryogenic Cooler Conf., USAF Academy, Colorado Springs, Colo., Oct. 16-17, 1973*, pp. 441-462 (Air Force Flight Dynamics Laboratory (FEC), Wright-Patterson Air Force Base, Ohio, Dec. 1973).

Key words: forced flow; heat transfer; helium; pump; refrigeration.

The operation of practical superconducting components usually generates some heat because of nonideality of the superconductors, particularly in a.c. applications. In many cases, e.g., pulsed magnets, system design and performance is strongly constrained by the available heat transfer between the superconductor and the surrounding helium. We have been studying the general problems of maintaining the required refrigeration by forced flow of helium.

The desired helium flow can be obtained either directly from the refrigerator system (i.e., room temperature compressors) or from aux-

iliary pumps which offer additional system flexibility at the cost of probable additional thermal load on the refrigerator. We have evaluated centrifugal pump performance in superfluid, normally boiling, and supercritical helium, with results in approximate accord with scaling laws and pump performance measurements in other fluids. Cavitation limits and other performance considerations in helium will be presented.

Kanda, M., Adams, J. W., **Amplitude statistics of electromagnetic noise in coal mines**, *Proc. Thru-the-Earth Electromagnetics Workshop, Colorado School of Mines, Golden, Colo., Aug. 15-17, 1973*, pp. 156-160 (1973).

Key words: amplitude probability distributions; electromagnetic compatibility; electromagnetic interference in coal mines; field strength measurement.

A system for measuring amplitude probability distributions (APD's) of electromagnetic noise in coal mines is described and typical APD's from an underground coal mine are presented. The APD is a basic statistic required for the design and analysis of communication systems, especially those intended for use in noisy environments, and where neither overdesign nor underdesign is acceptable. The rms and average field strengths are obtained by integration of the APD, and examples are shown at several frequencies. All field strength levels are given in absolute units. Selected frequencies cover the range from 10 kHz to 32 MHz.

Kearsley, E. A., **A test sample to standardize measurements of normal stress**, *Rheol. Acta* **12**, No. 4, 546-549 (1973).

Key words: molecular weight distribution; normal stress; polystyrene solutions; standard sample; streaming birefringence.

This paper is an account of the design of a test sample of polystyrene solution which will be distributed to research laboratories interested in participating in a comparison of techniques of measurement of normal stresses through a common sample. Questions of concentration, molecular weight distribution and solvent properties are considered.

Kessler, K. G., **Progress in the measurement of atomic transition probabilities and solar abundances**, *Comments At. Mol. Phys.* **11**, No. 5, Part D, 151-155 (Dec. 1970-Jan. 1971).

Key words: astrophysics; *f*-values; oscillator strengths; transition probabilities.

The exploitation, over the past decade, of new approaches to the measurement of atomic transition probabilities has produced data of greater accuracy than was available before. The value of these new data to astronomy is well illustrated by the recent work on the iron spectrum. Though it is a somewhat atypical example, it serves as an excellent illustration of the great progress in this field and its effect on astrophysics.

Kessler, K. G., **The role of resonance interactions in some molecular far-infrared laser systems**, *Comments At. Mol. Phys.* **11**, No. 2, Part D, 67-72 (June-July 1970).

Key words: Coriolis interactions; infrared lasers; molecular lasers.

An analysis of the HCN laser system is presented and generalized to explain the operating mechanism for molecular lasers systems in general.

Krauss, M., Neumann, D., **Multi-configuration self-consistent-field calculation of the dissociation energy and electronic structure of hydrogen fluoride**, *Mol. Phys.* **27**, No. 4, 917-921 (1974).

Key words: configuration interaction; dipole moment; dissociation energy; electronic structure; HF; quadrupole moment.

The optimized valence configuration method of Wahl and Das is applied to a study of the electronic structure of FH at the equilibrium internuclear separation. A compact eight configuration wave function is found to yield an accurate dissociation energy and dipole moment.

Kropschot, R. H., **Helium heat transfer**, *Proc. Application of Superconducting Cable in Electrical Engineering and High Energy Physics, Titisee, Germany, Oct. 9-13, 1972*, pp. D1-D32 (Gesellschaft fuer Kernforschung, Karlsruhe, Germany, 1973).

Key words: cryogenics; heat transfer; helium; refrigeration; thermodynamic properties.

Design of an optimum superconducting device such as a magnet, cavity, generator, motor, transmission line or electronic device requires careful consideration of heat transfer. Any transient or oscillatory electrical behavior will cause heat generation which must be removed in order to permit continuous operation. Helium is the only cooling medium for most applications and as system size, cost and complexity increase it may not be practical to immerse the conductor in a container of helium and depend upon pool boiling, commonplace in small laboratory magnets. The purpose of this paper is to present the state of the art of reliable data on helium properties and helium heat transfer necessary for serious engineering studies of superconducting systems.

Kusuda, T., **Effectiveness method for predicting the performance of finned tube coils**, *ASHRAE Symp. Bull.*, pp. 5-14 (1970).

Key words: air conditioning; cooling and dehumidifying capacities; effectiveness; finned tube coil; heat transfer; refrigeration.

In 1960 the author proposed using the effectiveness method for predicting the heat and mass transfer performance of chilled water coils. This method is reviewed and elaborated. Comparisons of predicted chilled water dehumidifying coil capacities using this method with observed experimental values given by Prof. Trapanese of Italy were made. The comparisons show that the effectiveness method is accurate if the parameters employed in the effectiveness equation are properly evaluated.

The effectiveness method also appears to be a powerful concept for predicting the performance of finned tube coils at conditions other than those originally selected for design purposes.

Kuyatt, C. E., Celotta, R. J., Mielczarek, S. R., **Applications of electron spectroscopy to air pollution measurements**, (Proc. VIII Int. Conf. on Physics of Electronic and Atomic Collisions, Belgrade, Yugoslavia, July 16-21, 1973), Paper in *Proceedings VIII International Conference on Physics of Electronic and Atomic Collisions—Invited Lectures and Progress Reports*, B. C. Cobic and M. V. Kurepa, Eds., pp. 681-701 (Institute of Physics, Belgrade, Yugoslavia, 1974).

Key words: air pollution; electron spectroscopy; energy-loss spectroscopy.

Recent developments in electron spectrometer design have made the application of inelastic electron scattering measurements to gas analysis competitive with other techniques. The energy distribution (energy loss spectrum) of electrons of an initially monoenergetic electron beam after an encounter with a gas target contains the optical absorption spectrum of the gas. This spectrum, by revealing the valence energy states of the gas, is an intrinsic "fingerprint" of the atom or molecule. An instrument has been built to explore the potentialities of this method. Its response is linear with concentration over a very wide range. The instrument is described and its performance as a trace analyzer for air pollution studies discussed.

Leasure, W. A., Jr., **Performance evaluation of personal noise exposure meters**, *Sound Vib.* **8**, No. 3, 36-40 (Mar. 1974).

Key words: exposure meters; noise; meters noise exposure; noise exposure meters; personal noise exposure meters.

The promulgation of Federal occupational noise exposure regulations has resulted in a proliferation of personal noise exposure meters. A wide variation in performance has been observed among the various instruments; therefore, the user should be cautioned to carry out enough evaluation tests to determine that the devices are performing adequately for his purpose.

Ledbetter, H. M., Reed, R. P., **Elastic properties of metals and alloys, I. Iron, nickel, and iron-nickel alloys**, *J. Phys. Chem. Ref. Data* **2**, No. 3, 531-617 (1973).

Key words: bulk modulus; compressibility; elastic constants; iron; iron alloys; Lamé constants; nickel; nickel alloys; Poisson's ratio; shear modulus; single-crystal elastic coefficients; Young's modulus.

A comprehensive compilation is given of elastic properties of iron-nickel alloys. When sufficient data exist, preferred values are recommended. This compilation covers, besides pure iron and pure nickel, the entire binary composition range, both b.c.c. and f.c.c. phases. Elastic constants included are: Young's modulus, shear modulus, bulk modulus (reciprocal compressibility), Poisson's ratio, and single-crystal elastic stiffnesses, both second-order and higher-order. Data are compiled for variation of elastic constants with composition, temperature, pressure, magnetic field, mechanical deformation, annealing, and crystallographic transitions. An overview is given from the vantage points of the electron theory of metals, elasticity theory, and crystallographic theory. Also included are discussions of isothermal and adiabatic elastic constants, interrelationships among engineering elastic constants, computation of the latter from single-crystal elastic stiffnesses, and similar topics. Where key data have not been measured, they were generated if possible from existing data using standard formulae. Other gaps, both theoretical and experimental, in the elastic properties of iron-nickel alloys are indicated. A few theoretical results are included where experimental data are nonexistent or scarce. A semantic scheme is proposed for distinguishing elastic constants of solids.

Lutz, G. J., **Determination of lead in paint with fast neutrons from a californium-252 source**, *Anal. Chem.* **46**, No. 4, 618-620 (Apr. 1974).

Key words: activation analysis; californium-252; lead; neutron irradiation; paint.

Large amounts of lead in the paint on walls in dwellings is potentially hazardous to children in certain susceptible age groups who may ingest it. Most analytical methods for screening suspect homes require lengthy dissolution or other chemical procedures. Activation analysis with unmoderated neutrons from a ^{252}Cf source inducing the nuclear reaction $^{204}\text{Pb}(n,n')^{204m}\text{Pb}$ followed by gamma spectrometry with a Ge(Li) detector is shown to be a convenient, reliable and potentially rapid nondestructive method for this determination. The lower limit of determination in a 1.5 gram sample of paint with a $600\ \mu\text{g}$ source of ^{252}Cf is of the order of one percent lead.

Lutz, G. J., **The analysis of biological and environmental samples for lead by photon activation**, *J. Radioanal. Chem.* **19**, 239-244 (1974).

Key words: biological samples; environmental samples; lead; photon activation analysis.

The photonuclear reaction $^{204}\text{Pb}(\gamma,n)^{203}\text{Pb}$ is used for the determination of lead in biological and environmental samples. Precision and accuracy were determined to be adequate by analyzing some samples which have been assayed for lead by other methods. With a rigorous post-irradiation separation, the limit of detection is of the order of tens of nanograms.

Lyerla, J. R., Jr., McIntyre, H. M., Torchia, D. A., **A ^{13}C nuclear magnetic resonance study of alkane motion**, *Macromolecules* **7**, 11-14 (Jan.-Feb. 1974).

Key words: alkanes; carbon-13; magnetic resonance; molecular motion; polyethylene; rotational potentials; spin-lattice relaxation.

Carbon-13 spin-lattice relaxation times (T_1) have been measured for resolved carbons in neat n -alkanes ($n = 7, 10, 13, 15, 18, 20$) and 2-methylnonadecane, and effective correlation times (τ_{eff}) have been calculated from the T_1 values. A self-consistent analysis of the τ_{eff} values is provided using a model which considers alkane carbon motion in terms of contributions from overall and internal rotations. This analysis yields values for the barriers to methyl rotation in the linear (2.6 kcal/mol) and branched (2.9 kcal/mol) alkanes that are in approximate agreement with previously reported values. One also obtains information on the effects of chain ends and branches on internal motion and an estimate of the number of carbons involved in segmental motion of long alkanes.

Lyndon, R. C., Newman, M., **Commutators as products of squares**, *Proc. Amer. Math. Soc.* **39**, No. 2, 267-272 (July 1973).

Key words: commutators; products of squares; squares, products.

It is shown that if G is the free group of rank 2 freely generated by x and y , then $xyx^{-1}y^{-1}$ is never the product of two squares in G , although it is always the product of three squares in G . It is also shown that if G is the free group of rank n freely generated by x_1, x_2, \dots, x_n , then $x_1^2 x_2^2 \dots x_n^2$ is never the product of fewer than n squares in G .

Mandel, J., **The evaluation of referee methods in clinical chemistry**, *Med. Instrum.* **8**, No. 1, 26-29 (Jan.-Feb. 1974).

Key words: accuracy; calcium in serum; clinical testing; inter-laboratory comparisons; precision.

The importance of clinical testing to health demands that both precision and accuracy be achieved. Proficiency testing has shown that generally this is not the case. The next task is to study some individual clinical methods in depth to provide the profession with well developed referee methods. An interlaboratory study of a test method involves five elements: the protocol, samples, laboratories, statistical design, and analysis of the data. These elements are discussed and illustrated in terms of determining calcium in serum by atomic absorption spectrometry, using isotope dilution mass spectrometry as a standard of accuracy. This study, consisting of five "exercises," shows that only through constant vigilance and an attitude of real concern can acceptable levels of precision and accuracy be achieved.

Mann, D. B., Diller, D. E., Olien, N. A., Hiza, M. J., **Measurements of liquefied natural gas in commerce**, *Proc. American Gas Association Operating Section, El Paso, Texas*, pp. D-206-D-214 (American Gas Association, Inc., Arlington, Va., 1973).

Key words: cryogenic; density; flow; importation; liquefied natural gas; measurement; methane.

The Cryogenics Division of the NBS Institute for Basic Standards is currently involved in a number of programs dealing with liquefied natural gas (LNG). The objective of these NBS programs is to bring to bear over 20 years of cryogenic experience on certain selected LNG problem areas. A description of the programs will be given in the following sections as well as a summary of progress of this five-year effort.

In addition, the objectives of past, present and projected LNG programs at NBS will be related to one specific LNG problem area, custody transfer, and suggestions will be made about maximum utilization of present and expected research results.

Marcus, M., Merris, R., **A relation between the permanental and determinantal adjoints**, *J. Australian Math. Soc.* **XV**, Pt. 3, pp. 270-271 (1973).

Key words: congruence; doubly stochastic matrix; positive definite hermitian matrix.

Let A be an n -square positive definite hermitian matrix and $A(i|j)$ be the submatrix of A obtained by deleting row i and column j . Let $P(A)$ be the n -square matrix whose ij entry is $\text{per } A(j|i)$. If $D(A)$ is the classical adjoint of A then $n(\text{per } A) D(A) - (\det A) P(A)$ is positive semidefinite.

Maryott, A. A., Malmberg, M. S., Gillen, K. T., **Effective collision numbers for angular momentum relaxation from nuclear relaxation studies of simple liquids**, *Chem. Phys. Lett.* **25**, No. 2, 169-174 (Mar. 15, 1974).

Key words: angular momentum relaxation; collision numbers; liquids; NMR relaxation; rotational diffusion; spin-rotation.

Angular momentum correlation times, τ_J , derived from nuclear relaxation studies of a number of liquids composed of small molecules of high symmetry are compared with hard sphere and cell model collision rates. Either model leads to the conclusion that collision efficiency is high (collision number of 1 to 2) and provides a useful and simple relationship for predicting τ_J semiquantitatively over the liquid range.

Mauer, F. A., Hubbard, C. R., Hahn, T. A., **Anisotropic thermal expansion of $\alpha\text{-Pb}(\text{N}_3)_2$** , *J. Chem. Phys.* **60**, No. 4, 1341-1344 (Feb. 15, 1974).

Key words: lead azide; thermal expansion.

The anisotropic expansion coefficients of orthorhombic $\alpha\text{-Pb}(\text{N}_3)_2$ in the temperature range 102-423 K were determined by a single crystal x-ray method. The cell parameters and rms deviations at 298.2 K are $a = 11.33344[17]$, $b = 16.28277[37]$, and $c = 6.64058[10]$ Å. The linear expansion coefficients change gradually from $\alpha_a = 5.7 \times 10^{-5}$, $\alpha_b = 0.3 \times 10^{-5}$, and $\alpha_c = 1.4 \times 10^{-5} \text{ K}^{-1}$ at 112, to $\alpha_a = 8 \times 10^{-5}$, $\alpha_b = 0.4 \times 10^{-5}$, and $\alpha_c = 2.0 \times 10^{-5} \text{ K}^{-1}$ at 412 K. The largest expansion is in the a direction, which is perpendicular to sheets of azide ions separated by lead atoms.

Maximon, L. C., O'Connell, J. S., **Sum rules for forward elastic photon scattering**, *Physics Letters* **48B**, No. 5, 399-402 (Mar. 4, 1974).

Key words: Compton scattering; dispersion relations; photon; proton; scattering; sum rules.

Relations between integrals over forward elastic photon scattering amplitudes, forward elastic cross sections and total cross sections are derived from dispersion relations. A new photon-proton interaction sum rule is derived and evaluated.

McAlister, A. J., Cuthill, J. R., Williams, M. L., Dobbyn, R. C., **Electronic structure of the diborides of the 3d metals**, *Proc. Int. Symp. X-Ray Spectra and Electronic Structure of Matter, Munchen, Germany, Sept. 18-22, 1972*, **II**, 426-448 (1973).

Key words: band structure; borides; density of states; emission spectra; soft x ray; transition metal diborides.

Reported here are the results of two studies of the electronic structure of the isostructural sequence of refractory hard metals ScB_2 , TiB_2 , VB_2 , and CrB_2 . Experimentally, we have obtained the Boron soft x-ray K-emission spectra of the series and, as in other physical properties, observed a systematic variation with metal atomic number. Computationally, we have carried out a model band calculation which predicts qualitatively both the observed soft x-ray behavior and other observed trends in the properties of these compounds.

McCall, R. C., Nelson, W. R., Wyckoff, J. M., Pruitt, J. S., **Angular distribution of thick target bremsstrahlung**, *Proc. Second Int. Conf. on Accelerator Dosimetry and Experience, SLAC, Stanford, Calif., Nov. 5-7, 1969*, Conference Report No. 691101, pp. 684-691 (1969).

Key words: angular distribution; depth-dose; photon energy; Ta target; thermoluminescent detectors; 30 and 57.4 MeV electrons.

The angular distributions of dose due to 30 and 57.4 MeV electron beams striking a thick Ta target have been measured using small thermoluminescent detectors. Depth-dose curves measured at 5 and 135° have been used to demonstrate the contribution of secondary electrons in free air, at a plexiglas surface and at 9.25 g/cm² inside the plexiglas. Comparisons are made with calculated angular distributions of the photon energy emitted showing fair agreement.

McCarty, R. D., **A modified Benedict-Webb-Rubin equation of state for methane using recent experimental data**, *Cryogenics* **14**, No. 5, 276-280 (May 1974).

Key words: equation of state; methane.

A 33 term modified Benedict-Webb-Rubin equation of state is presented for methane. The adjustable parameters in the equation of state have been estimated using recent experimental data and least squares techniques which include the thermodynamic equilibrium conditions for the co-existing liquid and vapour phases. Comparisons of the new equation of state and an older modified Benedict-Webb-Rubin equation of state to experimental data are given.

McClendon, L. T., LaFleur, P. D., **Determination of rare earths in standard reference material glass using neutron activation analysis and reversed-phase chromatography**, *J. Radioanal. Chem.* **16**, 123-126 (1973).

Key words: di(2-ethylhexyl) orthophosphoric acid, Corvic; NBS Standard Reference Material 480; neutron activation analysis; rare earths; reversed-phase chromatography.

Recently, the interest in quantitative determination of rare earth elements has grown considerably, especially in connection with the space programs. There has also been a need for quantitative methods for rare earth element determination in different matrices at the National Bureau of Standards. We have therefore applied some of our earlier qualitative investigations with di(2-ethylhexyl) orthophosphoric acid (HDEHP) to separations of these elements for their subsequent quantitative determination. The rare earth elements in NBS Standard Reference Material 480, Trace Elements in Glass, a sodium glass to which 61 trace elements, including the thirteen naturally occurring rare earths, were added, have been determined by neutron activation analysis with a chemical separation using a column (11 cm × 40 cm) of "Corvic" powder [poly(vinyl chloride-vinyl acetate)] loaded with HDEHP and operated at a constant temperature. Since our earlier solvent extraction studies with HDEHP had shown perchloric acid to be the most favorable of three acids (HCl, HNO₃, HClO₄) for rare earth separation, we established the best operating conditions (e.g., time, flow, acid concentration, etc.) using this acid. A detailed description of the separations procedure and the quantitative results will be discussed.

McCulloh, K. E., Walker, J. A., **Photodissociative formation of ion pairs from molecular hydrogen and the electron affinity of the hydrogen atom**, *Chem. Phys. Lett.* **25**, No. 3, 439-442 (Apr. 1, 1974).

Key words: deuterium; electron affinity; hydrogen atom; ion-pair formation; para-hydrogen; photodissociation.

Photodissociative production of ion pairs from H₂ has been observed in the wavelength range 706-718 Å at spectral resolutions of 0.4 and 0.22 Å. From measured thresholds for production of H⁻ from H₂ molecules in each of the three lowest rotational states, the lower

bound EA(H) ≥ 0.754 ± 0.002 eV is obtained, in excellent agreement with the theoretical electron affinity of 0.75421 eV. For formation of D⁻ from D₂, a threshold assigned to molecules in the rotational state J = 2 has been measured, from which the bound EA(D) ≥ 0.757 ± 0.005 eV is obtained. Negative ion yield curves are presented for hydrogen.

McDonald, D. G., Peterson, F. R., Cupp, J. D., Danielson, B. L., Johnson, E. G., **Josephson junctions at 45 times the energy-gap frequency**, *Appl. Phys. Lett.* **24**, No. 7, 335-337 (Apr. 1, 1974).

Key words: cryogenics; infrared; Josephson junctions; lasers; superconductivity.

Superconductive Nb-Nb point contacts have been studied with 9.5-μm radiation from CO₂ lasers. Two models are considered to explain the experiments: one is Werthamer's Josephson junction model and the other is a thermally modulated Josephson junction. The evidence favors Werthamer's model but is not conclusive.

McLaughlin, W. L., Holm, N. W., **Physical characteristics of ionizing radiation**, Chapter 1 in *Manual on Radiation Sterilization of Medical and Biological Materials, Tech. Reports Series No. 149*, pp. 5-12 (International Atomic Energy Agency, Vienna, Austria, 1973).

Key words: dosimetry; electrons; gamma rays; ionizing radiation; microdosimetry; radiation physics; radiation sterilization; radiobiology; x rays.

An important step in developing the background for the radiation sterilization process is to review the physics and chemistry of radiation interactions in matter and the quantities that are used for monitoring radiation energy depositions. From this basis we can go on in subsequent chapters to the practical considerations of how efficiently the most radiation-resistant living organisms (fungi, bacteria, viruses, etc.) can be inactivated without causing excessive damage to the host material.

Mihalas, D., Hummer, D. G., **Some observational implications of extended static O-star model atmospheres**, *Astrophys. J.* **189**, L39-L43 (Apr. 1, 1974).

Key words: astrophysics; energy loss; O-stars; radiative transfer; stellar atmospheres.

Some results and observational implications are presented for the first extended spherical non-LTE model atmospheres in hydrostatic and radiative equilibrium. These models all correspond to a star with $\mathcal{M} = 60 \mathcal{M}_{\odot}$, $L = 1.25 \times 10^6 L_{\odot}$, and $R = 24 R_{\odot}$, with an effective temperature $T_{\text{eff}} \approx 39,500$ K and surface gravity $\log g \approx 3.45$ (spectral type near O6). They are differentiated by the magnitude and radiative dependence of a radiation-force multiplier γ , inserted into the equation of hydrostatic equilibrium, to simulate the effect of radiation force on opacity sources (e.g., lines) that have not been included in the calculations. It has been possible to obtain models very close to the limit at which the radiation force balances the gravity. Hydrogen and helium ($Y = 0.1$) constitute the gas; six hydrogen lines are treated explicitly. These models show L α in emission, the lower Balmer lines in absorption, the Balmer jump in absorption, and both infrared and ultraviolet excesses relative to the visual. Continuum jumps and gradients, Strömgren-system colors, and equivalent widths of H α , H β , and H γ are tabulated and discussed briefly.

Mitchell, R. A., Woolley, R. M., Chwirut, D. J., **Analysis of composite-reinforced cutouts and cracks**, (Proc. 15th Structures, Structural Dynamics and Materials Conference, Las Vegas, Nev., Apr. 17-19, 1974), AIAA Paper No. 74-377, pp. 1-13 (American Institute of Aeronautics and Astronautics, New York, N.Y., 1974).

Key words: adhesively bonded joints; composite materials; composite-overlay reinforcement; contour plotting; cracks, reinforcement of; cutouts, reinforcement of; finite element analysis; joints, adhesively bonded; reinforcement, composite overlay; reinforcement, cutouts and cracks.

Finite element computer analyses of the reinforcement of cutouts and cracks in metal sheet, by bonded overlays of composite material, are described. The analyses articulate the separate responses of the sheet, the overlays, and the adhesive. Contour plots of computed stress and strain fields are automatically generated by the computer programs. Strains measured on the surfaces of several reinforced-sheet tensile specimens were, for the most part, in good agreement with strains predicted by the analyses. Significant correlations between certain failure modes observed in the test specimens and the stress distributions given by finite element analysis are apparent. The same analytical approach is currently being used to study weld/bond and fastener/bond joints, and it could be used to study other problems such as hole repair in metal or composite sheet and embedded defects in laminar material.

Molino, J. A., **Psychophysical verification of predicted interaural differences in localizing distant sound sources**, *J. Acoust. Soc. Amer.* **55**, No. 1, 139-147 (Jan. 1974).

Key words: auditory localization; diffraction patterns; earphone simulation; human audition; interaural differences; minimum audible angle; psychometric functions; psychophysics; space perception.

Subjects made forced choices to either side of a reference direction (0, 30, 60, and 75°) to locate the image of pure tones presented through earphones. Various combinations of interaural intensity differences (IID's) and interaural time differences (ITD's) were used, including some combinations which do not occur in nature. Psychometric functions confirmed the expected apparent azimuth of ITD/IID combinations based on free-field diffraction theory and microphone measurements. The relative dominance of the intensive and temporal cues was examined at each frequency (500, 1000, and 8000 Hz). The shape of the psychometric plane for the bidimensional matrix at the 1000-Hz 30° condition showed possible nonlinearities in the trading relation. Data were also collected from the same subjects using the same signals presented by means of distant loudspeakers in an open field. When the free-field data were compared with the data from earphone-simulated sounds, they showed similar angular acuities, being approximately the size of those reported in the literature.

Moos, H. W., Linsky, J. L., Henry, R. C., McClintock, W., **High-spectral-resolution measurements of the H I λ 1216 and Mg II λ 2800 emissions from arcturus**, *Astrophys. J.* **188**, No. 3, L93-L95 (Mar. 15, 1974).

Key words: late-type stars; OAO spectroscopic observations; stellar chromospheres; stellar ultraviolet observations.

High-spectral-resolution scans of H I λ 1216 and Mg II λ 2796, 2803 obtained using the ultraviolet spectrometer aboard the *Copernicus* satellite show broad and very asymmetrical emission profiles. The ratio of the line widths to the solar values is consistent with a law similar to the Wilson-Bappu relation for the calcium K reversal. A fit of the interstellar absorption profile indicates that the average H density toward this nearby star is low, 0.02 - 0.1 cm⁻³.

Mulholland, G. W., Rehr, J. J., **Coexistence curve properties of Mermin's decorated lattice gas**, *J. Chem. Phys.* **60**, No. 4, 1297-1306 (Feb. 15, 1974).

Key words: coexistence curve; critical azeotrope; critical double point; decorated lattice gas; maxithermal point; renormalization.

Mermin's decorated lattice gas, noteworthy for its singular coexistence curve diameter and previously studied in connection with the breakdown of the law of rectilinear diameters, is shown to display in addition a rich variety of coexistence curve shapes and kinds of critical behavior as the interaction parameters of the model are varied. For an attractive decoration interaction, the coexistence curve of the model resembles, and can closely approximate, the liquid-vapor coexistence curve of real fluids. For a sufficiently repulsive decoration interaction, however, the model is shown to possess (at fixed tempera-

ture) three transitions to increasingly dense phases. These coexistence curves may feature peculiar shapes, such as necks and cusps, and they can appear inverted near the critical point; these curves terminate at either a critical point or at a maxithermal point (an analog of an azeotropic point). For discrete values of the interaction parameters, the model possesses a critical double point (the coalescence of two critical points) or a *cuspidal* critical point (critical azeotropy), in which cases the critical exponents become renormalized. Qualitatively these results are found to be independent of lattice structure and spatial dimensionality $d \geq 2$, and representative coexistence curves are plotted for the simple cubic lattice. Possible applications of these results are mentioned.

Naimon, E. R., Weston, W. F., Ledbetter, H. M., **Elastic properties of two titanium alloys at low temperatures**, *Cryogenics* **14**, No. 5, 246-249 (May 1974).

Key words: bulk modulus; compressibility; Debye temperature; elastic constant; Poisson's ratio; shear modulus; sound velocity; titanium alloys; Young's modulus.

Sound velocities and elastic constants were determined semi-continuously for two annealed polycrystalline titanium alloys between 4 and 300 K. Results are given for: longitudinal sound velocity, transverse sound velocity, Young's modulus, shear modulus, bulk modulus, Poisson's ratio, and elastic Debye temperature. A pulse-superposition technique was used.

Negas, T., Roth, R. S., Parker, H. S., Minor, D., **Subsolidus phase relations in the BaTiO₃-TiO₂ system**, *J. Solid State Chem.* **9**, 297-307 (1974).

Key words: barium-titanium oxides; BaTiO₃-TiO₂ system; crystal structure; phase equilibria.

Ba₆Ti₁₇O₄₀, Ba₄Ti₁₃O₃₀, BaTi₄O₉, and Ba₂Ti₉O₂₀ are the only compounds which were found to have a stability range in the subsolidus of the BaTiO₃-TiO₂ system. BaTi₂O₅ and BaTi₅O₁₁, reported in other studies, apparently are not stable. The compound reported as Ba₂Ti₅O₁₂ appears to have been mistaken for Ba₆Ti₁₇O₄₀. X-ray diffraction powder data are given for this phase which is monoclinic with $a=9.890$, $b=17.117$, $c=18.933$ Å and $\beta=98^\circ 42.6'$. The phase formulated previously as BaTi₃O₇ is shown to be Ba₄Ti₁₃O₃₀ based on structural and density considerations, phase equilibria, and single crystal and powder x-ray diffraction data. This compound is orthorhombic with $a=17.072$, $b=9.862$, and $c=14.059$ Å, probable space group, *Cmca*. An idealized structure for this phase is proposed. Ba₂Ti₉O₂₀ decomposes above 1300 °C in the solid state to BaTi₄O₉ plus rutile. Single crystals were grown using BaF₂ as a mineralizer.

Newell, A. C., Crawford, M. L., **Planar near-field measurements on high performance array antennas**, *Proc. 23d U.S. Air Force Antenna Symp., Urbana, Ill., Oct. 10-12, 1973* (Wright-Patterson Air Force Base, Dayton, Ohio, Oct. 1973).

Key words: antennas; near-field measurements; phased arrays.

The results of measurements are described which apply the planar near-field measurement technique to phased array antennas. Fast and efficient tests are used to determine the required scan area and data point spacing. The use of these tests can reduce the amount of data required for some antennas without seriously increasing the errors in computed results.

Measurements were made at different distances from the antennas, with the probe transmitting and receiving, and for both sum and monopulse difference patterns. Comparisons between the far-field patterns computed from the near-field data and those measured on far-field ranges are presented.

Newman, M., **Diophantine equations in cyclotomic fields**, *J. Reine Angew. Math.* **265**, 84-89 (1974).

Key words: cyclotomic fields; diophantine equations; units.

Let K_p be the cyclotomic field $Q(\zeta_p)$, where $\zeta_p = \exp(2\pi i/p)$, Q is the field of rationals, and p is a prime > 3 . The principal result of this paper is that the equation $\xi = \eta^n - 1$ has no solutions in units ξ, η of K_p which are not roots of unity, provided that $n > 2$. MOS Numbers - 10.66, 10.10.

Oettinger, F. F., Gladhill, R. L., **Thermal response measurements for semiconductor device die attachment evaluation**, 1973 *IEDM Tech. Digest*, pp. 47-50 (1973).

Key words: die attachment evaluation; diode die attachment; screen, die attachment; transistor die attachment.

This paper discusses an improved technique, based on transient thermal response measurements, to nondestructively evaluate die attachment in semiconductor devices. The technique was confirmed with studies performed on diodes bonded to TO-5 headers and transistors bonded to both TO-5 and TO-66 headers with voids intentionally incorporated into the die attachment. The advantages of using the transient thermal response technique for screening semiconductor devices for poor die attachment are emphasized.

Okabe, H., **Production of electronically excited species in photodissociation of simple molecules in the vacuum ultraviolet**, (Proc. Advanced Study Institute on Chemical Spectroscopy and Photochemistry in the Vacuum Ultraviolet, NATO, Valmorin, Quebec, Canada, Aug. 1973), Paper in *Chemical Spectroscopy and Photochemistry in the Vacuum Ultraviolet*, C. Sandorfy, P. J. Ausloos, and M. B. Robin, Eds., **8**, Series C, 513-523 (D. Reidel Publishing Co., Dordrecht, Holland, 1974).

Key words: bond energy; fluorescence; photodissociation; predissociation; spin conservation rules; vacuum ultraviolet.

Recent studies of the primary process in the photodissociation of small molecules have been reviewed. The process of producing fluorescing excited species in photodissociation in particular has been studied as a function of incident wavelength. The determination of the threshold wavelength of incident photons required for the production of the excited species provides information on bond dissociation energies and other thermochemical data. The nature of the primary process (i.e., direct dissociation, predissociation, the spin conservation rule, and the configuration of an upper state) has been discussed for some small molecules.

Olver, F. W. J., **Error bounds for stationary phase approximations**, *SIAM J. Math. Anal.* **5**, No. 1, 19-29 (Feb. 1974).

Key words: asymptotic approximations; error analysis; generalized integrals; special functions; stationary phase; Watson's lemma.

An error theory is constructed for the method of stationary phase for integrals of the form

$$I(x) = \int_a^b e^{ixp(t)} q(t) dt.$$

Here x is a large real parameter, the function $p(t)$ is real, and neither $p(t)$ nor $q(t)$ need be analytic in t . For both finite and infinite ranges of integration, explicit expressions are derived for the truncation errors associated with the asymptotic expansion of $I(x)$. The use of these explicit expressions for the computation of realistic error bounds is illustrated by means of an example.

Penn, D. R., **Field emission from adsorbate covered surfaces. II**, *Phys. Rev. B* **9**, No. 3, 844-847 (Feb. 1, 1974).

Key words: adsorbate density of states; adsorbate energy level; chemisorb; field emission; surface; total electronic energy distribution.

A previous calculation of the total energy distribution of field-emitted electrons in the presence of chemisorbed atoms by Penn, Gomer, and Cohen (PGC) is reexamined with respect to the following point. PGC assumed that the metal-adsorbate system could be

represented by the Anderson model; however, the Anderson model is phenomenological. Anderson and McMillan have shown how the model can be reformulated in a way which makes it more quantitative. Use of the reformulated model leads to a significant change in the PGC result for the field-emission current. We find $\Delta j(\omega)/j_0(\omega) = R^{-1} u'^2 \rho_a$, where $\Delta j(\omega)$ is the change in the current at energy ω due to the presence of the adsorbate and $j_0(\omega)$ is the current in the absence of the adsorbate. ρ_a is the density of states at the adsorbate and u'^2 and R^{-1} are given in the text. This result differs from that of PGC by the factor $R = [1 + \xi^{3/2} (\pi\alpha)^{-1/2}]^2$, where $\xi = (-2mE_F/\hbar^2)^{1/2}$ and $\alpha = 2mEF/\hbar^2$. Energies are measured from the vacuum level, E_F is the metal Fermi energy, and F is the strength of the external electric field. For typical experimental conditions $R^{-1} \approx 1/16$.

Penn, D. R., Plummer, E. W., **Field emission as a probe of the surface density of states**, *Phys. Rev. B* **9**, No. 4, 1216-1222 (Feb. 15, 1974).

Key words: field emission; metal surface; photoemission; surface density of states; total energy distribution.

Field-emission measurements of the total-energy distribution from a clean metal surface are shown to provide information about the density of states near the surface. Specifically, we find the field-emitted current per unit energy at energy ω to be given approximately by $j(\omega) \approx (2\hbar/m) S \lambda^{-2}(\omega) \sum_m D_0^2 (E_m^m) \times |\psi_m(\chi_m)|^2 \delta(\omega - \epsilon_m)$, where D_0^2 is the usual barrier-penetration probability with image potential corrections, $E_m^m = \omega - \hbar^2 k_{||}^2/2m$, where $k_{||}$ is the electron momentum parallel to the surface, $|\psi_m(\chi_m)|$ is the amplitude of the metal electron at the classical turning point ($\chi_m \sim 1.2 \text{ \AA}$), $\lambda(\omega)$ is a slowly varying function of ω , and S is the metal surface area. The D_0^2 factor in $j(\omega)$ strongly weights electron states with small $k_{||}$ and consequently $j(\omega)$ measures the density of states at χ_m arising from the component of the bulk band structure normal to the surface. Measurements of $j(\omega)$ for several single-crystal planes of tungsten will be presented and compared to the relevant photoemission data.

Powell, R. L., Fickett, F. R., Birmingham, B. W., **Programs on large scale applications of superconductivity in the United States**, (Proc. NATO Advanced Study Institute, Superconducting Machines and Devices-Large Systems Applications, Entreves, Italy, Sept. 5-14, 1973), Chapter 17 in *Superconducting Machines and Devices-Large Systems Applications*, S. Foner and B. B. Schwartz, Eds., pp. 651-675 (Plenum Publishing Corp., New York, N.Y., 1974).

Key words: electrical machinery; land transportation; power transmission; propulsion systems; superconducting devices; superconducting magnets; superconductivity.

A brief overview is given of U.S. programs on large-scale applications of superconductivity. Tables are presented listing for each project: the organization; the manager; a description of the device; a comment on the type of program; the source and amount of funding; the current status and the projected plans. The seven major project categories are: (1) Generators for electric power systems; (2) Power transmission; (3) Machinery for propulsion systems; (4) Magnets for energy storage, MHD and CTR systems; (5) Magnets and cavities for high energy physics experiments; (6) Magnets for industrial and medical applications; (7) Land transportation systems.

Pummer, W. J., Wall, L. A., **The burning and thermal properties of some γ -irradiated polymers**, *Proc. 165th Dallas Meeting of the American Chemical Society—Division of Organic Coatings and Plastic Chemistry, Dallas, Texas, Apr. 8-13, 1973*, **33**, No. 1, 490-498 (1973).

Key words: combustion; DTA; γ -irradiation; LOI; polymers; TGA.

Very little data are available which are concerned directly with the burning characteristics of γ -irradiated polymers. In this report, samples of six commercially available polymers were exposed to γ -rays

from a cobalt-60 source for 24 and 72 hour periods of time. Data was collected and compared between the nonirradiated and exposed polymers in the following areas: (1) the limiting oxygen index values, (2) the differential thermal analysis, (3) thermogravimetric analysis, and (4) temperature profiles of the polymers burning at or near their oxygen index values. The behavior of the polymers towards γ -rays is dependent upon the structure of each polymer. For example, Plexiglas (PMMA), Celcon (acetal copolymer), and poly- α -methylstyrene are degraded by γ -rays, while polystyrene, polyethylene, and Surlyn A ionomer undergo mainly crosslinking types of reactions although some degradation may also occur in the latter two polymers. In turn, the changes that may occur in thermal properties of the γ -treated polymers depend upon the severity of the radiation damage caused by the γ -rays to the polymers under our conditions of exposure. The amount of radiation damage sustained by each polymer would also be expected to affect the burning characteristics of each polymer. Thus, Celcon and Plexiglas, severely degraded by γ -rays, show the largest variations in their LOI values. Polystyrene, poly- α -methylstyrene and the ionomer, show no changes in their values after γ -irradiation, and polyethylene shows a slight rise in the LOI value on longer exposure times.

Pyke, T. N., Jr., Blanc, R. P., **Computer networking technology—A state of the art review**, *Computer* **6**, No. 6, 13-19 (Aug. 1973).

Key words: computer-communications; computer network architecture; computer networks.

Computer networking technology as represented by existing and planned computer networks is reviewed. Functional capabilities of alternative approaches to networking are considered particularly in terms of terminal and host computer system interfaces. Commonalities and differences in network architecture are identified. The limitations of existing network technology are discussed to clearly identify current problems and to indicate areas where further research and development is needed.

Pyke, T. N., Jr., **Some technical considerations for improved service to computer network users**, (Proc. 7th Annual IEEE Computer Conference, San Francisco, Calif., Feb. 27-Mar. 1, 1973), Paper in *Computing Networks from Minis through Maxis—Are they Real?*, *Digest of Papers*, pp. 53-55 (1973).

Key words: computer network; computer service; man-computer interface.

A variety of required and desired communications support services to users of computer networks are described. The general framework for these services is a large resource sharing network in which a number of host computer systems provide service to users through suitable communication facilities. Both interactive and noninteractive users are considered, and some alternatives are outlined for implementation necessary to provide these user services.

Radziemski, L. J., Jr., Kaufman, V., **Wavelengths, energy levels, and analysis of the second spectrum of chlorine (Cl II)**, *J. Opt. Soc. Amer.* **64**, No. 3, 366-389 (Mar. 1974).

Key words: chlorine; energy levels; spectra; wavelengths.

We have observed the spectrum of singly ionized chlorine (Cl II) with grating spectrographs from 500 to 11 000 Å using a ring discharge and a pulsed rf-discharge source. The accuracy of the observed wavelengths is about 0.002 Å from 500 to 3000 Å and 0.01 Å from 3000 to 11 000 Å. The number of known energy levels has increased from 140 to 270 and the number of classified lines from 600 to over 1100. We have found 25 levels of $3p^3\ ng(n=5-8)$ and 59 levels of $3p^3\ nf(n=4-10)$, including all 20 levels of $3p^3\ (^2D)4f$. Combinations with the latter levels gave new information on the singlets in the $3p^3\ 3d$ configuration, which led to the rejection of some levels, the establishment of others, and many changed assignments. *Ab initio* energy-level and spectrum calculations and least-squares energy-

level fits showed large interactions between the $3s\ 3p^5$, $3s^2\ 3d$, and $3s^2\ 3p^3\ 4d$ configurations. The ionization limit of Cl^+ is $192070 \pm 1\ \text{cm}^{-1}$.

Risley, E. W., Jr., **Discontinuity capacitance of a coaxial line terminated in a circular waveguide: Part II—Lower bound solution**, *IEEE Trans. Microwave Theory Tech.* **MTT-21**, No. 8, 564-566 (Aug. 1973).

Key words: coaxial line; lower bound; open circuit termination.

This calculation provides a lower bound (complementing the upper bound solution given earlier) to the discontinuity capacitance of a coaxial line terminated in a circular waveguide. A 50- Ω 0.9525-cm (3/4-in) open-circuited coaxial termination with a solid center conductor was fabricated with center- and outer-conductor diameters of 0.82723 ± 0.00005 and 1.90487 ± 0.00005 cm (1 cm = 0.393703 in), respectively. The measured value of capacitance of this termination at 1000 Hz was 216.4 ± 1.0 fF, as compared with the calculated lower bound of 215.0 fF. (The upper bound for this case was 217.7 fF.)

Risley, E. W., Jr., **Discontinuity capacitance of a coaxial line terminated in a circular waveguide. II. Lower bound solution**, (Proc. Conf. Precision Electromagnetic Measurement, Boulder, Colo., June 26-29, 1972), *CPEM Digest*, p. 111 (1972).

Key words: coaxial line reactance termination; discontinuity capacitance; lower bound.

The standard of reflection for coaxial line is the quarter wave short circuit termination. There are shortcomings to this standard; the fabrication cost is high and each termination is usable at only one frequency. However, an open-circuited coaxial line with extended outer conductor and solid inner conductor could be used advantageously as a standard termination because fabrication can be made using commercially available components, the device is broadband and losses are minimal. In addition to the high-frequency application, the termination can also be used at low frequencies as a standard of capacitance.

In an earlier paper (Discontinuity Capacitance of a Coaxial Line Terminated in a Circular Waveguide, Vol. MTT-17, No. 2, Feb. 1969), the input admittance y_{in} of this termination was calculated, assuming perfect conductivity, using a variational technique. A stationary form was derived for y_{in} which determined an upper bound to the discontinuity capacitance of the termination.

Roberts, R. W., **Freedom and social responsibilities**, *IEEE Spectrum* **11**, No. 4, 59-60 (Apr. 1974).

Key words: computer privacy; freedom of information; information; public information.

The guiding principle of the Freedom of Information Act is promotion of the public interest. Effective use of technical information requires more than "freedom," if by freedom one means merely unrestricted access. It requires a sense of responsibility and an activist approach toward evaluation and distribution to assure adequate dissemination of correct information. This is our approach at NBS.

Roder, H. M., **ASRDI oxygen technology survey. Volume V: Density and liquid level measurement instrumentation for the cryogenic fluids oxygen, hydrogen, and nitrogen**, *NASA Spec. Publ.* **3083**, 67 pages (National Aeronautics and Space Administration, Washington, D.C., 1974).

Key words: density; instrumentation; liquid level; phase detection; quantity gaging.

This volume of the survey presents information on instrumentation for density measurement, liquid level measurement, quantity gaging, and phase measurement. Information directly concerned with oxygen was given primary emphasis, work not specifically designated for oxygen, but considered of potential value in oxygen service was included. The information available on each instrument is presented under the headings: reference(s), instrumentation type, physical prin-

iple, phase of operation, a description of the instrument, materials of construction significant to oxygen compatibility, calibration method, performance characteristics, oxygen service, and limitations. The report also presents a discussion of problem areas in density and liquid level measurement, and recommends areas for further research and development.

Rook, H. L., LaFleur, P. D., Suddueth, J. E., **Trace element determination using a high yield electromagnetic isotope separator and neutron activation—the determination of cadmium**, *Nucl. Instrum. Methods* **116**, 579-586 (1974).

Key words: cadmium; high yield mass separator; neutron activation.

The use of isotope separators capable of producing high beam currents as applied to neutron activation analysis is discussed. The specificity of mass separation in this application allows beta or gross gamma counting to be used thereby providing increased sensitivity. The definition of instrument operational parameters and capabilities are discussed. Such parameters as yield, memory, resolution, overlap, and sputtering are considered. The optimized use of the mass separator as applied to the determination of cadmium in submicrogram quantities is presented.

Rook, H. L., Lutz, G. J., LaFleur, P. D., **The use of a high efficiency mass separator in activation analysis**, (Proc. Int. Conf. on Modern Trends in Activation Analysis, Saclay, France, Oct. 1972), *J. Radioanal. Chem.* **15**, 557-565 (1973).

Key words: activation analysis; cadmium; lead; mass separator.

The application of high yield mass separators to problems in activation analysis is discussed. The identification of separation parameters including separator yields, memory, resolution and overlap, and sputtering are considered. The use of the mass separator in determining lead by photon activation analysis is described.

Ruff, A. W., **Grain orientation dependence of reactivity in polycrystalline titanium after anodic polarization**, *Met. Trans.* **5**, 601-603 (Mar. 1974).

Key words: corrosion; crystallographic orientation; electrochemical polarization; electron channeling; titanium.

Selected area electron channeling patterns were obtained from individual grains down to 10 μm size in polycrystalline titanium after different anodic polarization treatments in 1 N H_2SO_4 . The crystallographic orientations of the more resistant and less resistant grains were determined and correlated with their relative reactivity. The results were in agreement with previously reported single crystal studies on titanium.

Sadowski, W. L., Lozier, D. W., **A unified standards approach to algorithm testing**, (Proc. ACM SIGPLAN Symp. on Computer Program Test Methods, Chapel Hill, N.C., June 21-23, 1972), Paper in *Program Test Methods*, Part VIII, pp. 277-290 (1973).

Key words: algorithms; mathematical functions; performance; standards; testing; validation.

A system of standards is proposed for the testing and validation of mathematical function subroutines. The system is based on a standards chain of the type that has been used successfully in metrology. This chain consists of a primary standard, a transfer standard, and a working standard. Their main characteristics are described and examples are given to illustrate the considerations that determine the writing of each of the above standards. The validation and testing process with the aid of these standards is discussed.

Schoenwetter, H. K., **An ultra-stable ac power supply for an absolute volt determination**, *Metrologia* **10**, No. 1, 11-15 (Mar. 1974).

Key words: absolute volt experiment; feedback control system; power amplifier; power supply oscillator; stable ac supply; voltage monitor.

A 159.2 Hz power supply with 85 VA power output and very stable amplitude was designed and constructed for use in an absolute volt experiment. The rms value of the ac voltage is regulated at the level of a dc reference voltage (based on unsaturated standard cells), using a feedback control circuit. The measured amplitude drift is less than 0.5 ppm/h and is typically less than 1 ppm in 4 h. The measured amplitude temperature coefficient is 0.6 ppm/ $^{\circ}\text{C}$ and the distortion is less than 0.02 percent.

Somes, N. F., **Progressive collapse risk**, (Proc. Int. Conf. on Planning and Design of Tall Buildings, Lehigh Univ., Bethlehem, Pa., Aug. 21-26, 1972), Paper in *Tall Building System and Concepts*, **1b**, 727 (1972).

Key words: accident occurrence; building; gas explosion; hazards; progressive collapse; tall buildings.

The National Bureau of Standards is undertaking an extensive study on behalf of the U.S. Department of Housing and Urban Development. The objectives are to determine the nature and frequency of occurrence of the various forms of extreme local loads on high rise buildings and to develop criteria necessary to reduce the risk of progressive collapse to an acceptable level.

Soulen, R. J., Jr., **Calibration of paramagnetic thermometers using superconductive fixed points**, *Cryogenics* **14**, No. 5, 250-252 (May 1974).

Key words: fixed points; paramagnetism; superconductivity; temperature.

A new method for calibration of paramagnetic materials is described. The technique consists of fitting the temperature-dependent mutual inductance of a coil set surrounding a paramagnetic material to a Curie Law using the superconductive transitions of several elements as thermometric fixed points. As a particular demonstration of this technique, the paramagnetic salt, cerous magnesium nitrate, was calibrated using the superconductive transitions of aluminium, zinc, and cadmium. The temperature scale obtained in this way was used in a study of the superconductive properties of iridium.

Soulen, R. J., Finnegan, T. F., **A microwave resistive SQUID for noise thermometry**, *Rev. Phys. Appl.* **9**, No. 1, 305-307 (Jan. 1974).

Key words: Josephson junction; superconductivity; temperature.

A SQUID magnetometer has been shown to work at 10 GHz with a significant enhancement of signal-to-noise over 30 MHz devices. This article describes how such enhancement could lead to faster determinations of absolute temperature using a resistive SQUID, i.e., a noise thermometer. A prototype 10 GHz resistive SQUID is described and its performance evaluated. The feasibility of using a 10 GHz system is clearly established.

Spiegel, V., **Age of californium-252 fission neutrons to indium resonance energy in water**, *Nucl. Sci. Eng.* **54**, 28-34 (1974).

Key words: age; ^{252}Cf ; fission spectrum; neutron; neutron age.

The age of ^{252}Cf fission neutrons to indium resonance energy (1.44 eV) was measured in water using a source encapsulated in a 7.6-mm-diam by 7.6-mm-high cylinder. The correction for the displacement of the moderator by the source was experimentally determined to be -0.13 cm^2 or about -0.5 percent in approximate agreement with calculation. The distribution of indium resonance energy neutrons close to the source was measured to be Gaussian. The age measured for this experiment was $28.69 \pm 0.39 \text{ cm}^2$. An average energy for the ^{252}Cf neutron spectrum of $2.21 \pm 0.05 \text{ MeV}$ is inferred from this age.

Spiegel, V., **The effective half-life of californium-252**, *Nucl. Sci. Eng. Tech. Note* **53**, No. 3, 326 (Mar. 1974).

Key words: activation analysis; californium-252; manganese activity; neutron irradiation.

The effective half-life of ^{252}Cf has been determined as 2.638 ± 0.007 yr. The method utilized the ratio of the manganese activity induced in a manganous-sulfate bath by a ^{252}Cf spontaneous-fission neutron source and the National Bureau of Standards photoneutron source to measure the change in emission rate of the ^{252}Cf source over a period of 1.77 half-lives. The data were corrected for the activity of radium (1622-yr half-life) in the photoneutron source (-0.2%) and for the competing neutron production from ^{250}Cf .

Stevens, W. J., Billingsley, F. P. II, **Coupled multiconfigurational self-consistent-field method for atomic dipole polarizabilities. II. Application to the first-row atoms, lithium through neon**, *Phys. Rev. A* **8**, No. 5, 2236-2245 (Nov. 1973).

Key words: atoms; correlation; dipole polarizabilities; excited states; ground state; multiconfiguration.

Static dipole polarizabilities, accurate to within 5 percent are presented for the ground states and some valence excited states of the first-row atoms. The polarizabilities are obtained from multiconfigurational self-consistent-field wave functions, which were computed with the perturbing electric field included directly in the Hamiltonian. The use of the multiconfigurational framework allows any state of both degenerate and nondegenerate atoms to be considered, and also allows for the explicit introduction of electron-correlation effects. Detailed discussions of basis-set selection and the effects of electron correlation are presented along with comparisons with experimental and other theoretical polarizability results.

Treu, S., Pyke, T. N., Jr., **Project-oriented collaboration via a computer network**, *Proc. Computer Science Conference, Columbus, Ohio, Feb. 1973*, p. 27 (1973).

Key words: computer network; interpersonal communications; task group collaboration.

Given a commitment to collaborate on a particular project, but hampered by geographical separation, a telecommunications triangle was established within the context of the ARPA Network. The triangle consisted of NBS, Pitt and ECOM. Several staff/faculty members at the first two institutions employed facilities of the Network Information Center (SRI) in order to formulate plans, exchange ideas, and produce specific results in support of a project at ECOM. That project involved interactive graphics for computer-aided design and engineering. ECOM personnel were able to "observe" and supply feedback when appropriate. A set of written ground rules for participation and data collection sheets for recording individual experiences were designed in advance. Results of this project-oriented collaboration have been analyzed in terms of feasibility, productivity, and required network capabilities.

Tsang, W., **Comparisons between experimental and calculated rate constants for dissociation and combination reactions involving small polyatomic molecules**, *Int. J. Chem. Kinet.* **5**, 947-963 (1973).

Key words: ammonia; combination; cyanogen; decomposition kinetics; nitric acid; nitril chloride; ozone; RRKM.

The experimental results on decomposition and combination reactions involving O_3 , HNO_3 , NH_3 , C_2N_2 , and NO_2Cl over extended temperature and pressure ranges are compared with the deductions from RRKM calculations. Quantitative fits of the data over the entire range are possible only if the external (overall) rotations are assumed to be involved in the reactions. Recommended rate constants for the reactions $\text{O} + \text{O}_2 + \text{N}_2 \rightarrow \text{O}_3 + \text{N}_2$ and $\text{OH} + \text{NO}_2 + \text{N}_2 \rightarrow \text{HNO}_3 + \text{N}_2$ are presented.

Tsang, W., **Pyrolysis of 2,4-dimethylhexene-1 and the stability of isobutenyl radicals**, *Int. J. Chem. Kinet.* **5**, 929-946 (1973).

Key words: bond strength; combination rate; decomposition; 2,4-dimethylhexene-1; isobutenyl; shock tube.

2,4-Dimethylhexene-1 has been decomposed in single-pulse shock tube experiments. Rate expressions for the initial reactions are

$$k(\text{C}_4\text{H}_7\text{-s-C}_4\text{H}_9 \rightarrow \text{C}_4\text{H}_7\text{-(isobutenyl)} + \text{s-C}_4\text{H}_9) = 10^{15.6} \exp(-33,200/T) \text{ sec}^{-1}$$

and

$$k(\text{C}_4\text{H}_7\text{-s-C}_4\text{H}_8 \rightarrow \text{iC}_4\text{H}_8 + n\text{-C}_4\text{H}_8) = 10^{12.5} \exp(-26,900/T) \text{ sec}^{-1}$$

at 1.5-5 atm and 1050 K. This leads to $\Delta H_{300}^\circ(\text{CH}_2 = \text{C}(\text{CH}_3)\text{CH}_2) = 124$ kJ/mol, or an allylic resonance energy of 50 kJ/mol. Rate expressions for the decomposition of the appropriate olefins which yield isobutenyl radicals and methyl, ethyl, isopropyl, *n*-propyl, *t*-butyl, and *t*-amyl radicals, respectively, are presented. The rate expression for the decomposition of isobutenyl radical is

$$k(\text{C}_4\text{H}_7\text{-(isobutenyl)} \rightarrow \text{C}_3\text{H}_4(\text{allene}) + \text{CH}_3) = 10^{13.3} \exp(-25,200/T) \text{ sec}^{-1}$$

(at the beginning of the fall-off region). For the combination of isobutenyl and methyl radicals, the rate constant at 1020 K is

$$k(\text{C}_4\text{H}_7\text{-(isobutenyl)} + \text{CH}_3 \rightarrow 2\text{-methylbutene-1}) = 10^{10.3} \text{ l./mol sec}$$

Combination of this number and the calculated rate expression for 2-methylbutene-1 decomposition gives $S \text{ C}_4\text{H}_7$, (1100) = 470 J/mol K. This yields

$$k(\text{CH}_3 + \text{C}_3\text{H}_4(\text{allene}) \rightarrow \text{C}_4\text{H}_7\text{-(isobutenyl)}) = 10^{8.2} \exp(-2,500/T) \text{ l./mol sec}$$

It is demonstrated that an upper limit for the rate of hydrogen abstraction by isobutenyl from toluene is

$$k(\text{C}_4\text{H}_7 + \phi\text{CH}_3 \rightarrow \text{iC}_4\text{H}_8 + \phi\text{CH}_2) \leq 10^{8.3} \exp(-6,000/T) \text{ l./mol sec.}$$

Van Brunt, R. J., Kieffer, L. J., **Electron energy dependence of the energy and angular distributions of O^- from dissociative ion pair formation in O_2** , *J. Chem. Phys.* **60**, No. 8, 3057-3063 (Apr. 15, 1974).

Key words: dissociation; electron; ionization; molecular oxygen.

The energy and angular distributions of O^- produced from O_2 by dissociative ion pair formation have been measured at selected incident electron energies from threshold to 100 eV. The kinetic energy distributions show well-defined maxima near 2.0 and 3.3 eV with appearance potentials, respectively, at 20.0 and 23.0 eV. The angular distributions are peaked in the forward and backward directions relative to electron beam and exhibit nondipolar structure. The shape of the distributions depends on electron energy, becoming more isotropic with increasing energy. An attempt has been made to explain the behavior of the angular distributions in terms of a superposition of final states using a multipole expansion of the differential cross section which includes the effects of higher-order partial waves.

VanderHart, D. L., **Low capacitance electrical feedthrough and simple, reusable closure seal for hydrostatic pressures to 7 kilobar and temperatures to 200 °C: Application to NMR**, *Rev. Sci. Instrum.* **45**, No. 1, 111-113 (Jan. 1974).

Key words: closure seal; electrical feedthrough; high pressure; hydrostatic; NMR; temperature.

An electrical feedthrough having a capacitance of 7 pF is described. It consists of a stack of two right circular cylinders, one an insulator, and one a metal with polyimide gaskets appropriately placed. A very simple, reusable, polymeric closure seal is also described. The seal is patterned after the "C" seal and features easy

extraction and sealing on the small bore of the pressure vessel. The closure seal and feedthrough have been tested to 7 kilobar at room temperature and 5 kilobar at 200 °C without failure.

Wachtman, J. B., Jr., **Determination of elastic constants required for application of fracture mechanics to ceramics**, (Proc. Symp. on Fracture Mechanics of Ceramics, University Park, Pa., July 11-13, 1973), Paper in *Fracture Mechanics of Ceramics*, R. C. Brandt, D. P. H. Hasselman, and F. F. Lange, Eds., 1, 49-68 (Plenum Publishing Corp., New York, N.Y. 1974).

Key words: anisotropy; elastic constants; elasticity; fracture; fracture mechanics; Griffith criterion.

Elastic properties enter into fracture mechanics most simply in the case of plane stress in an elastically isotropic body for which $EG_1 = \Pi K_1^2$ where G_1 is the energy release rate, K_1 is the stress intensity factor, and E is Young's modulus. For an elastically orthotropic body the same result holds provided $1/E$ is replaced by $(s_{11}s_{22}/2)^{1/2} [s_{22}/s_{11}]^{1/2} + (2s_{12} + s_{66})/2s_{11}]^{1/2}$ where the s_{ij} are the single crystal elastic compliances. These equations may be used to establish a Griffith type fracture criterion by setting $G_1 = G_{1c} = 2\gamma_f$ where γ_f is the fracture surface energy. Elastic moduli or compliances can usually be determined more accurately than either G_{1c} or γ_f . Methods for their determination by resonance or by ultrasonic wave propagation are briefly described. Values of the elastic factors in the energy release rates for material in polycrystalline form are compared with values for materials in single crystal form for various orthotropic orientations of cracks to indicate the effectiveness of single crystal elastic isotropy in causing variation in the fracture condition. This theory is shown to predict an anisotropic fracture criterion for certain crystal planes.

Wachtman, J. B., Jr., Schneider, S. J., **Measurements and standards for high temperature materials in energy conversion and clean fuel production**, *Stand. News* 1, No. 8, 16-23 (Aug. 1973).

Key words: clean fuel; coal; energy; gas; gas turbine; MHD; slag.

The serious energy situation in the United States requires greatly increased use of fossil fuel over the next thirty years despite the projected growth of nuclear power generating capacity. More efficient generation of electric power from coal and very large production of clean fuel from coal are urgently needed. Both require high temperatures and highly reactive chemical conditions.

The severe environments existing in high temperature gas turbines, MHD power generators, and coal gasifiers are briefly summarized. Data and test methods needed for process optimization, engineering design of hardware, and reliability assurance are analyzed. Early results are presented on slag characterization and on reaction of slag components with refractories. Typical data on viscosity of slag and on electrical conductivity of slag and alumina insulating material are given. A procedure to insure required lifetime under service stress is described. The implications of the present work for practical test methods for mechanical lifetime assurance, corrosion resistance, electrical conductivity measurements, viscosity measurements, and wear are assessed.

Wachtman, J. B., Jr., **The influence of surface features on the strength of polycrystalline alumina**, (Proc. 1971 Int. Conf. Mechanical Behavior of Materials, Kyoto, Japan, Aug. 13-31, 1971), Chapter in *Mechanical Behavior of Materials* 4, 432-442 (The Society of Materials Science, Kyoto, Japan, 1972).

Key words: fracture surface energy; machining damage; plastic deformation; polycrystalline alumina; strength; surface features; thermal expansion anisotropy.

Fracture surface energy of polycrystalline alumina measured with large cracks ranges from 10 to 46 J/m²; the critical surface energy de-

pends on the size of the fracture nucleus. For single crystals, values depend on the plane of the crack with a minimum of 6 J/m² for (10 $\bar{1}$ 1). On this basis failure results from surface microcracks only one fourth the average grain diameter. The thermal expansion anisotropy stress acting on this size crack is 1.5 times the value calculated for an internal crack due to surface proximity. Hardness indentations produce cracks at high loads but reduce strength only when a greater critical load, which increases with decreasing grain size, is exceeded. This behavior apparently corresponds to a range of safe machining.

Wagner, H. L., Hoeve, C. A. J., **Mark-Houwink relations for linear polyethylene in 1-chloronaphthalene and 1,2,4-trichlorobenzene**, *J. Polymer Sci.* 11, 1189-1200 (1973).

Key words: fractionation; limiting viscosity number; linear polyethylene; Mark-Houwink; molecular weight; Stockmayer-Fixman; unperturbed dimensions; viscosity; 1-chloronaphthalene; 1,2,4-trichlorobenzene.

The parameters in the Mark-Houwink relationship, $[\eta] = K'M_r^a$, for linear polyethylene in 1-chloronaphthalene and 1,2,4-trichlorobenzene at 130 °C have been estimated. They were found by measuring the limiting viscosity numbers of a series of fractions with molecular weights ranging from less than 10,000 to almost 700,000. The results are for 1-chloronaphthalene, $[\eta] = 0.0555 \bar{M}_r^{0.684}$ (with a standard error of 0.0064 in K' and 0.010 in a) and for 1,2,4-trichlorobenzene, $[\eta] = 0.0392 \bar{M}_r^{0.725}$ (with a standard error of 0.00703 in K' and 0.015 in a), where $[\eta]$ is expressed in ml/g. The unperturbed end-to-end distance calculated from the viscosity-molecular weight data agrees with the theoretically expected value.

Wagner, H. L., **The polymer standard reference materials program at the National Bureau of Standards**, *Adv. Chem. Series No. 125*, pp. 17-24 (1973).

Key words: gel permeation chromatograph calibration; limiting viscosity number; molecular weight; molecular weight distribution; polyethylene standard; polystyrene standard; standard reference materials; standard reference polymers.

The National Bureau of Standards now distributes four polymer Standard Reference Materials designed for use in the calibration of instruments employed in polymer characterization. Polystyrene is available in narrow (SRM 705) and broad (SRM 706) distributions and polyethylene in high-density linear (SRM 1475) and low-density branched (SRM 1476) whole polymer. These materials are characterized with respect to many but not necessarily all of the following properties: weight and number-average molecular weight, limiting viscosity number in several solvents, ASTM density, and ASTM melt flow rate. In addition the molecular-weight distribution of the linear polyethylene is given, making it suitable for the calibration of gel-permeation chromatographs at high temperatures.

Wait, D. F., Beatty, R. W., **The 1973 International Microwave Symposium**, *IEEE Trans. Microwave Theory Tech.* MTT-21, No. 12, 747-751 (Dec. 1973).

Key words: exhibits; microwave; symposium.

The 1973 IEEE G-MTT International Microwave Symposium was held June 4-6, 1973, in Boulder, Colo. The theme was "Microwave Applications in the 70's."

Wakeford, O. S., Robinson, D. E., **Lateralization of tonal stimuli by the cat**, *J. Acoust. Soc. Amer.* 55, No. 3, 649-652 (Mar. 1974).

Key words: animal audition, cats; animal psychophysics; auditory lateralization; auditory localization; avoidance; binaural hearing; earphones for animals; interaural differences.

The ability of the cat to "lateralize" tonal signals having interaural intensive or interaural temporal disparities was measured. Interaural intensive differences were studied at 0.5, 1.0, and 3.0 kHz. Interaural temporal differences were studied at 0.5, 1.0, 2.0, and 3.0 kHz. Minia-

ture audio transducers were employed to present the stimuli to the animals. The transducers were held in a fixed spatial relation to the auditory canal by means of "pinna inserts" and leather helmets. An avoidance response in a shuttle box was used as the dependent variable. The animals' task involved the detection of a right-left reversal in a gated sequence of tone bursts. The cat appears to be about as sensitive as the human to both interaural intensive and temporal disparities at each of the frequencies studied.

Walls, F. L., Dunn, G. H., **Measurement of total cross sections for electron recombination with NO^+ and O_2^+ using ion storage techniques**, *J. Geophys. Res.* **79**, No. 13, 1911-1915 (May 1, 1974).

Key words: ion storage technique; recombination of NO^+ ; recombination of O_2^+ .

The total cross section as a function of electron energy for recombination of electrons with room temperature NO^+ has been measured with a trapped ion technique. Measurements were made in the electron energy range 0.045-4 eV with an energy resolution between 0.045 and 0.120 eV, and the cross sections, which showed some structure, ranged from $1.25 \times 10^{-14} \text{ cm}^2$ at the lowest energy to $1.7 \times 10^{-16} \text{ cm}^2$ at the highest energy. Similar measurements were made on O_2^+ , the species used to calibrate the apparatus geometry. A Maxwellian distribution of electron velocities was used with the measured cross sections to calculate rate constants, giving values extending to electron temperatures as high as 40,000 K. Comparison with previously measured rate coefficients at lower temperatures is quite satisfactory.

Wells, J. S., McDonald, D. G., Risley, A. S., Jarvis, S., Cupp, J. D., **Spectral analysis of a phase locked laser at 891 GHz, an application of Josephson junctions in the far infrared**, *Rev. Phys. Appl.* **9**, 285-292 (Jan. 1974).

Key words: frequency noise; HCN laser; infrared frequency synthesis; Josephson junction; laser frequency measurements; laser linewidth; laser stabilization; phase locked laser.

We have used a Josephson junction to investigate the spectral purity of an HCN laser which is used in an infrared frequency synthesis chain. To obtain a narrower linewidth from the laser it has been phase locked to a multiplied microwave reference chain. A calculated value for this linewidth was based upon the measured noise spectrum of the microwave source and a theory due to Middleton. One can take advantage of the unique properties of the Josephson junction as a frequency multiplier and mixer for use in measuring this linewidth. The Josephson junction is driven by an x-band signal which is derived from a specially designed cavity stabilized klystron system of high spectral purity. The 92nd harmonic of the x-band signal is generated in the Josephson junction. In addition, the Josephson junction acts as a mixer of the harmonic signals and the 891 GHz output of the HCN laser. The 92nd harmonic beat signal is taken from the Josephson junction, amplified, and sent to a spectrum analyzer for frequency domain analysis. Details of the experiment, results, and relation to predicted linewidths are presented.

Wright, R. N., **Survey of fire and live loads**, (Proc. Int. Conf. on Planning and Design of Tall Buildings, Lehigh Univ., Bethlehem, Pa., Aug. 21-26, 1972), Paper in *Tall Building System and Concepts*, **1b**, 128-130 (1972).

Key words: buildings; design; fire loads; fire rating; floor loadings; live loads; stochastic models.

This discussion, presented at the session on gravity loads and temperature effects of the ASCE-IABSE Conference on Tall Buildings, outlines a program of survey of fire and live loads which the National Bureau of Standards is beginning under the auspices of the Building Research Advisory Board and the sponsorship of the Public Building Service of the General Services Administration. Its objectives are to improve the technical bases for criteria for fire ratings of buildings

and for floor loadings used in building design. The surveying will employ stochastic models for representation of loadings developed at NBS. It will provide a data base for immediate improvements in building standards for fire resistance and design live loads. The information surveyed also will provide an information basis for long-range scientific studies to develop new design concepts for control of building fires and new criteria for mitigation of fire effects. The live loads information will allow theoretical studies of design load configurations leading to more consistent probabilistic formulations of combinations of loadings from the building's own weight, the effects of occupancy, effects of wind, effects of earthquake, etc.

Yakowitz, H., **X-ray microanalysis in scanning electron microscopy**, *Proc. Annual Scanning Electron Microscopy Symp. sponsored by IITRI, Chicago, Ill., Apr. 7-9, 1974*, pp. 1029-1042 (IIT Research Institute, Chicago, Ill., Apr. 1974).

Key words: analytical accuracy; electron probe microanalysis; elemental mapping; energy dispersive analysis; scanning electron microscopy; specimen preparation.

This tutorial paper touches briefly on a number of aspects of qualitative and quantitative x-ray analysis. The way in which energy dispersive detectors can be used for qualitative and quantitative analysis is described. Automatic qualitative analysis and background subtraction for energy dispersive methods are described. Crystal spectrometer systems are considered and compared with energy dispersive techniques. The question of identification and analysis of elements of atomic number eleven or less is discussed. A great many practical problems can be solved by elemental distribution mapping. Therefore, this technique is outlined and an example given. A brief compendium of the classical theoretical basis for quantitative analysis is given; histograms of results indicate what accuracy can be expected from optimum specimens. Other quantitative analysis methods such as the hyperbolic approximation are also touched upon. An on-line quantitative analysis computer routine is outlined. Special specimen geometries such as thin films, either free standing or on a substrate or small spheres, or inclusions require special handling. Finally, a few comments on specimen preparation are offered.

Yates, J. T., Jr., Madey, T. E., Erickson, N. E., **ESCA study of carbon monoxide and oxygen adsorption on tungsten**, *Surface Sci.* **43**, 257-274 (1974).

Key words: carbon monoxide; chemical shift; chemisorption; ESCA; oxygen; tungsten.

The chemisorption of both CO and O_2 on a clean tungsten ribbon has been studied using an ultrahigh vacuum x-ray photoelectron spectrometer. For CO , the energy and intensity of photoemission from $\text{O}(1s)$ and $\text{C}(1s)$ core levels have been studied for various adsorption temperatures.

At adsorption temperatures of $\sim 100 \text{ K}$, the "virgin"- CO state was the dominant adsorbed species. Conversion of this state to more strongly-bound $\beta\text{-CO}$ is observed upon heating the adsorbed layer to $\sim 320 \text{ K}$. Thermal desorption of CO at $300 \leq T \leq 640 \text{ K}$ causes sequential loss of $\alpha_1\text{-CO}$ and $\alpha_2\text{-CO}$ as judged by the disappearance of $\text{O}(1s)$ and $\text{C}(1s)$ photoelectron peaks characteristic of these states.

Oxygen adsorption at 300 K gives a single main $\text{O}(1s)$ peak at all coverages, although at high oxygen coverages there exist small auxiliary peaks at $\sim 2 \text{ eV}$ lower kinetic energy. The photoelectron $\text{C}(1s)$ and $\text{O}(1s)$ binding energies observed for these adsorbed species are all lower than for gaseous molecules containing C and O atoms. For CO adsorption states there is a systematic decrease in photoelectron binding energy as the strength of adsorption increases. These observations are in general accord with expectations based on electronic relaxation effects in condensed materials.

Yokel, F. Y., Wright, R. N., **Summary report—Technical Committee No. 26, Limit states design**, (Proc. Int. Conf. on Planning and Design of Tall Buildings, Lehigh Univ., Bethlehem, Pa., Aug. 21-26, 1972), Paper in *Tall Building System and Concepts*, **III**, 949-953 (1972).

Key words: deterioration; failure; limit states design; mode of failure; reliability; structural failures.

A limit state has been defined as "a particular state, in which a structure ceases to fulfill the function or to satisfy the condition for which it is designed" (1). By this definition a limit state is a mode of failure, which includes failure to perform a specific function or to provide a desired attribute. The goal of limit states design as presently defined is to give explicit consideration to all failure modes and to assure a suitably low probability that the structure or any of its components reach a limit state in service.

The state of the art reports presented in behalf of Committee 26 identify limit states of reinforced concrete structures and survey our knowledge with respect to the application of limit states design. In

this paper the state of the art reports are summarized and some new definitions are suggested for consideration.

Zwanzig, R., Bishop, M., **Tunnel model of liquid diffusion**, *J. Chem. Phys.* **60**, No. 1, 295-296 (Jan. 1974).

Key words: liquid diffusion; tunnel model; velocity correlation function.

A tunnel model of liquid diffusion, analogous to Barker's thermodynamic model, is constructed by separating particle motion into components parallel and perpendicular to a tunnel axis. By combining exact results for hard rod systems, one is able to predict both the tunnel diffusion coefficient and the corresponding velocity correlation function. The ratio of the tunnel diffusion coefficient to the Enskog value at the same density and temperature is obtained by matching the virial and the temperature. The value predicted lies outside the range investigated by Alder *et al*; therefore direct comparison to molecular dynamics results is not possible. However, the velocity correlation function has the negative region characteristic of dense fluids. It is suggested that the derivation of the tunnel model dynamics may be valid at close packed densities.